

THE PHYSICAL BASIS OF THE METHOD

Thesis for Degree of Ph.D.

OF

D. F. OJO

DIFFERENTIAL THERMAL ANALYSIS

Changes and Corrections made on the  
grounds of Instructions of the Examiners

-----  
The copies hereby submitted are those originally submitted, but the following alterations have been

Thesis submitted by

- (a) Page 50, line 11 to Page 53 line 5. Entirely new material which is equivalent paragraphs of original thesis, with the addition of new illustrations.
- (b) Fig. 16 (Page 37). A revised form of Fig. 16 of original thesis to allow correction of graph 1 and to include necessary labelling in accordance with text.
- (c) Page 57 and Fig. 37. Phrasing of paragraph 3 slightly altered and the curves of Fig. 37 extrapolated to zero for the sake of amplification.
- (d) Binding: Changed in order to allow the inclusion of the fresh material and correction of spine lettering.
- (e) Minor corrections: As pointed by the Examiners.



DIFFERENTIAL THERMAL ANALYSIS

Thesis for Degree of Ph.D.

D. F. OJO

Changes and Corrections made on the  
instructions of the Examiners

The copies hereby submitted are those originally submitted, but the following alterations have been made:-

- (a) Page 50, line 11 to Page 53 line 5. Entirely new material which replaces equivalent paragraphs of original thesis, with the addition of new illustrative data in Table V(a).
- (b) Fig.16 (Page 37). A revised form of Fig.16 of original thesis to allow correction of graph I and to include necessary labelling in accordance with text.
- (c) Page 57 and Fig.37. Phraseology of paragraph 2 slightly altered and the curves of Fig.37 extrapolated to zero for the sake of amplification.
- (d) Binding: Changed in order to allow the inclusion of the fresh material and correction of spine lettering.
- (e) Minor corrections:. As pointed by the Examiners.

P R E F A C E.

The material reported in this thesis represents some of the results of investigations carried out by the author over a number of years at University College, Ibadan, under the direct supervision of Professor N.S. Alexander, to whom I am most grateful for his encouragement and help, both personal and official, and for the facilities afforded me in his department.

Part of the work was done with the assistance of the Government of Nigeria under a two-year research scholarship, which I hereby gratefully acknowledge.

In the construction of the apparatus, most valuable help was given by Mr. N. Gardiner, Superintending Technician, University College of Ghana, and the rotary switch was entirely made by him. Mr. E.H. McKoy Senior Technician, University College, Ibadan, made the drawings for Figures 5, 6 and 14. Mrs. Mona Irvine helped in reducing some of the records and drawing some of the graphs. To all these people, and to Dr. R.W.R. Wright, Professor of Physics, Ghana, and Dr. A.J. Lyon, University College, Ibadan, both of whom gave valuable suggestions on the theoretical work, I am deeply indebted.

III.3. Crystalline Inversion,  
Including Recrystallization  
from amorphous form, in  
the solid state

<u>TABLE OF CONTENTS</u>		Page
PREFACE		i
CONTENTS		ii
LIST OF ILLUSTRATIONS		iv
CHAPTER		
I. INTRODUCTION		1
I.1. Mainly Historical		
I.2. Description of Method		
I.3. Applications of D.T.A.		
I.4. Two types of Problems		
II. DESCRIPTION OF APPARATUS		9
II.1. The Calorimeter		
II.2. The Furnace		
II.3. Temperature Regulation		
II.4. Measurement of Furnace or Surface Temperature		
II.5. Thermocouple arrangement for measurement of internal temperatures		
II.6. Photographic Recorder and ancillary equipment		
II.7. Electronic Recording		64
III. EXPERIMENTAL TECHNIQUE		26
III.1. Preparation of Specimen		
III.2. Crystalline Inversion, including Recrystallisation from amorphous form, in the solid state		

	Page
VI. III.3. Melting and Solidification	77
APPENDIX III.3.1. Sintered Glass	80
REFERENCES III.3.2. Calcium Sulphate	82
III.3.3. Impregnation	
III.3.4. Choice of test substance and inert base	
IV. EXPERIMENTAL RESULTS	37
IV.1. Melting and Solidification	
IV.1.1. Differential Thermal Curves	
IV.1.2. Propagation of Reaction (a) Heating Curves	
IV.1.3. Propagation of Reaction (b) Equation of Propagation.	
IV.2. Crystalline Inversion of Potassium Nitrate	
IV.2.1. Summary of general results	
IV.2.2. Effects of Heating Rate	
IV.2.3. Effects of the Concentration of Reacting Material	
IV.2.4. Notes on Results.	
V. THEORETICAL ANALYSIS OF THE STEFAN PROBLEM	64
V.1. Symmetrical radial heat flow with $\theta = kt$ at $r = a$	
V.2. Inclusion of the Source	
V.3. Properties of the Differential Temperature	
V.4. Evaluation of the Differential Temperature	
V.5. Discussion	

	Page
<u>LIST OF ILLUSTRATIONS</u>	
VI. CONCLUSION	77
APPENDIX	80
REFERENCES	82
3. Idealized dehydration and D.T.A. curves for kaolinite	4
4. The Calorimeter or Specimen-Holder	11
5. Furnaces Types I & II	13
6. Furnace Type III	14
7. Ancillary Heaters	15
8. Regulating Potentiometer and Thermocouple Circuit	16
9. Regulating Resistances for Furnaces I and II	16
10. Thermocouple Patterns	18
11. Spark-welding of Thermocouple Wires	19
12. Principle of Constant-Damping Shunt	22
13. Circuit Diagram of Shunt	22
14. Rotary Switch	23
15. Complete Recording System	24
16. Vapour Pressure Curves	26
17. D.T.A. Curves for zinc chloride	30
18. " " " m-nitroaniline (I)	30
19. " " " " (II)	30
20. Idealized D.T.A. Curve	40
21. Position of Peak with respect to Surface Temperature for different r	42
22. Height of Peak and r	43
23. Heating Curves for zinc chloride	45

Figure LIST OF ILLUSTRATIONS

Figure		Page
1.	Temperature-Time Curves after Wohlin	2
2.	Arrangement of Thermocouples in D.T.A.	3
3.	Idealized dehydration and D.T.A. curves for kaolinite	4
4.	The Calorimeter or Specimen-Holder	11
5.	Furnaces Types I & II	13
6.	Furnace Type III	14
7.	Ancillary Heaters	15
8.	Regulating Potentiometer and Thermocouple Circuit	16
9.	Regulating Resistances for Furnaces I and II	16
10.	Thermocouple Patterns	18
11.	Spark-welding of Thermocouple Wires	19
12.	Principle of Constant-Damping Shunt	22
13.	Circuit Diagram of Shunt	22
14.	Rotary Switch	23
15.	Complete Recording System	24
16.	Vapour Pressure Curves	36
17.	D.T.A. Curves for zinc chloride	39
18.	" " " m-nitroaniline (I)	39
19.	" " " " (II)	39
20.	Idealized D.T.A. Curve	40
21.	Position of Peak with respect to Surface Temperature for different r	42
22.	Height of Peak and r	43
23.	Heating Curves for zinc chloride	45

Figure	Page
24. Heating Curves for m-nitroaniline (I)	45
25. " " " " (II)	45
26. Comparison of Heating and D.T. Curves	46
27. Propagation Curves of Melting	49
28. Empirical Relation between $r_1$ and $t$	52
29. $a^2 - r_1^2$ against $t$	53
30. Heating Curves for potassium nitrate (I)	55
31. D.T. " " " " (I)	55
32. Heating " " " " (II)	55
33. D.T. " " " " (II)	55
34. D.T. Curves for $r = 1.5$ cm. for various heating rates	56
35. Variation peak height with heating rate	57
36. Propagation curves for inversion of potassium nitrate	57
37. $a^2 - r_1^2$ vs. $t$ for various heating rates	57
38. Graph of propagation rate against heating rate	58
39. Maximum differential temperature as a function of Concentration	59
40. Propagation Curves for various concentrations	60
41. Theoretical D.T.A. Curves for Inversion of Potassium Nitrate (I)	72
42. Theoretical D.T.A. Curves for Inversion Of Potassium Nitrate (II)	72
43. Deviation of the d.t. curve	75



## Chapter 1.

### I N T R O D U C T I O N

#### I. 1. Mainly Historical:

Thermal analysis of naturally occurring substances seems to have been first performed by Le Chatelier<sup>(1)</sup> in 1887. His method consisted in setting up simple apparatus to measure and record thermal reactions taking place in a material when it is heated at a more or less uniform rate, and using such recorded data as analytical criteria to study the material. Little use was made of the method by mineralogists, except sporadically and hesitatingly by Italian ceramists, until 1910, when several investigators used it in the study of clays. In these early studies the procedure generally followed was to place the material in a small platinum crucible with a single thermocouple (usually platinum - platinum + 10% iridium) in the centre of the material. The whole mass was placed in a furnace and heated at a rapid and relatively uniform rate. The thermocouple was attached to a galvanometer which was read periodically or recorded photographically. Thermal reactions in the material caused variations in the record as compared with that obtained when the furnace contained no sample. The record obtained showed the thermal reactions of the material superimposed on the heating curve of the furnace.

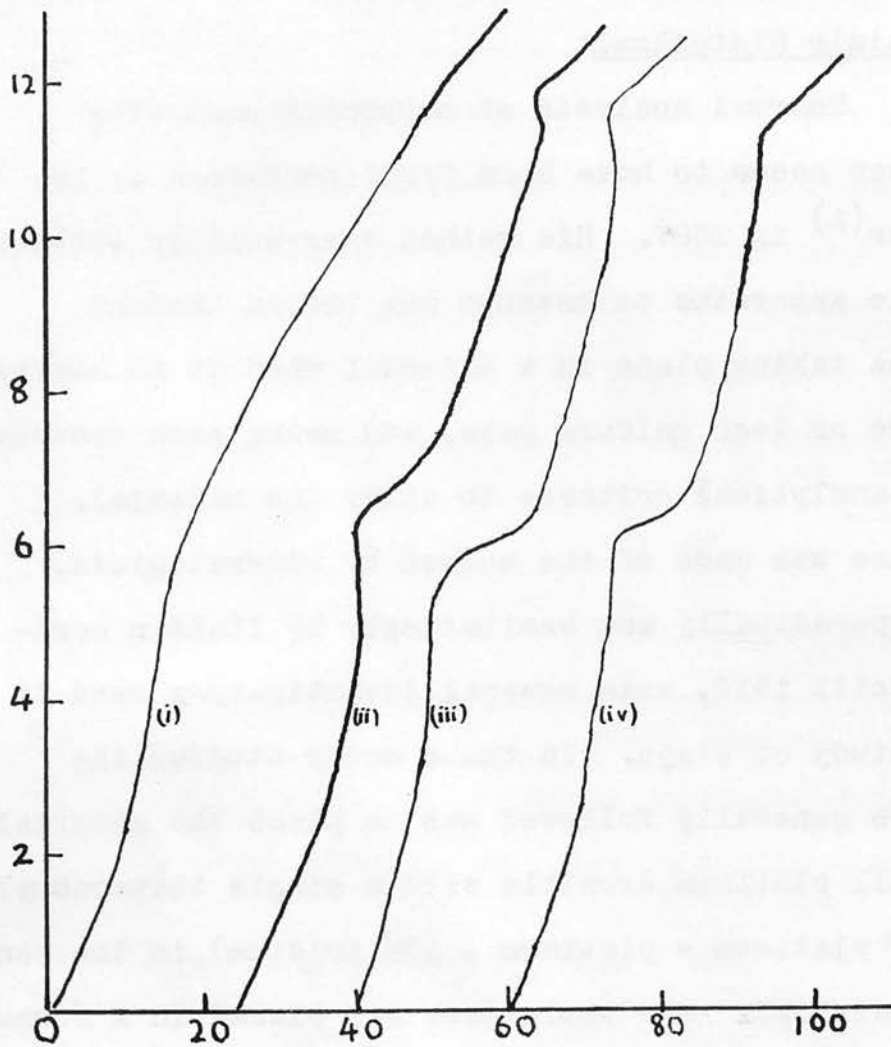
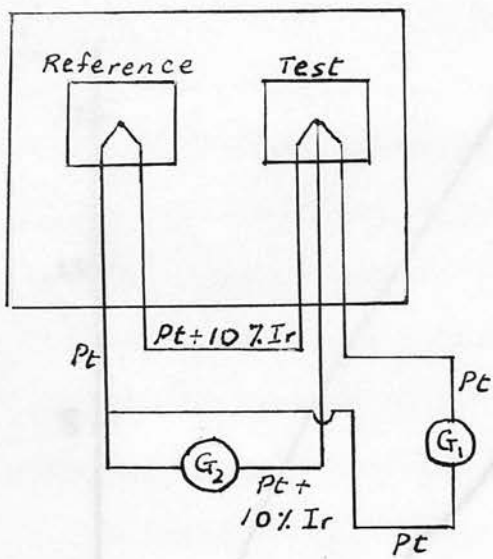


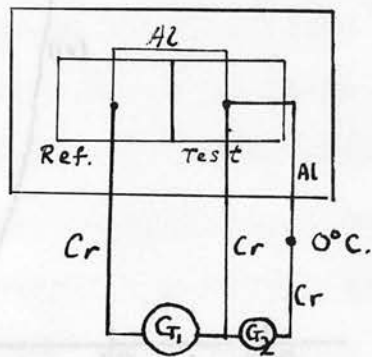
FIG. 1 TEMP. vs. TIME CURVES, AFTER WOHLIN.

(i) Furnace heating Curve.

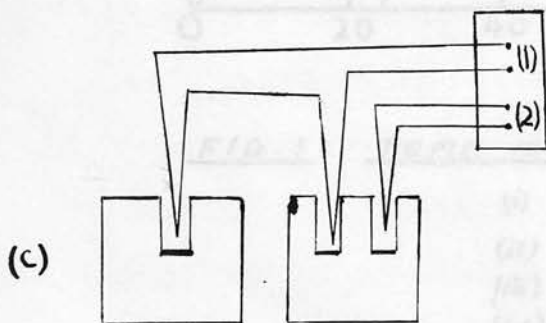
(ii) }  
 (iii) } Furnace heating with reactions  
 (iv) } in clays superimposed.



(a)



(b)



(c)

(1) To Galvanometer

(2) To Potentiometer

Fig. 2. Arrangement of Thermocouples in D.T.A.  
(a) Roberts-Austen's (b) & (c) Two  
Modern Arrangements

In 1899, Roberts-Austen<sup>(2)</sup>, a metallurgist, devised the differential-thermocouple method for measuring temperature differences between a material and a reference unit. But following the work of Roberts-Austen the method aroused little interest except among metallurgists, and Fenner (1913) in his study of the stability relations of the silica minerals<sup>(3)</sup>, appears to have been the first to apply the method outside the field of metallurgy. Fenner's technique is substantially the same as is used today.

#### I. 2. Description of Method:

In the method as generally used today, the sample to be studied is placed in one hole of a specimen holder, and an inert material that experiences no reaction when heated to the temperature of the experiment, (usually calcined aluminium oxide -  $\alpha$ - $\text{Al}_2\text{O}_3$ ), is placed in another hole of the specimen holder. One junction of the difference thermocouple (Fig. 2) is placed in the centre of the sample and the other junction in the centre of the inert material. The holder and thermocouples are placed in a furnace so controlled as to produce a uniform rate of temperature increase, usually 5 to 12°C. per minute. The temperature of the inert material increases <sup>regularly as the temperature of the furnace increases.</sup> When a thermal reaction takes place in the sample, the temperature of the sample

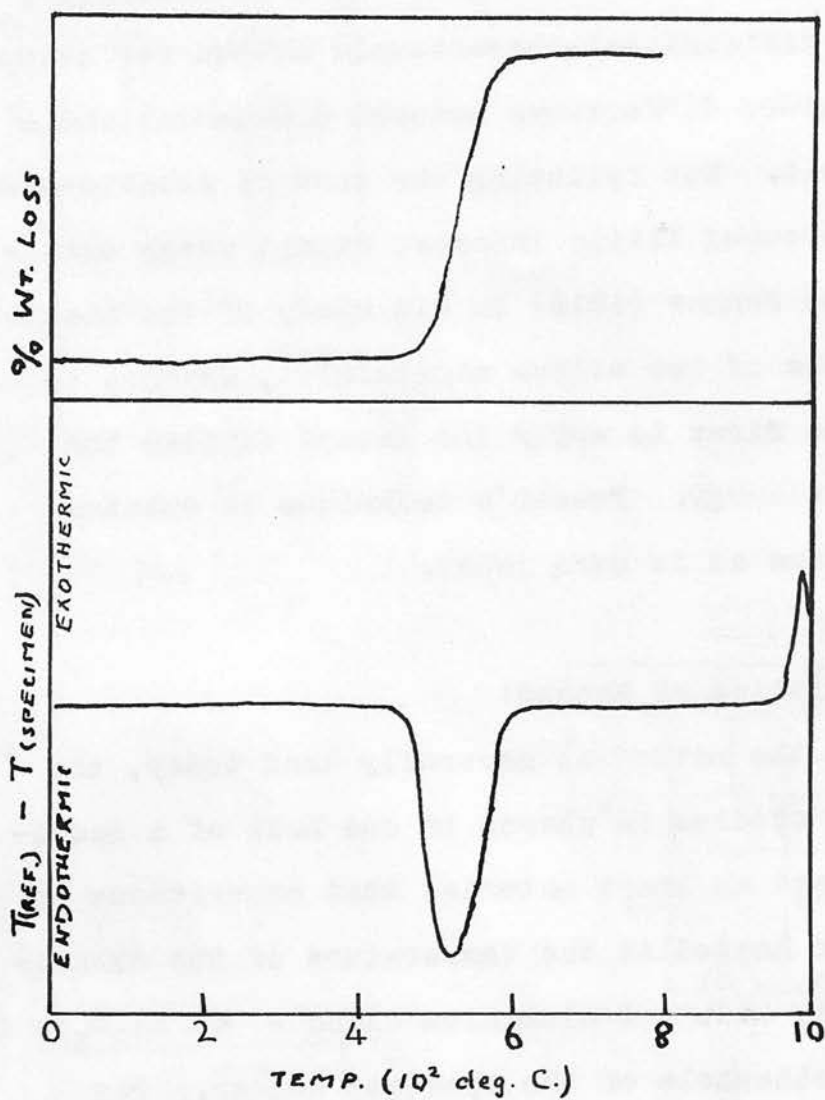


FIG. 3. IDEALIZED DEHYDRATION AND D. T. CURVES FOR KAOLINITE (SPEIL).

becomes greater or less than that of the inert material depending on whether the reaction is exothermic or endothermic, for an interval of time until the reaction is completed, and the temperature of the sample again comes to the temperature of the furnace. Consequently, for an interval of time the temperature of one junction of the difference-thermocouple is different from that of the other junction, and an e.m.f. is set up in the thermocouple circuit which is recorded as a function of time or of the furnace temperature. In the absence of thermal reactions, the differential e.m.f. is either zero or constant, and the record is a straight line parallel to the time (or temperature) axis. During a reaction, the direction of the differential e.m.f., of course, depends on whether the reaction is exothermic or endothermic. Figure 3 shows an idealized equilibrium dehydration curve and a differential thermal curve for kaolinite. The endothermic reaction between  $500^{\circ}\text{C}$  and  $700^{\circ}\text{C}$ . corresponds to the dehydration of the mineral. A comparison of the curves illustrates that the method of differential thermal analysis is a dynamic rather than a static one. The reactions in some cases are not instantaneous, and they are recorded as functions of time or as functions of furnace temperature, which is continuously increasing as the reaction takes place.

be called the "latent heat" type of reaction since they

### I. 3. Applications of Differential Thermal Analysis

Following the work of Fenner, the method has been used by various workers for the investigation of a wide variety of physico-chemical problems including phase equilibria<sup>(4, 5, 6, 7)</sup>, crystalline polymorphism<sup>(8, 9, 10, 11, 12)</sup>, solid phase reactions and chemical reaction velocity<sup>(13, 14, 15)</sup>, higher-order transformations<sup>(16, 17, 18)</sup>, analysis of organic systems and solid solutions<sup>(19, 20)</sup>, and, since 1935, due to the work of Orcel<sup>(21, 22)</sup>, Caillere<sup>(23)</sup>, and Grim<sup>(24)</sup>, the method has become an important and conventional approach to the study not only of clay minerals but also of carbonates, sulphates, hydrates, and ammonium compounds. The main interest of the present study is primarily in the last mentioned field, namely, the differential thermal analysis of reactions of simple systems.

### I. 4. Two types of problems:

Two types of reactions are important in this respect<sup>(26)</sup>:

(a) phase inversions, characterised by reversibility and a fixed transition temperature,  $T_i$ , irrespective of the rate of heating. Melting and solidification, the  $\alpha \rightleftharpoons \beta$  or I  $\rightleftharpoons$  II inversion of quartz, and other crystalline inversions, fall into this class, which may be called the "latent heat" type of reaction since they

involve the evolution or absorption of a definite amount of heat per unit mass at the temperature of the reaction. They are often called 'Stefan reactions' since Stefan<sup>(25)</sup> was the first to make a systematic mathematical study of the temperature relationships involved in such reactions; reaction and the effect of the energy of activation

(b) unimolecular first-order type of reactions, such as occur during dehydration, loss of sulphur dioxide, ammonia, carbon dioxide, etc., and oxidation, which are governed by the rate of diffusion of gaseous products or reactants out of or into the material. In these reactions the rate of reaction and hence the heat absorbed or evolved depend on the temperature according to the equations:

$$dw/dt = k \exp.(-E/RT), \text{ and}$$

$$dT/dt = -q dw/dt \text{ in the}$$

adiabatic case, where

$E$  is the energy of activation,

$R$  is the gas constant,

$k$  is a constant for any given system,

$T$  is the absolute temperature

$w$  is the fraction of substance reacted in time  $t$ .

Until recently only half-hearted attempts

have been made by d.t.a.\* workers to distinguish between these two types of reactions.

\* d.t.a. = Differential Thermal Analysis



So long as the method was used mainly in the empirical identification of clays and the qualitative classification of clay constituents, this distinction was not important. But the quantitative interpretation of d.t.a. records requires a more exact knowledge of the nature of each reaction and the effect of the energy of activation or the latent heat of the reaction, and the mathematical approach to the two problems are quite different.

Most of the reactions of the second type occur at low temperatures (less than 500°C.) and are mainly endothermic, whereas most of the Stefan reactions in clays and clay minerals are exothermic and take place at higher temperatures (700 to 1,000°C.). The low-temperature endothermic peaks and the high-temperature exothermic peaks in d.t.a. records occur at temperatures and temperature ranges characteristic of the mineral constituents of each specimen. The method of differential thermal analysis has therefore been perfected and refined to the stage where it has now become a ready tool for the accurate qualitative analysis of clay materials, and a very useful ancillary technique in other investigations involving physical and/or chemical changes. But only rudimentary work has been done on the extraction from d.t.a. records of quantitative information as to the amount of reactive material present or its thermal constants, owing to the difficulty of finding the exact relationships between the temperature, height, width, and

shape of the peak on the one hand, and the quantity of material present, its latent heat or energy of activation, and the rate of heating on the other. The solution of this problem is of rather great~~er~~ mathematical difficulty, and although a number of attempts have been made to obtain solutions using approximation and numerical methods, no general analytical solutions seem to have been made.

In the present study, it is intended to concentrate on Stefan Problems exclusively, and to attempt a partial solution making use of experimental data relating to (a) the temperature distribution in a finite medium of given shape before, during, and after a thermal reaction, and (b) the rate of propagation of such a reaction through the medium. For this type of problem a number of analytical solutions have appeared<sup>(27,- 36)</sup>, but so far only the solution for semi-infinite media has been carried to a stage suitable for numerical calculation. The essential feature of the problem is the existence of a moving boundary at which heat is generated or removed, and one obstacle to complete solution is that the history of this interface as it moves is unknown. To determine the history (a space-time curve) of the interface, it is necessary to solve the heat equation, which is a linear homogenous parabolic equation, with the appropriate boundary conditions and with a suitable discontinuity in the first-order space

derivatives across the unknown interface<sup>(37)</sup>. Such a solution, in most cases, is either very difficult or impossible. In this study a spherical vessel was chosen, both for the sake of mathematical simplicity and for experimental convenience. The test material was placed in a spherical steel chamber of 6 cm. diameter, and thermocouple junctions were placed at intervals of 0.6 cm. along one radius. The temperature of the chamber was then raised at a uniform rate until the reaction was complete. The temperature at each junction was recorded either photographically at intervals of 30 seconds or by means of a six-point electronic recorder having a 30-second cycle. To improve the resolution of the record, instead of measuring the actual temperatures at each junction, which could be as high as 400 to 500°C., a differential arrangement was adopted, whereby only the differences between these temperatures and the steadily increasing surface temperature were measured. This is simply an extension of the principle used in actual differential thermal analysis. The records obtained by measurement of actual values of temperatures are, in fact, the heating curves for six points within the material, whereas, the second type of records are the differential thermal records for each point.

From these records the following data could be obtained:-

(a) the Chapter II distribution in a uniformly  
DESCRIPTION OF APPARATUS material before,

In this study a spherical model was chosen, both for the sake of mathematical simplicity and for experimental convenience. The test material was placed in a spherical steel chamber of 6 cm. diameter, and thermocouple junctions were placed at intervals of 0.6 cm. along one radius. The temperature of the chamber was then raised at a uniform rate until the reaction was complete. The temperature at each junction was recorded either photographically at intervals of 30 seconds or by means of a six-point electronic recorder having a 36-second cycle. To improve the resolution of the record, instead of measuring the actual temperatures at each junction, which could be as high as 400 to 500°C., a differential arrangement was adopted, whereby only the differences between these temperatures and the steadily increasing surface temperature were measured. This is simply an extension of the principle used in actual differential thermal analysis. The records obtained by measurement of actual values of temperatures are, in fact, the heating curves for six points within the material, whereas, the second type of records are the differential thermal records for each point.

From these records the following data could be obtained:-

one face of the cylinder was lat a hemispherical recess measuring accurately 6 cm. in diameter. A flange, 5.5 cm. in diameter, was

- (a) the temperature distribution in a uniformly heated sphere of reacting material before, during, and after the reaction;
- (b) the temperature at any point in the sphere at the moment when the moving interface between two phases passes that point, i.e. the transition temperature;
- (c) the temperature difference between the furnace and any point in the sphere after the reaction had commenced, and the dependence of this on
  - (i) the density of the reacting material;
  - (ii) the thermal constants, especially the heat of transition,  $H_{tr}$ , of the material,
  - (iii) the rate of increase of surface temperature;
- (d) the rate of propagation of the reaction through the sphere, i.e. the history of the moving interface. This will be described in more detail in Chapter IV.

## II. 1. The Calorimeter or Specimen Holder.

This consisted of two cylindrical halves, of outside diameter 6.7 cm., each half having been machined out of a mild steel block 4" x 4" x 2". Into one of the plane faces of the cylinder was let a hemispherical recess measuring accurately 6 cm. in diameter. A flange, 8.5 cm. in diameter, and

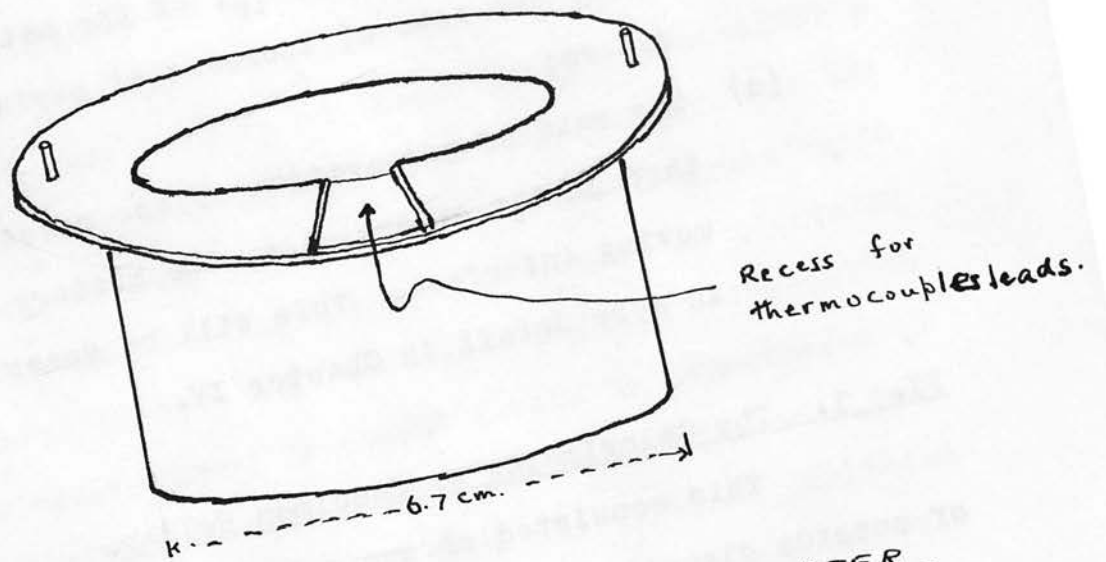
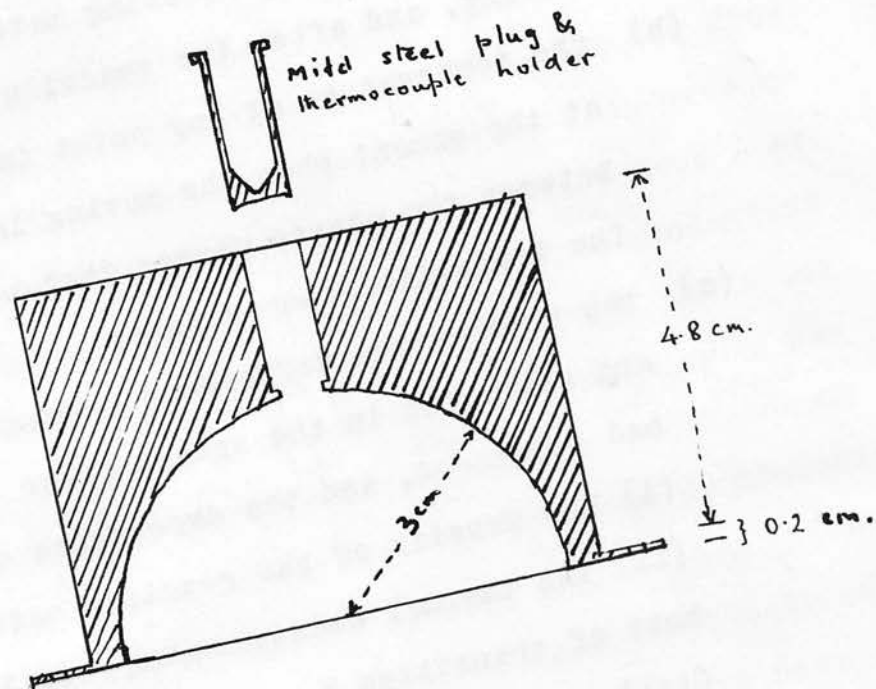


FIG. 4. THE CALORIMETER

and 0.2 cm. thick, was left round the outside of the open end. The two halves when put together constituted a cylinder of diameter 6.7 cm. and height 10 cm., enclosing in its centre a spherical chamber of diameter 6.0 cm. Round the middle of the assembled cylinder was a flange, 0.9 cm. wide and 0.4 cm. thick, by means of which the two halves could be clamped together. Riveted to the face of the flange on one block were two pins which let into corresponding holes on the other block, and by means of these the two halves were accurately fitted whenever the calorimeter was assembled. The face of the flange on the lower half also carried a recess 1 inch wide and  $1/32$  inch deep, so that when the two blocks were fitted together, a gap was left, 1 inch long, serving as outlet for thermocouple wires and their insulation. The upper block also carried, at its pole, a hole used for filling the chamber. The hole was  $27/64$  inch in diameter over all but the last  $1/16$  inch of its length where it emerged into the chamber. After the chamber had been filled and the apparatus assembled, this hole was plugged with a small hollow steel cylinder, closed at one end, of outside and inside diameters  $25/64$  and  $21/64$  inch respectively. Into this cylinder was introduced the thermocouple which regulated the furnace temperature, the junction of the thermocouple being then about  $1/8$  inch from the inside surface of the specimen holder. (Fig.4)

## II. 2. The Furnace

Three types of furnace were used:-

(a) Type I: This was a mains voltage furnace of nichrome wire wound directly on the calorimeter and insulated from it by means of micanite, mica, alumina cement, or syndanio strips. The resistance of each half was approximately 100 ohms at room temperature, making a 50-ohm furnace when the two were connected in parallel. The furnace was controlled manually by means of a variac transformer and operated between 100 and 180 volts, attaining a temperature of  $700^{\circ}\text{C}$ . in about 65 minutes at its fastest rate. This furnace did not give satisfactory performance over any considerable period, owing to frequent <sup>destruction of the winding or breakdown of</sup> electrical insulation. The latter trouble was the more serious, and, of the four insulators mentioned above, micanite gave the best results provided the resin bonding was slowly and carefully baked out before the furnace was put into use. Even then, leakage from the mains to the thermocouples and thence to the measuring instruments was never completely eliminated, especially at temperatures above  $300^{\circ}\text{C}$ , owing probably to the presence of incompletely incinerated carbon in the insulation or the poor quality of the mica.

(b) Type II: This was similar in construction to Type I but the winding was of thick vacrom strip, the resistance of each half at room temperature being only



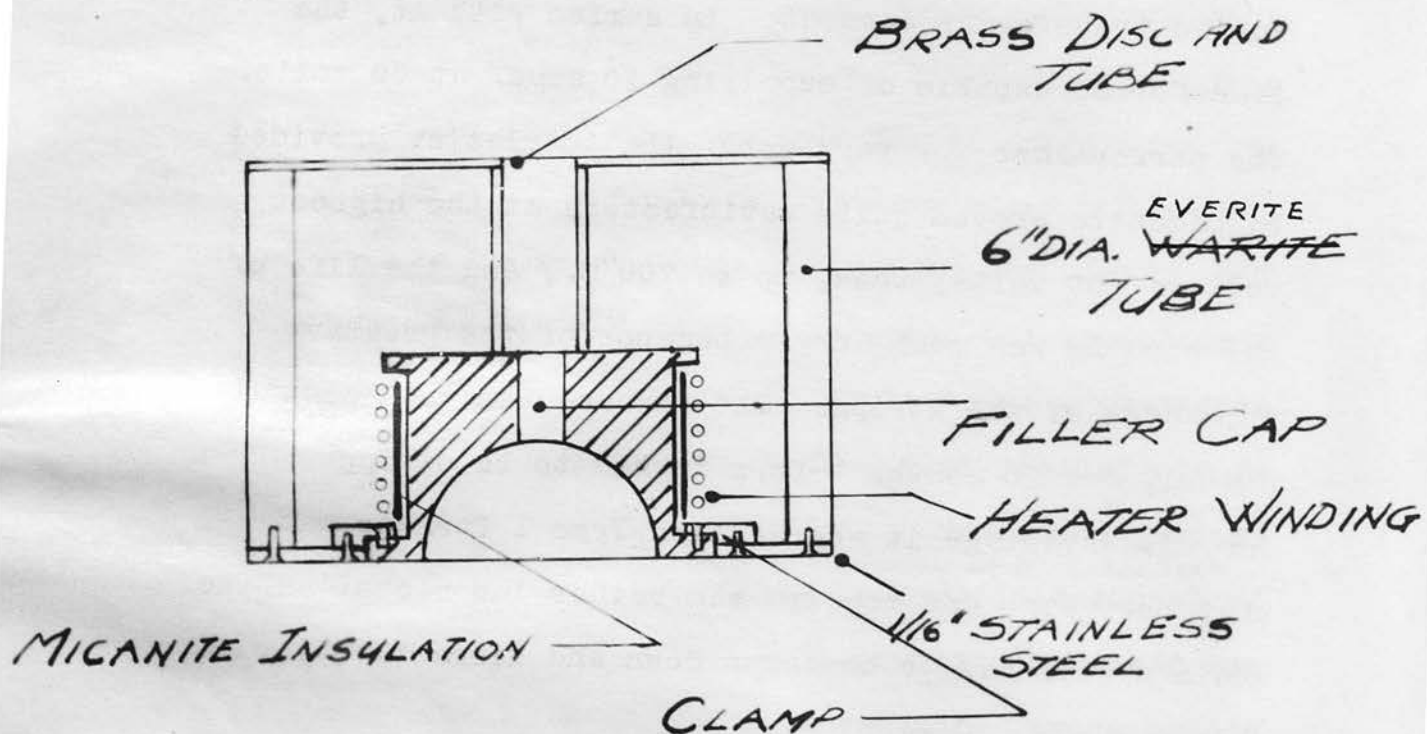
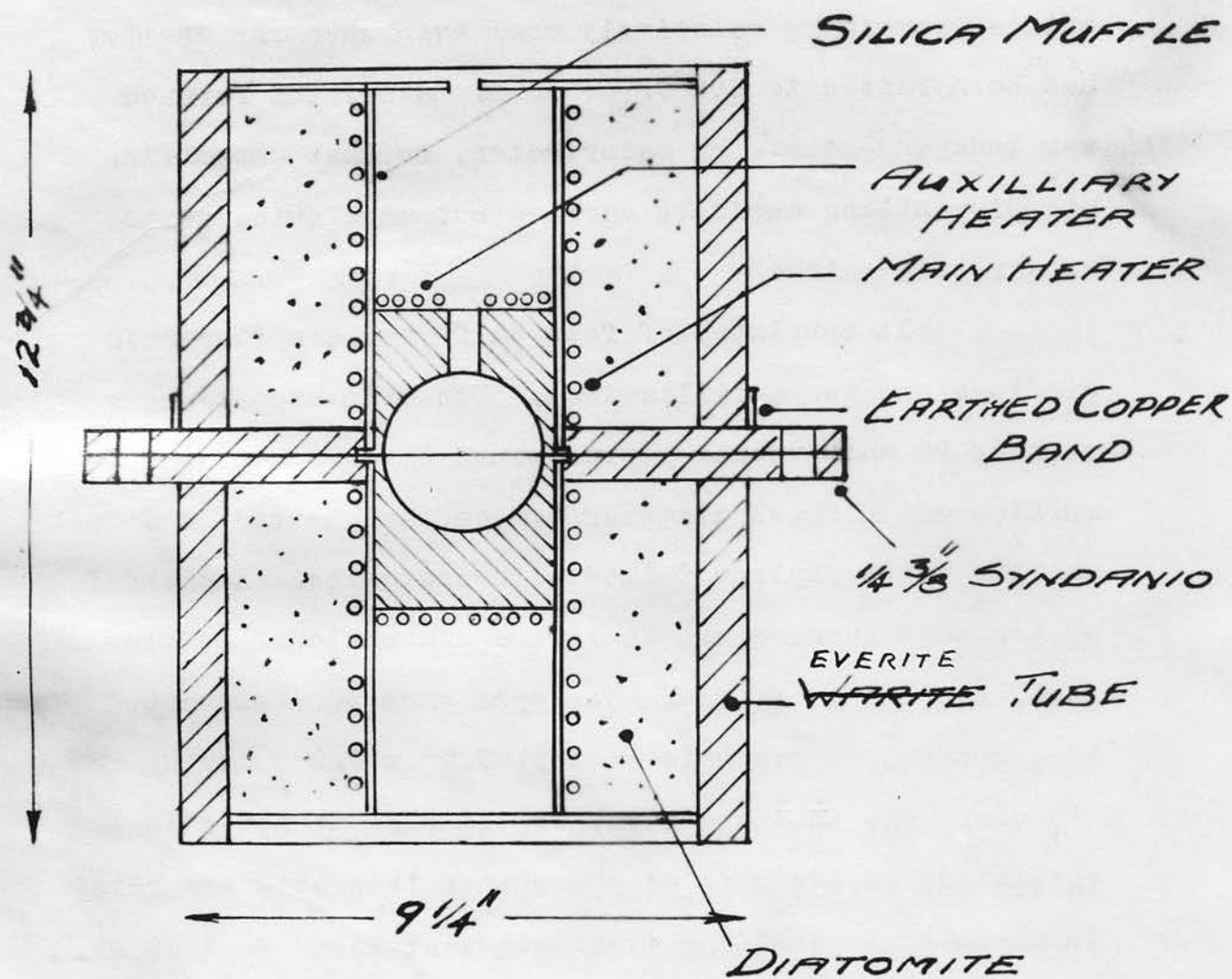


FIG. 5 UPPER HALF OF  
FURNACE TYPES I & II

12 ohms, giving a double furnace of 6 ohms when assembled. The insulation was of micanite. It was a low-voltage high-current furnace controlled by a 230/60-volt transformer fed through a 0 - 270-volt variac transformer connected in series with it, the ~~transformer~~ transformer capable of supplying 10 amps. at 60 volts. The performance was very good: the insulation provided by micanite proved quite satisfactory at the highest voltage (60 volts) used, up to 700°C., and the life of the winding was much longer because of the greater thickness of the strips. The furnace was used continuously for 15 months before it had to be stripped down. One disadvantage it shared with <sup>the</sup> Type I furnace was that servicing and repairs was rather laborious, as the whole system had to be taken down and dismantled for this purpose. (Fig.5)

For these two types of furnace, thermal insulation was provided by fixing the two separate blocks to circular face plates of 1/16-inch stainless steel which were then screwed on to drums of 6-inch <sup>everite</sup> ~~wacrite~~ water piping. The drums were then filled with diatomite. But, for either type, accurate control of heating rate was difficult owing partly to inadequate lagging and partly <sup>to</sup> inefficient electrical insulation.



**FIG. 6 SECTION OF FURNACE TYPE III**  
SCALE: 1/3" = 1"

(c) Type III. This proved the most suitable and differed radically from the first two types. Being a larger furnace the loss of heat was negligible, the outside remaining relatively cool even when the chamber had been raised to 600°C. or more. Also, the furnace was independent of the calorimeter, so that assembling and dismantling could be carried out more quickly and at any temperature.

It consisted of four half-heaters (two main windings and two <sup>auxiliaries</sup> auxiliaries). The main heaters were each of 98 ohms vacrom strips wound on to fused silica muffles of internal diameter 6.8 cm. and housed in 9-inch waerite water pipings filled with diatomite. Each half of the main furnace was therefore <sup>a</sup>conventional muffle furnace open at one end. The open ends were supported by quarter-inch syndanio plates, 9.2" x 9.2", having a circular hole in the centre, of the same diameter as the inside of the muffle; the rim of this hole was rebated to accommodate the flange on the calorimeter so that when this was dropped into position, the face of the calorimeter was flush ~~d~~ with the face of the furnace, <sup>and</sup> ~~the~~ there was no gap between the two halves of the assembled apparatus. (Fig. 6)

The main windings alone were capable of raising the temperature of the calorimeter quite rapidly to 750°C. in about 50 minutes, and at such a rapid rate of heating

the control was accurate to within 2%, i.e. giving a heating rate of  $(0.250 \pm 0.005)^{\circ}\text{C.}$  per second. For slower heating rates such as were actually employed in the present work, the control, however, was rather poor, owing to the thickness and low thermal conductivity of the muffle. (N.B. The control was maintained at a point as near as to the surface of the specimen as possible, i.e. relatively remote from the heater windings.) Hence, for more exact control at low heating rates, an <sup>auxiliary</sup> ~~auxilliary~~ heater was placed in contact with the plane closed end of each half of the calorimeter. Each such heater was wound on an annular disc of mica, outside and inside diameters 6 cms. and 1.5 cms. respectively (Fig.7). The heater was then insulated with two further discs (one on either side) of good quality mica (muscovite) and the whole was clamped between two 1/16-inch steel plates. Each heater had a resistance of 50 ohms, and were connected in parallel. They were fed independently through a 230/60 volts transformer connected in series with one pair of secondary terminals of a 0 - 270 volts double variac, and operated between 45 and 25 volts. The main heaters, on the other hand, were controlled directly by the variac and operated between 50 and 150 volts.

With both sets of heaters in use, and employing manual control only, a heating rate of

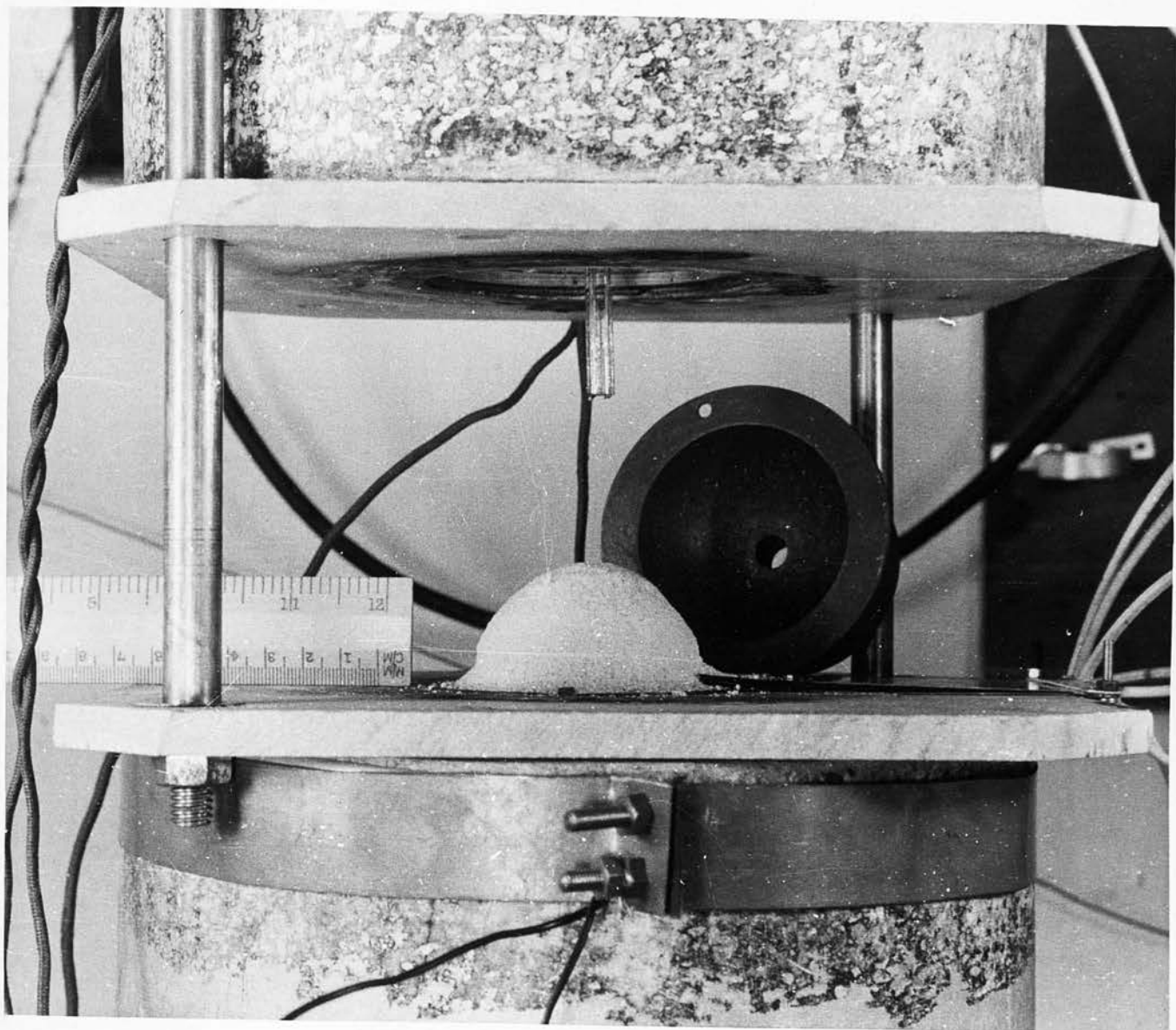


Plate I. Photograph of Furnace Assembly.

$(0.021 \pm .001)^{\circ}\text{C}$ . per second could be maintained for a wide range of temperatures, i.e. accurately to about 5%, as against  $(0.031 \pm .004)^{\circ}\text{C}$ . per second, or accurately to about 13%, without the double control.

### II. 3. Temperature Regulation:

The actual temperature of the calorimeter at a point as close as possible (about  $\frac{1}{8}$  inch) to its internal surface was used to indicate the direction and magnitude of mains regulation required to keep the furnace on a predetermined heating course. The e.m.f. of the control thermocouple was made to oppose a constantly increasing potential difference across a motor-driven helical potentiometer, and the heating of the furnace was adjusted so that a sensitive galvanometer in the thermocouple circuit always read zero. The circuit was so arranged that a positive deflection of the galvanometer always indicated overheating, and the sensitivity of the galvanometer (a Tinsley Type 3270) was such that a potential difference of 1 microvolt across its terminals produced a deflection of 0.27 mm., which, for a chromel-alumel thermocouple, corresponds to a deflection of about 100 mm. per degree C. departure from the heating programme.

The regulating potentiometer consisted of 100 turns vacrom wire of resistance 26 ohms, driven at

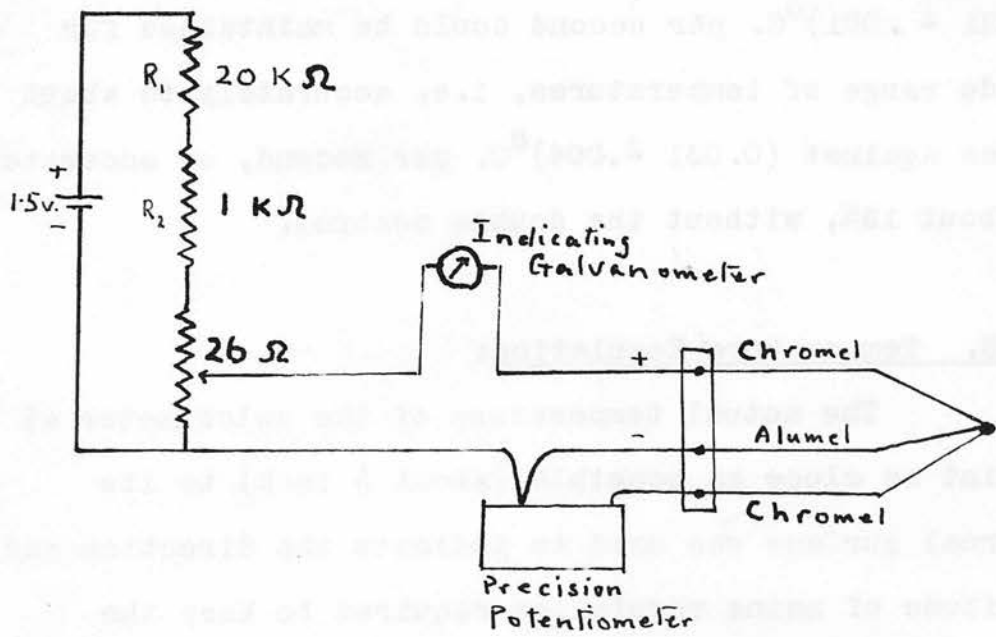


FIG. 8

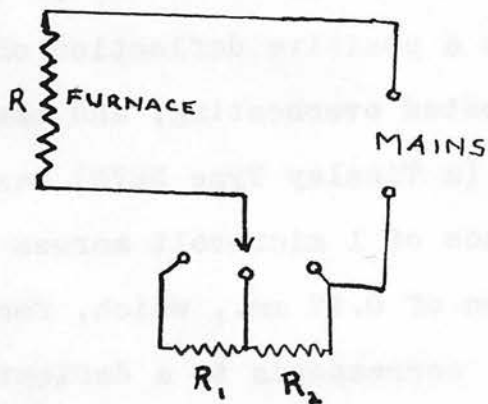


FIG. 9.

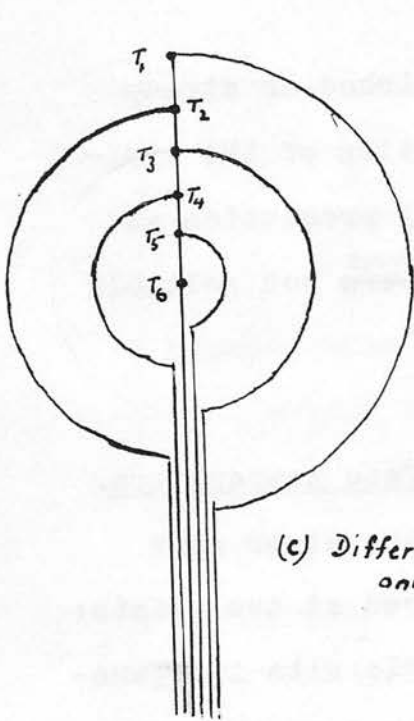


the rate of one turn per minute, and the p.d. per turn was adjusted by means of two rheostats  $R_1$  and  $R_2$  (Fig.8) to correspond to the desired rate of increase of temperature in degrees C. per minute.

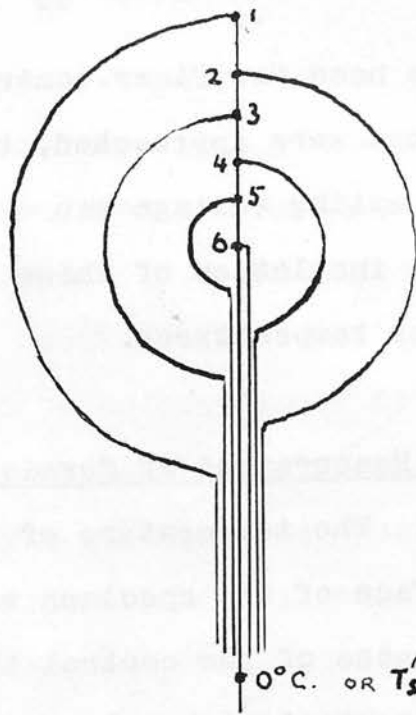
The furnaces Types I and II were roughly controlled by alteration of the variac output voltage, but further fine adjustment was obtained by means of two resistances  $R_1$  and  $R_2$  placed in series with the furnace windings and connected to a three-position switch as shown (Fig.9).  $R_2$  was normally left in series with the heater R, so that with  $R_2$  out the current was increased a predetermined amount above normal, and with both  $R_1$  and  $R_2$  the current was reduced the same amount below normal.  $R_1$  and  $R_2$  were so chosen that in the initial stages of heating when hunting was likely to be most serious these changes were up to 10%, and later, when steady conditions had been attained, only 5%.

For <sup>the</sup> Type III furnace, rough adjustment was made by altering the input to the main heater only, and fine control by switching on or off the <sup>auxiliary</sup> ~~auxilliary~~ heaters. In the initial stages of heating, the power dissipated by the <sup>auxiliary</sup> ~~auxilliary~~ heaters <sup>was</sup> ~~were~~ made as high as possible, up to 100 watts, but as the furnace settled down to steady heating the voltage on the main heater was gradually increased and that on the auxilliary heaters reduced until the latter dissipated only 25 watts. Apart from the fact

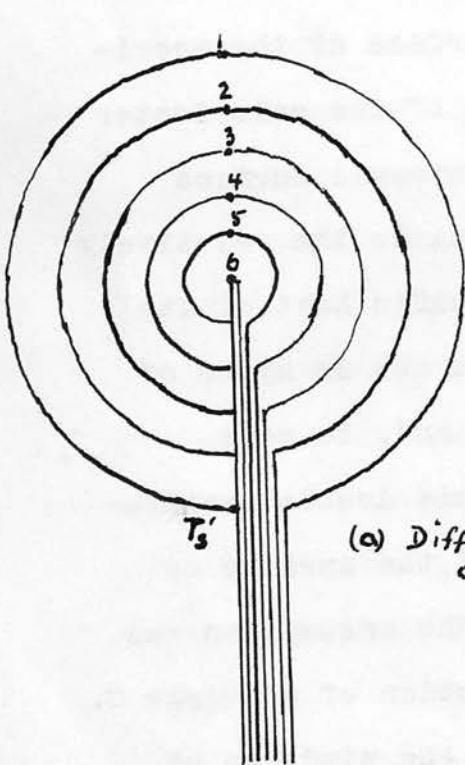
in contact with the furnace wall were thinnest, as



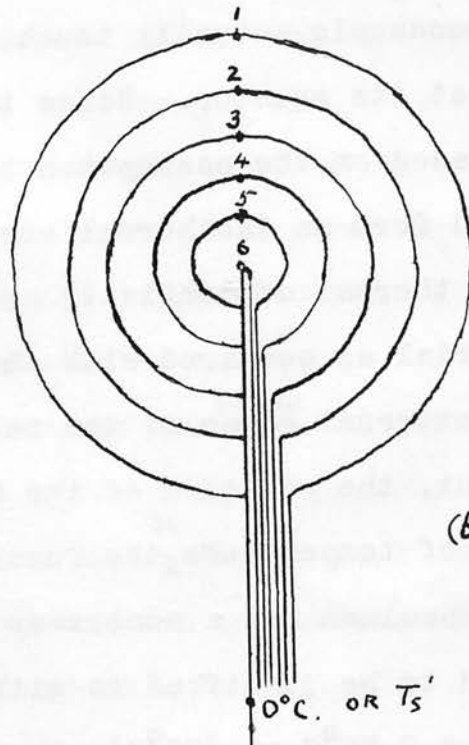
(c) Differential only



(d)



(a) Differential only



(b)

Fig. 10. Thermocouple Patterns

otherwise the temperature at the poles tended to lag behind the equatorial temperature.

II. 5. Thermocouple arrangement for measurement of internal temperatures.

Two methods were employed to determine the temperature distribution in the sphere, viz., (a) a direct measurement of the temperature at six (later five) equally spaced points along a radius, and (b) measurement of the difference in temperature between the surface (or furnace) and six (or five) equally spaced points along a radius. In both methods there were two alternative arrangements of the thermocouples within the sphere but both arrangements were designed to conform as closely as possible to the requirements (i) that the paths of the wires within the sphere should be as great as possible, (ii) that the wires were as thin as possible, and (iii) that, wherever possible, the paths of the wires should lie on an isothermal surface. In this way heat conduction along the wires into or out of the system was minimised and a low heat capacity in the thermocouple system was maintained. The arrangements employed are shown in Fig.10. It will be seen that the arrangements (a) and (b) conform more nearly to these requirements, but <sup>in</sup> a series of test runs, no appreciable difference was noticed in the records obtained by using either set of arrangements.

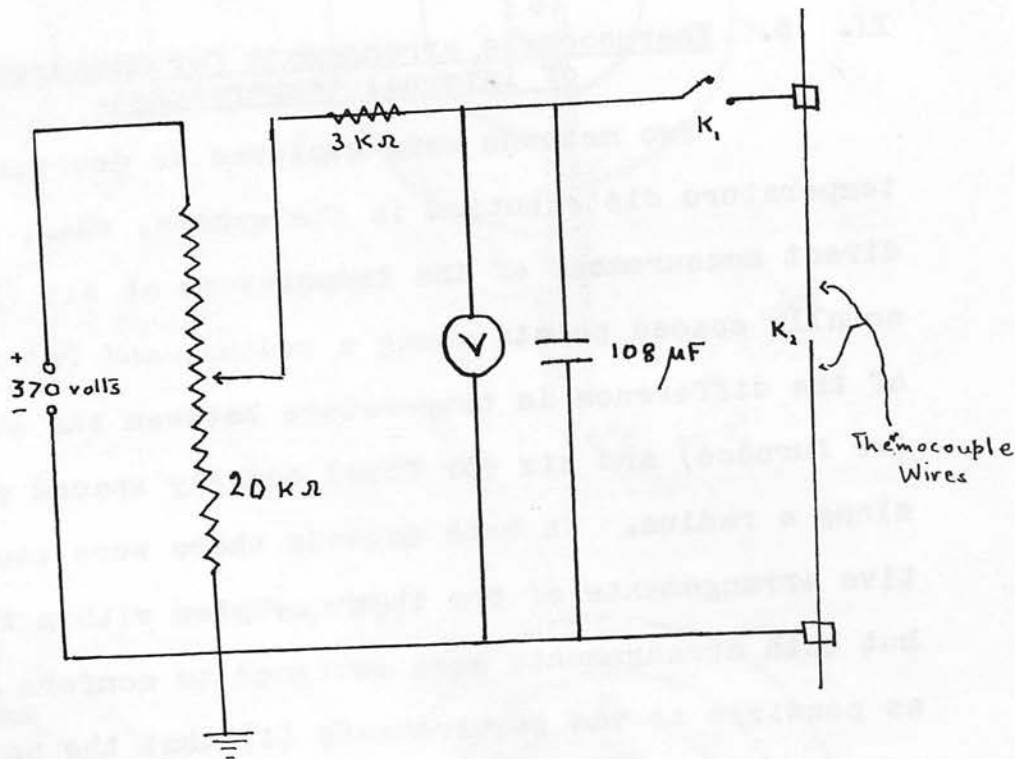


FIG. 11.      SPARK-WELDING OF  
THERMOCOUPLE WIRES.

agent. The junctions  $T_1, T_2 \dots T_6$  and  $T_1'$  were at distances  $r = a, 0.8a, 0.6a, 0.4a, 0.2a,$  and  $0,$  from the centre of the sphere, where  $a$  is the radius of the sphere. For the direct measurement of temperatures, (Fig.10),(b) and (d), a cold junction was provided outside the system by melting ice, but this arrangement was also used for differential measurements by placing this outside junction by the side of the regulating thermocouple with the advantage that the "reference junction" could not be affected by the reaction of the specimen. In both arrangements all the wires were connected to terminals in a closed junction box constructed of tufnol and lined internally with sheet aluminium for temperature equalisation. The terminals in the junction box were of brass and connections from them to the measuring or recording instruments were of enamelled copper wire.

experiment All temperature junctions were spark-welded, using the arrangement shown in Fig.11. Spark-welding gives junctions of very small dimensions, (and hence of low heat capacity), and also minimises oxidation of the wires and so increases the consistency in performance of various batches of finished junctions. This is essential as each set of thermocouples could be used for one specimen only. Oxidation was further prevented by closing the gap  $K_2$  between the flat end of a carbon rod and a clean glass plate, the carbon acting as a reducing

agent. The thinnest wire found suitable was 33 SWG, as the wires became brittle after being heated only once in the furnace up to 600°C. in the presence of glass (which was used extensively as an inert base in the earlier experiments). For this gauge, the optimum voltage to which the 108  $\mu$ F condenser must be charged was 220 to 270 volts, depending on the resistance of the discharge circuit, i.e. the length of chromel and alumel wire included in the circuit: these together may not exceed 4 to 5 inches.

The system, after welding, was formed into the required shapes or patterns of Fig.10 on a brass template machined for the purpose, the pattern being retained by fine threads stuck on with thin adhesive before transferring it to the specimen. The thread and the adhesive were burnt out at the temperature of the experiments.

## II. 6. Photographic recorder and ancillary equipment.

These consisted of a drum camera, a mirror galvanometer, a constant-damping variable shunt, and a double-pole rotary switch.

(a) The drum camera was a home-made unit of conventional design, consisting of a light-tight tufnol box with a 1 mm. horizontal slit, 9 inches long, along one side. The lens of the galvanometer lamp was coated

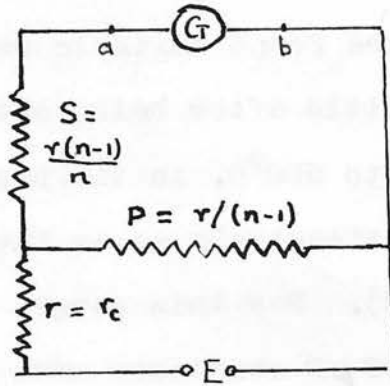


FIG. 12

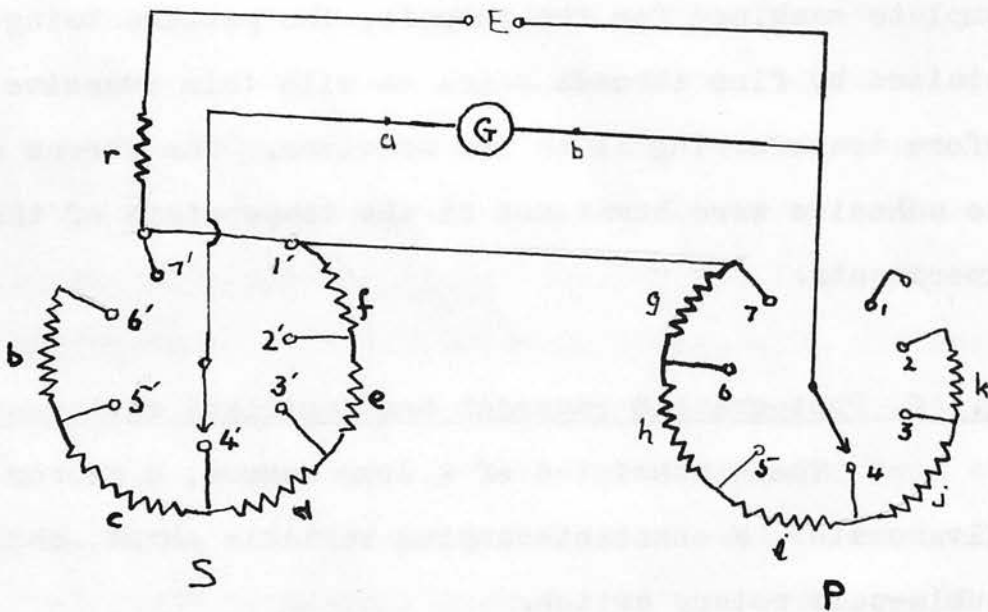


FIG. 13

$r = j = k = 9 \text{ K}\Omega$   
 $b = e = 750 \Omega$   
 $c = d = h = 1.5 \text{ K}\Omega$   
 $f = 2.25 \text{ K}\Omega$   
 $g = 3.0 \text{ K}\Omega$   
 $i = 4.5 \text{ K}\Omega$

RANGES

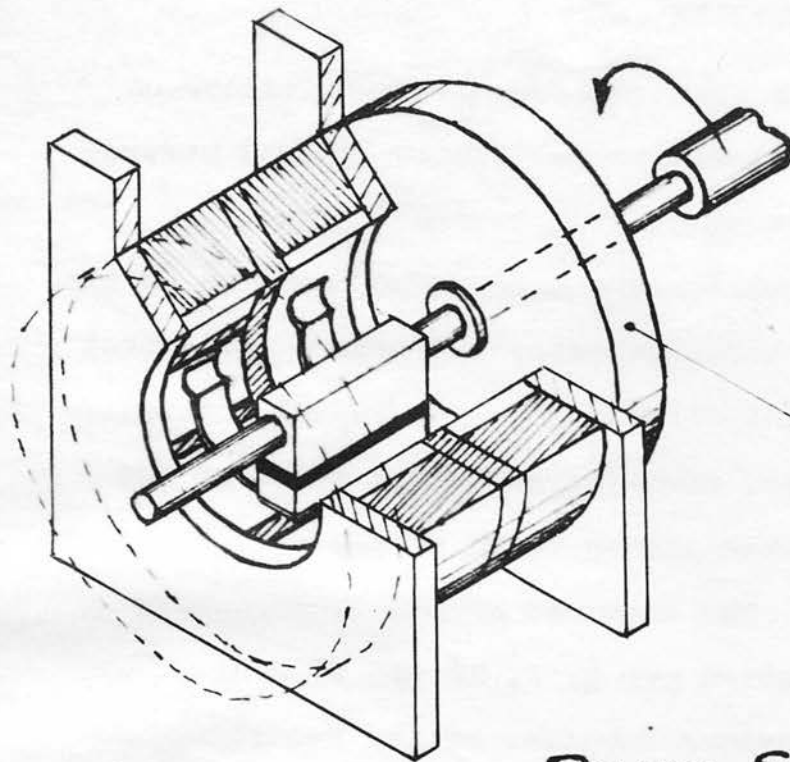
1-1'	$n = 1$
2-2'	$n = 4/3$
3-3'	$n = 3/2$
4-4'	$n = 2$
5-5'	$n = 3$
6-6'	$n = 4$
7-7'	$n = 0$

with black wax, and a 1mm. vertical slit was etched on to this, so that its image on the camera box was perpendicular to the camera slit, this giving on the drum behind the slit a 1 mm. square spot. The drum was  $8\frac{3}{4}$  ins. long and 48 cms. in circumference, and was fixed so that its front part was not more than  $\frac{1}{8}$  inch behind the slit, in order that the spot <sup>focused</sup> focussed on to the front of the camera was also practically in focus at the surface of the photographic paper. The drum was driven by clockwork at speeds of one revolution per  $\frac{1}{2}$ , 1,  $1\frac{1}{2}$  and  $2\frac{1}{2}$  hours, depending on the expected duration of the recording and the resolution desired.

(b) The galvanometer was a 450-ohm Cambridge Moving Coil Mirror Galvanometer with a periodic time of 2.5 seconds on open circuit, and <sup>an effective deflection time of</sup>  $\sqrt{3.5}$  seconds when critically damped. The resistance for critical damping was 9,000 ohms, and the maximum sensitivity when critically damped was 7.0 microvolt per 1 mm. deflection at a distance of 75 cm.

(c) Damping and Shunting: In order to vary the sensitivity in accordance with requirement and maintain critical damping, a specially constructed shunt was placed in the same housing as the rotary switch, based on the principle of (Fig.12) in which  $R_c$  is the resistance for critical damping. With this arrangement,  $V_{ab} = E/n$  and  $R_{ab} = R_c$ ,  $n$  being the multiplying factor for the





TUFNOL END PIECE

FIG. 14

PART-SECTIONED VIEW  
OF ROTARY SWITCH

SHADED AREAS SHOWN  
INDICATE INSULATING  
MATERIALS. SWITCH  
SEGMENTS HAVE RADIAL  
LEADS. (NOT SHOWN)

SCALE: FULL SIZE

galvanometer and shunt. The construction of the shunt and the ranges available by means of it are shown in Fig.13.

(d) Rotary Switch: This was specially designed and constructed for the purpose. It is a completely enclosed unit and the details of construction are shown in Fig. 14. Since all the contacts are completely enclosed, errors from outside sources of radiation are eliminated. The double-pole wiping arrangement eliminates errors due to wiping friction. Since the driving motor was on continuously and was therefore likely to generate a great deal of heat, the motor was mounted in the open, 12 inches away from the switch and coupled to it by the long driving shaft of the switch. Also, any heat conducted to the contacts by this shaft would be evenly distributed to all metallic surfaces within the switch, as the shaft is placed centrally within the cylindrical chamber. Although the input terminals to the switch are on the outside of the case, this was not considered a serious drawback, as the whole switch was enclosed in a thermally insulated box with three walls, the outside layer being of  $\frac{1}{4}$ -inch tufnol followed by  $\frac{1}{4}$ -inch asbestos board and then <sup>sheet</sup> ~~shut~~ aluminium to assist in temperature equalisation. The box was divided internally into two chambers by insulating material, one to house the switch proper, and the other to house the

galvanometer shunt described in (c) above, so that all connections between shunt and switch were also enclosed. In order to reduce contact resistance to the minimum, all the metallic parts of the switch were silver-plated, and the deposit was renewed periodically as it wore off between the wiping surfaces. All connections, external and internal, between the thermocouple circuit and the switch and shunt were of copper, and the transition from copper to thermocouple material was enclosed in a metal-lined junction box.

The switch was run at 2 r.p.m., so that each of the six points of the thermocouple system was in the circuit for approximately 5 seconds, and, allowing 3.5 seconds for the galvanometer deflection, the spot, therefore, remained stationary for 1.5 seconds. This 'exposure time' proved quite ample for the commercial bromide paper used.

The system worked very efficiently, and repeated blank tests run with thermocouple junctions maintained at temperatures from 30°C. to 400°C. showed it to be remarkably free from spurious e.m.f.'s originating in the recording system itself. The only drawback of the arrangement was the time consumed in photographic work.

## II. 7. Electronic Recording:

For the latter part of the work a six-point Cambridge Electronic Recorder became available. The input potential difference for full scale deflection is 1 mV, but the range was increased and made variable by placing a 20 K-ohms wire-wound potentiometer across the output from the recorder's amplifier.

at distances  $r = 0.3, 0.9, 1.5, 2.1$  and  $2.7$  cms. from the centre, the thermocouples being arranged either to give actual temperatures at these points or to indicate the difference in temperature between each point and the surface. In the latter case an additional thermocouple was placed at the surface to measure its temperature directly. The preparation of the specimen for these measurements depends on the nature of the reaction being investigated, i.e. either a crystalline inversion or a melting/solidification reaction.

## III. 2. Crystalline inversion, including recrystallization from amorphous form, in the solid state

Since this takes place in the solid state, the material was simply reduced to powder, placed in the calorimeter with the thermocouples, and the whole mass transferred to the furnace. This kind of reaction, therefore, is the simplest to examine experimentally, provided that it is a genuine 'latent heat' type and not a rate-controlled type, i.e. one that takes place over a

## Chapter III

### EXPERIMENTAL TECHNIQUE

#### III. 1. Preparation of Specimen:

The specimen was in the form of a sphere of radius 3 cm., with either six thermocouple junctions placed at distances  $r = 0, 0.6, 1.2, 1.8, \text{and } 2.4 \text{ cm. and } 3.0 \text{ cm.}$  from the centre, or five junctions placed at distances  $r = 0.3, 0.9, 1.5, 2.1 \text{ and } 2.7 \text{ cms.}$  from the centre, the thermocouples being arranged either to give actual temperatures at these points or to indicate the difference in temperature between each point and the surface. In the latter case an additional thermocouple was placed at the surface to measure its temperature directly. The preparation of the specimen for these measurements depends on the nature of the reaction being investigated, i.e. either a crystalline inversion or a melting/solidification reaction.

#### III. 2. Crystalline inversion, including recrystallisation from amorphous form, in the solid state

Since this takes place in the solid state, the material was simply reduced to powder, placed in the calorimeter with the thermocouples, and the whole mass transferred to the furnace. This kind of reaction, therefore, is the simplest to examine experimentally, provided that it is a genuine 'latent heat' type and not a rate-controlled type, i.e. one that takes place over a

TABLE I - TRANSITION POINTS

Substance	First Transi- tion Temp. °C	Second Transition Temp. °C	Separation
Potassium Nitrate	129	339 (Fusion)	210
Sodium Sulphate	240	890 ( " )	650
Potassium Hydroxide	248	400 ( " )	152
Lithium Sulphate	575	859 ( " )	284
Potassium Sulphate	587	1074 ( " )	487

a range of temperatures with the rate of transformation depending on the temperature. It has the further advantage that both the state of aggregation and the density of packing can be varied at will if it ~~was~~<sup>is</sup> desired to study the effect of these on the rate of propagation of the reaction through the sphere. But, unless the size of the sphere is small, there are not many phase inversions that can be studied in this way, owing to overlapping of reactions. For the size of sphere used, and depending on the heat of reaction per unit volume, and on whether the reaction was endothermic or exothermic, the duration of the reaction, (i.e. from commencement at the surface to completion at the centre), was of the order of 20 to 30 minutes in most cases. An additional 30 to 40 minutes was also always required for the system to resume steady conditions, depending on the diffusivity of the reacted substance. This additional period is of the same order as the time required for the sphere to reach steady state when heated at a uniform rate from room temperature, as is to be expected. Hence, suppose the rate of rise of temperature at the surface is  $k^{\circ}\text{C. per second}$  and the temperature of inversion is  $\theta_i^{\circ}\text{C.}$ , then temperature at the surface when reaction is complete at the centre is:

$$\theta_s^{\circ}\text{C} = \theta_i + kt \dots\dots\dots (1)$$

where  $t$  seconds is the duration of the reaction.

Now, if the material undergoes another reaction at a temperature  $\theta_m$ , less than  $\theta_s$ , then there will be an overlapping of the 'peaks' due to the two reactions, and it is impossible to analyse the contribution of each reaction to the composite peak produced on the records. Most crystals either exhibit more than one inversion, or in some cases, inversion takes place a few degrees below the melting point.

Another limitation to the choice of material is that the interpretation of the data is unduly complicated unless the temperature gradient in the material becomes steady before the reaction commences. Hence the need for a uniform heating rate. Now, for the sphere of radius  $a$  initially at temperature  $\theta_0$  and surface temperature subsequently ~~maintained at  $\theta_0 + kt$~~  <sup>increasing as  $\theta_0 + kt$</sup> , the temperature at  $r$  at time  $t$  is given by

$$\theta(r,t) = \theta_0 + kt - k(a^2 - r^2)/6K - (2ka^3/K\pi^3 r) \sum_{n=1}^{\infty} (1/n^3) (-1)^n (\sin n\pi r/a) \exp(-Kn^2 \pi^2 t/a^2) \dots \dots \dots (2)$$

Where  $K$  is the thermal diffusivity of the material <sup>(38)</sup>.

The exponential ~~time~~ <sup>term</sup> on the right side of equation (2) becomes negligible after a time  $t$  depending on the magnitudes of  $K$  and  $a$ , and the steady state temperature becomes

$$\theta = \theta_0 + kt - k(a^2 - r^2)/6K \dots \dots \dots (3)$$

For the purpose of these experiments, the exponential term was considered negligible if it was not greater



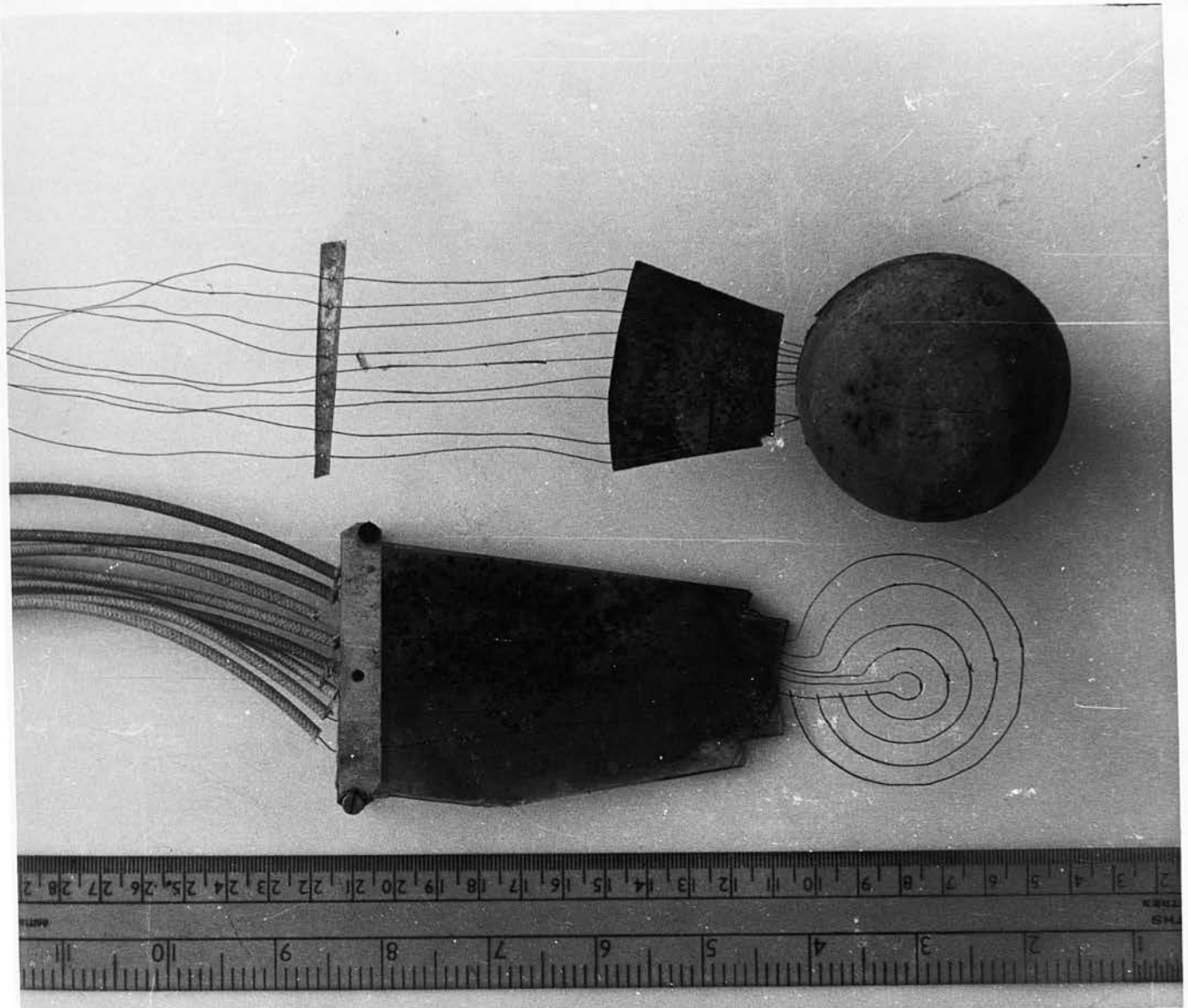
than  $0.1^{\circ}\text{C}$ . For a solid of diffusivity 0.004, say, and radius 3 cm., this occurs after about 40 minutes. In practice, 36 minutes was found sufficient for the mass to attain steady state conditions at the heating rates employed. Hence allowing for a maximum heating rate of  $2.5^{\circ}\text{C}$ . per minute, and a maximum room temperature of  $30^{\circ}\text{C}$ ., the transition temperature must be at least  $120^{\circ}\text{C}$ ., and any other reaction following this must be separated from it by at least  $150^{\circ}\text{C}$ . Of those compounds known to have a definite transition point, the substances shown in Table I meet these conditions. Potassium hydroxide, although meeting the above conditions, is difficult to handle and would have a deleterious effect on all metallic parts. Lithium and potassium sulphates also show transition points at temperatures too high for convenience. In the event, potassium nitrate gave excellent results with the minimum of trouble.

### III. 3. Melting and Solidification:

Since one of the phases involved is liquid, it is necessary to prevent convection in the liquid state. This problem was solved by casting a porous sphere of some 'inert' material with which the test substance was impregnated, i.e. a material which would not show any reactions at the temperature of the experiment and which would not react with the test substance.

P L A T E

Photograph of used specimen and thermocouples



Two substances were used for this purpose, namely, glass and calcium sulphate, the latter only for organic compounds.

control the heating accurately near the maximum temperature.

### III. 3. 1. Sintered Glass

Ordinary bottle glass was reduced to powder by pounding and sifted to remove all particles above a certain size<sup>\*</sup> so as to leave a high proportion of fine particles. These fine particles, it was found, assisted in bonding, but unfortunately, also reduced the porosity of the finished mould. The calorimeter was filled, with the thermocouples in position, and the temperature of the mass was raised rapidly to about 620°C., then more slowly to a maximum of 650°C over a period of about 20 minutes. It was then cooled slowly to about 620°C. over the same ~~period~~<sup>period</sup> of time, then rapidly in air to room temperature, after which it was removed from the calorimeter as a solid sphere in which thermocouples were embedded. It was found that the minimum density of packing required to obtain an undeformed sintered-glass sphere was about 1.5 gms. of powdered glass per cm.<sup>3</sup>, corresponding to about 40% porosity. Looser packing resulted in slight settling of the glass in the calorimeter as a result of the slight softening of the glass required for bonding; e.g. a powder density of 1.3 gm/cm.<sup>3</sup> gave a sphere whose diameter from pole to pole was only 5.8 cm.

\* 0.6 mm. maximum particle size

The sintering temperature is fairly critical but since at this temperature glass is slightly conducting (electrolytically), it was often difficult to control the heating accurately near the maximum temperature if the furnace winding insulation was imperfect. It was also found that the thermocouples became brittle after being in contact with glass at those temperatures and had to be handled with great care after the sphere had been removed from the calorimeter. Again, the softened glass tended to corrode the inside of the calorimeter and so impair the accuracy of the internal dimensions. To prevent this, and also to facilitate the removal of the sphere from the calorimeter, the inside of the latter was smeared with a preparation of graphite in vaseline.

### III. 3. 2. Calcium Sulphate:

This was found very useful for low-melting substances. The sphere was cast from ordinary plaster of Paris. The best results were obtained by mixing 130 grams of exsiccated calcium sulphate with 80 cc. of water containing 1 gm of borax in solution, the purpose of the borax being to delay setting of the plaster during handling. These proportions resulted in an undeformed sphere of about 40% porosity when completely dried. Setting was complete in about one hour, and the hard mass,



PLATE III.  
Fig. 16. Arrangement for Vacuum Impregnation.

with the thermocouples embedded, could be removed easily from a previously greased calorimeter. Afterwards it was dried by heating for about 40 minutes at 250°C. Heating at 120 - 130°C. removes all uncombined water as well as  $1\frac{1}{2}$  H<sub>2</sub>O, and at 210°C., the rest of the combined water is removed, leaving the anhydrous calcium sulphate. This drying was necessary in order to render the mould 'inert'. For reactions likely to be completed below 200°C., e.g. the melting of m-Nitroaniline (m.p. 112°C) the second stage of drying was dispensed with, especially as the block of anhydrous calcium sulphate was rather brittle.

### III. 3. 3. Impregnation.

III. 3. In order to achieve a uniform distribution of the test material in the inert base, impregnation was carried out by vacuum, using the arrangement shown in <sup>Plate III</sup> Fig. 16. Sufficient of the material was placed, together with the porous sphere, in the impregnating jar and the system evacuated to a pressure not less than the vapour pressure of the test substance at its melting point. This precaution was necessary in order to prevent loss of material by boiling or excessive vaporisation. The system was then shut off and the vessel heated until the substance had melted completely and the sphere was totally immersed in the liquid. Heating was continued

for a few minutes further to allow the sphere to attain throughout the temperature of the molten substance.

Air was then let into the system.

For the quantity of material involved, it was often necessary to keep the mass for a considerable period (up to 60 minutes) at a temperature greatly in excess of the melting point before it could be completely melted, and this was often a nuisance in view of the fact that at such temperatures it was not easy to maintain the low pressure necessary for efficient impregnation without renewed pumping which then upset the equilibrium between vapour and liquid, leading to extensive vaporisation and loss of material.

### III. 3. 4. Choice of test-substance and inert base.

In the choice of material, the lower limit for fusion temperature is set, as in the case of crystalline inversion, by the maximum uniform heating rate that is intended to be used and by the necessity to prevent melting until steady state is reached. This, as before, is about  $100^{\circ}\text{C}$ .

Secondly, the test material must have a low vapour pressure at temperatures considerably in excess of the melting point, for, apart from the fact that impregnation would otherwise be difficult to carry out, it may also be necessary to allow up to  $150^{\circ}\text{C}$ . in excess

of melting point in order to carry the test to completion. For example, it was found that while it was possible to impregnate with salicylic acid (m.p.  $158^{\circ}\text{C}.$ ), a great deal of vaporisation took place as soon as melting commenced, so that it was impossible to study melting in isolation. A simple test soon showed that the vapour pressure of salicylic acid was quite high at temperatures below its melting point (25 mm. Hg at  $158^{\circ}\text{C}.$ ), rising sharply.

This second requirement is to some extent at variance with the first as far as organic compounds are concerned. Of all the common organic compounds with melting points below  $200^{\circ}\text{C}.$ , more than fifty percent. have melting points below  $100^{\circ}\text{C}.$  Also, for organic compounds, a melting point in excess of  $100^{\circ}\text{C}.$  must be considered high, and it was found that such compounds became rather unstable near their melting points, possessing rather high vapour pressures with consequent tendency towards sublimation or considerable vaporisation. Furthermore, organic compounds with low vapour pressures and very high melting points (up to and above  $200^{\circ}\text{C}.$ ) tend to decompose at those temperatures.

Another limitation to the maximum temperature that may be employed is the nature of the inert material with which the test substance is impregnated. If calcium sulphate is used, the temperature at any part



of a sphere of up to 3 cm. radius should not exceed  $150^{\circ}\text{C}$ . if the sulphate was only partially dehydrated, and  $220^{\circ}\text{C}$  if the anhydrous sulphate was used. The latter limit is set by the fact that anhydrous calcium sulphate exhibits a slow but distinct exothermic reaction of its own at 320 to  $370^{\circ}\text{C}$ .<sup>(39)</sup> Glass would be more generally suitable for ordinary temperatures up to  $500^{\circ}\text{C}$ . at which it begins to soften, but even this limit would be limited (to as low as  $300^{\circ}\text{C}$ .) because of the need for vacuum impregnation which, for the mass of material involved, is difficult to carry out at temperatures exceeding  $300^{\circ}\text{C}$ . Glass was used for studies on zinc chloride and m-nitroaniline, and calcium sulphate for m-nitroaniline, salicylic acid, and adipic acid.

Now it has been shown that very few organic compounds with melting points in the desired range have been found amenable to the kind of treatment involved in these experiments. On the other hand, very few, if any, inorganic compounds can be found with melting points below  $200^{\circ}\text{C}$ ., except those which are liquid or gas at ordinary temperatures. Those with melting points between 200 and  $300^{\circ}\text{C}$ . are usually highly hygroscopic or even deliquescent, and are, therefore, difficult to handle. But they do possess the advantage, over organic compounds, of a low or even negligible vapour pressures over a very large range of temperatures, and, therefore,

TABLE II. Vapour Pressures of some compounds  
with melting points between 90 and 300°C.

[Handbook of Chemistry and Physics, 35th ed. (Chemical Rubber Publishing Company)].

Compounds	M.P.	Temperatures °C. at which V.P. = x mm Hg					
		1 mm	10 mm	40 mm	100 mm	400 mm	760 mm
Zinc chloride $\text{ZnCl}_2$	265	428	508	566	610	689	732
Stannic iodide $\text{SnI}_4$	145	solid	176	219	254	316	348
Salicylic acid	159	114	146	172	193	231	256
m-Nitroaniline	112	119	168	204	232	280	306 decompose
Glutaric acid $\text{HOOC}(\text{CH}_2)_3\text{COOH}$	98	156	196	226	247	284	303
Adipic Acid $\text{HOOC}(\text{CH}_2)_4\text{COOH}$	152	160	206	241	265	313	338
Pimelic Acid $\text{HOOC}(\text{CH}_2)_5\text{COOH}$	103	163.4	212	247	272	319	342
Suberic Acid $\text{HOOC}(\text{CH}_2)_6\text{COOH}$	142	173	220	255	279	323	346
Azeläic Acid $\text{HOOC}(\text{CH}_2)_7\text{COOH}$	107	178	226	260	287	333	357 decompose
Sebacic Acid $\text{HOOC}(\text{CH}_2)_8\text{COOH}$	135	183	232	268	295	333	352 decompose

would appear to be more suitable than organic compounds, provided they have a low electrical conductivity in the molten state and do not corrode the metallic holder or the thermocouple wires. Compounds of metals with a marked tendency to covalent bonds would fulfil these conditions.

A list is appended (Table II) of compounds which seem to meet all or most of the requirements. Experiments with zinc chloride, salicylic acid, m-nitroaniline and adipic acid are described in the next chapter. Examination of the series of saturated dicarboxylic acids seems to suggest that they possess, more than other organic compounds, the properties desired in this kind of work, but this fact was discovered too late to be used in the present studies.

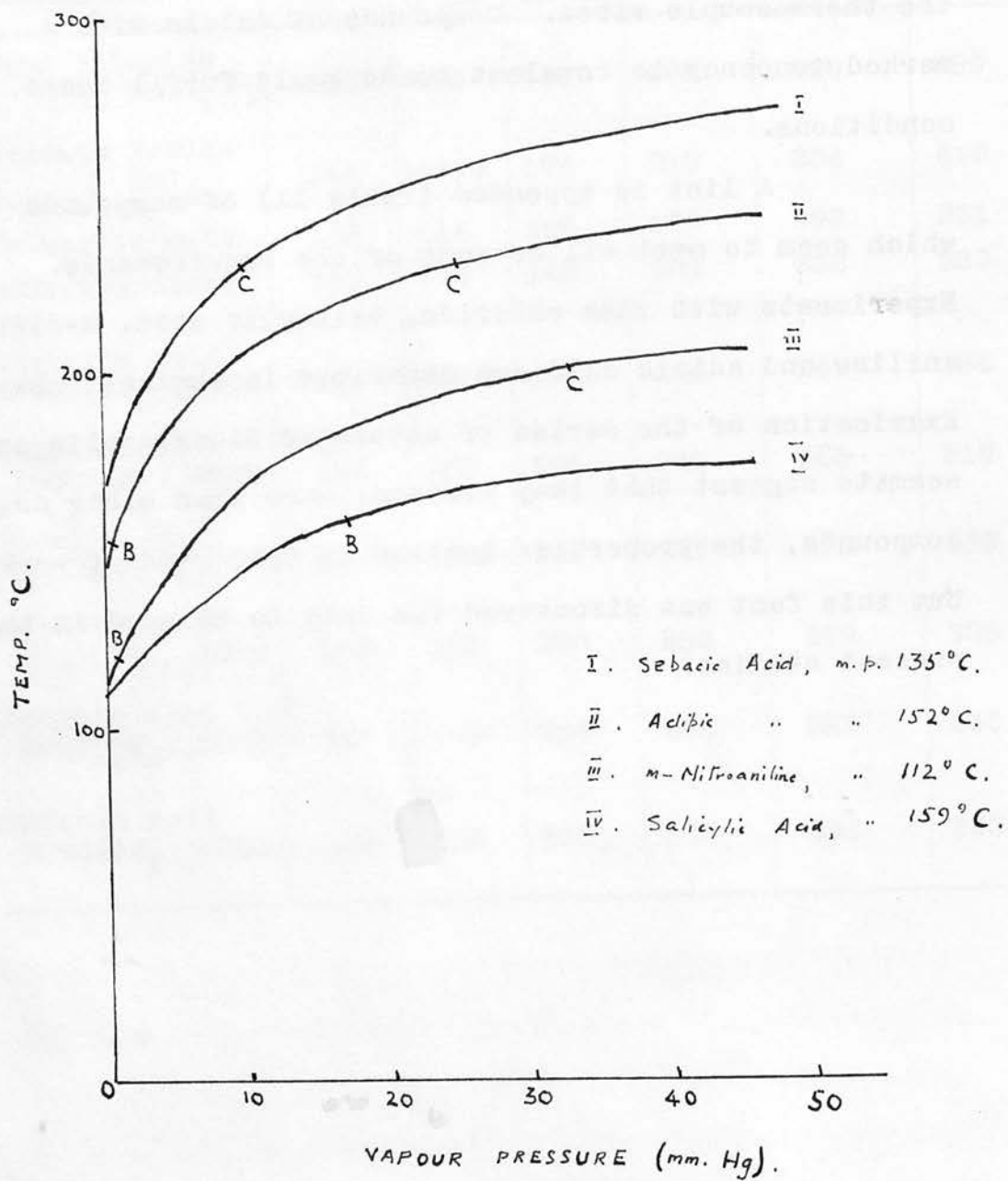


FIG. 16. VAPOUR PRESSURE CURVES.

Chapter IV.

EXPERIMENTAL RESULTS.

IV. 1. Melting and Solidification:

The chief difficulty with experiments in which a large quantity of the material has to be melted is the incidence of extensive vaporisation and, in the case of organic compounds, decomposition. It has been shown that, in all cases, a low vapour pressure at temperature of the experiment is necessary, which also implies that the melting and boiling points of the substance must be separated by a large temperature interval. Figure 16 shows the temperature-vapour pressure curves for four substances whose melting and boiling points are sufficiently separated. The points C on each curve represent (approximately) 'critical' conditions: the vapour pressures attained at the maximum temperatures likely to be used in a spherical specimen of about 6 cm. diameter, while points B represent conditions at the melting point.

(a) Salicylic acid melts at  $159^{\circ}\text{C}$ . and boils at  $256^{\circ}\text{C}$ ., and a maximum temperature of  $220^{\circ}\text{C}$ . was found necessary for completion of fusion, at which its vapour pressure is about 270 mm. Hg., an excessively large value.

(b) ~~m~~-Nitroaniline with melting and boiling points of  $112$  and  $285^{\circ}\text{C}$ . respectively has a vapour pressure of 31 mm. Hg. at  $200^{\circ}\text{C}$ ., the maximum temperature; hence,

although vaporisation was significant, it was not sufficiently serious to upset the operations.

(c) Adipic acid, melting at  $152^{\circ}\text{C}$ . and boiling at  $338^{\circ}\text{C}$ ., has a vapour pressure <sup>of about 25 mm.</sup> ~~less than 1 mm.~~ Hg. at the maximum temperature of about  $230^{\circ}\text{C}$ ., which renders it ~~eminently~~ <sup>even more</sup> amenable to the type of treatment required. It is the middle member of the saturated di-carboxylic acid series of which sebacic acid is the highest, and this property is shown to an increasing extent as the series is ascended, and, fortunately, the highest member of the series is also the cheapest and commonest.

(d) The only inorganic compound used was zinc chloride (m.p.  $262^{\circ}\text{C}$ .), which has a negligible vapour pressure, less than 1 mm. Hg. at the highest temperature of  $364^{\circ}\text{C}$ . for which measurements were taken. But, being highly deliquescent, it required special handling. After impregnation, the mass was dried at  $150^{\circ}\text{C}$ . for 24 hours and subsequently kept at slightly above  $100^{\circ}\text{C}$ .

Some of the records were obtained by taking measurements of the absolute values of temperature, using thermocouples of Type (b) or (d) (see Fig.10), but the majority of measurements were obtained using the more sensitive differential arrangements (Types a and c). In either case it was necessary to reduce the records so as to obtain both the absolute values and the differential values of temperature, in order to make a fuller

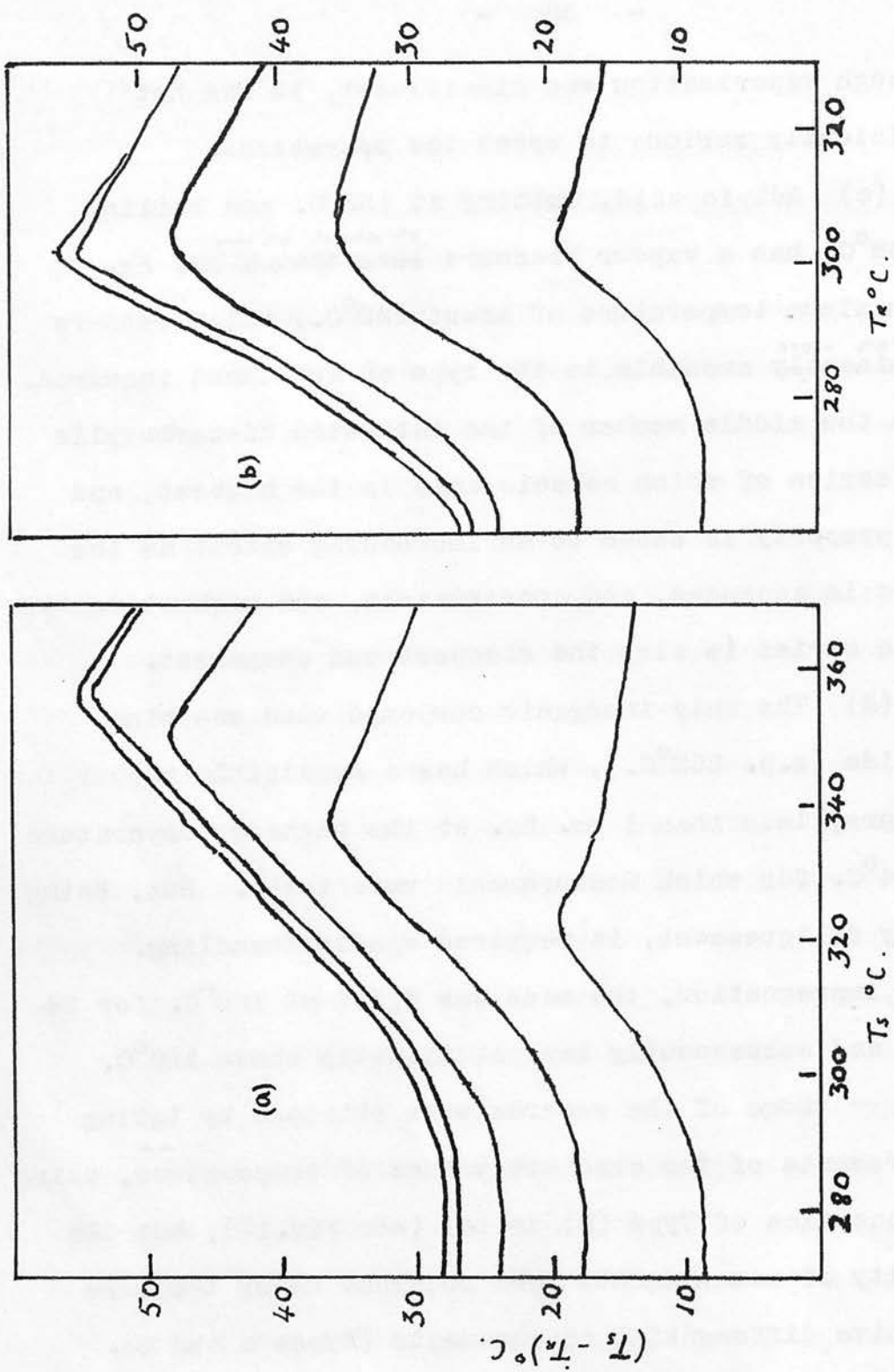


FIG. 17. DIFFERENTIAL TEMPERATURE CURVES FOR SINTERED GLASS SPHERE IMPREGNATED WITH ZINC CHLORIDE

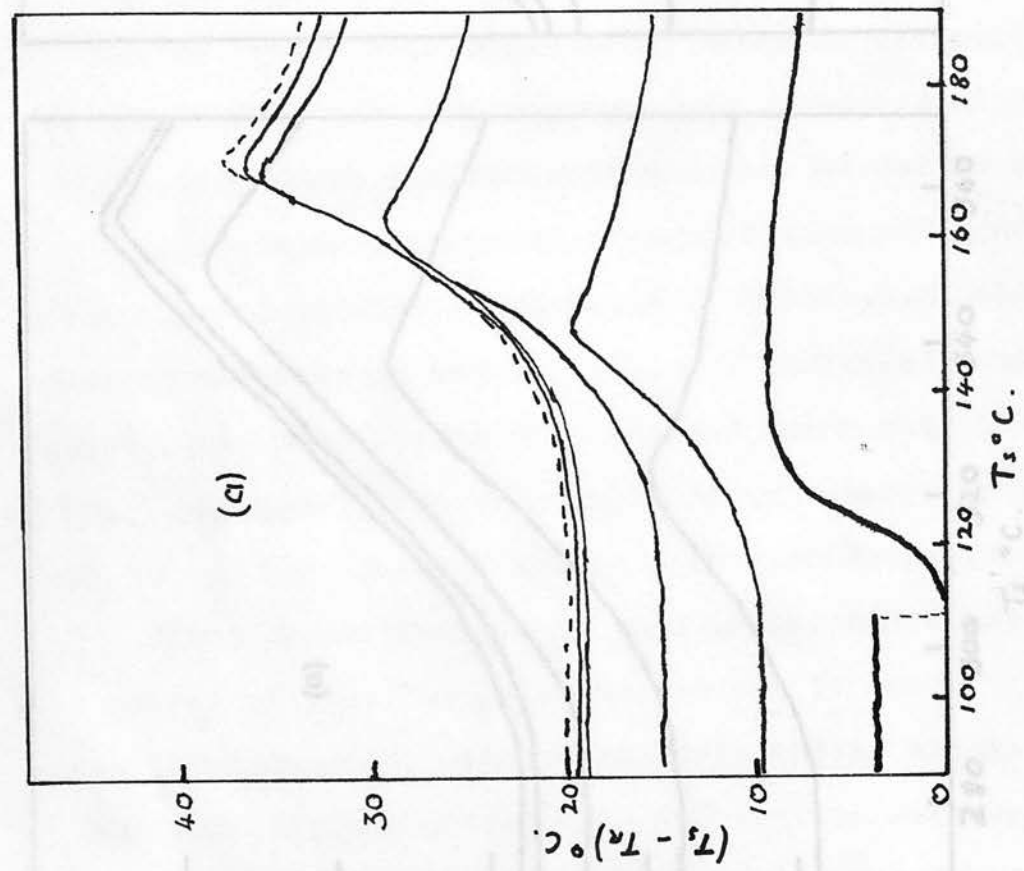
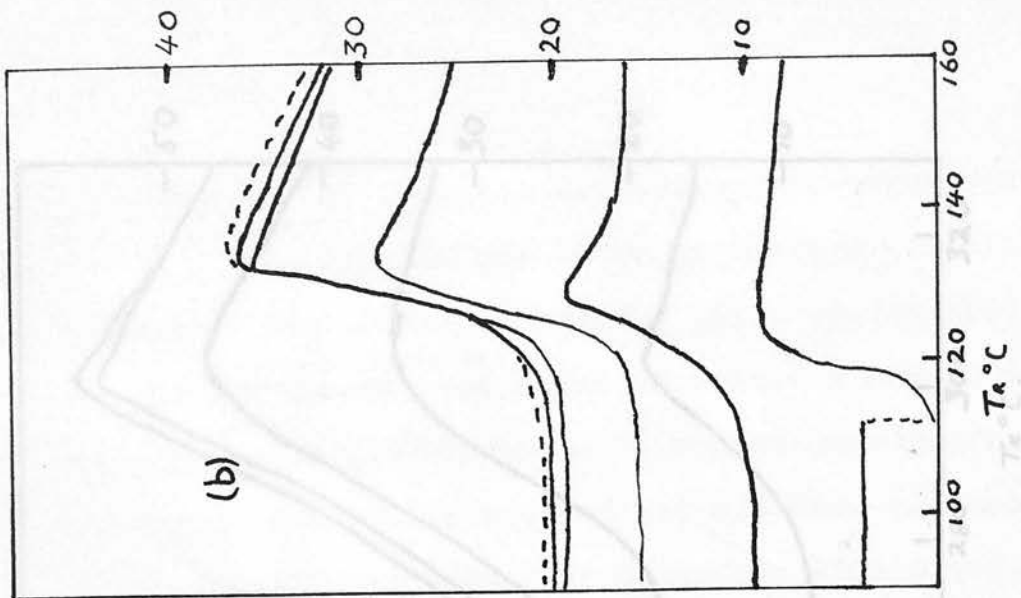


FIG. 18. DIFFERENTIAL THERMAL CURVES FOR SINTERED GLASS  
 SPHERE IMPREGNATED WITH m-NITROANILINE.

SINTERED GLASS SPHERE IMPREGNATED WITH  
 ZINC CHLORIDE



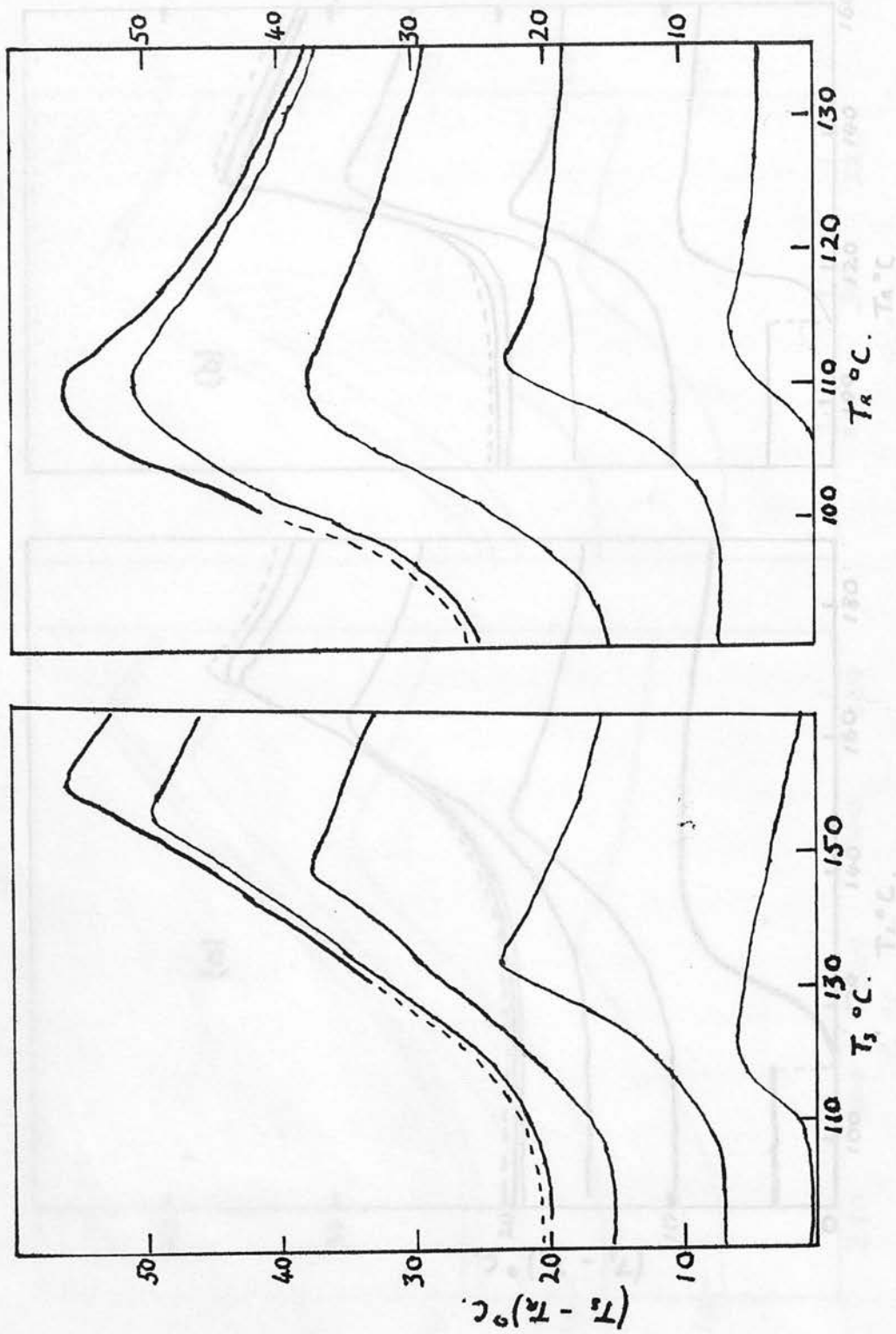


FIG. 19. DIFFERENTIAL TEMPERATURE CURVES FOR SPHERE  
OF ANHYDROUS CALCIUM SULPHATE IMPREGNATED  
WITH m - NITROANILINE

interpretation of the results possible. A reference table for chromel/alumel thermocouples was used. (40)

#### IV. 1. 1. Differential thermal curves.

Figure 17 shows a set of typical differential thermal curves for various points in a sphere of sintered glass impregnated with zinc chloride, figure 18 another set for m-Nitroaniline with sintered glass as base, and figure 19 a third set with anhydrous calcium sulphate as base. It is impossible to make quantitative comparison as between one specimen and another, except in so far as the general character of the curves are concerned, owing to the difficulty of ensuring uniformity of impregnation for the two different base materials and even for the same material impregnated with the same or different substances. Hence, each specimen (inert base + test substance) was treated as a separate unit, and, where quantitative comparison of effects was desired all measurements for that effect were made on one unit. The difficulty with this procedure, however, was that successive measurements become progressively less reliable owing to gradual loss of material during each run, except in the case of zinc chloride where vaporisation was negligible.

In figures 17 - 19, (a) is a plot of the differential temperature ( $T_s - T_r$ ) against the temperature

$T_s$  of the inside of the calorimeter, which, in this case, is also taken as equal to the temperature at the surface of the specimen, and (b) is the plot of differential temperature against temperature  $T_r$  at the point  $r$  cms. from the centre. These in conventional d.t.a. terminology, correspond respectively to differential thermal curves with temperature of inert material as reference, and differential thermal curves with temperature of specimen as reference temperature:

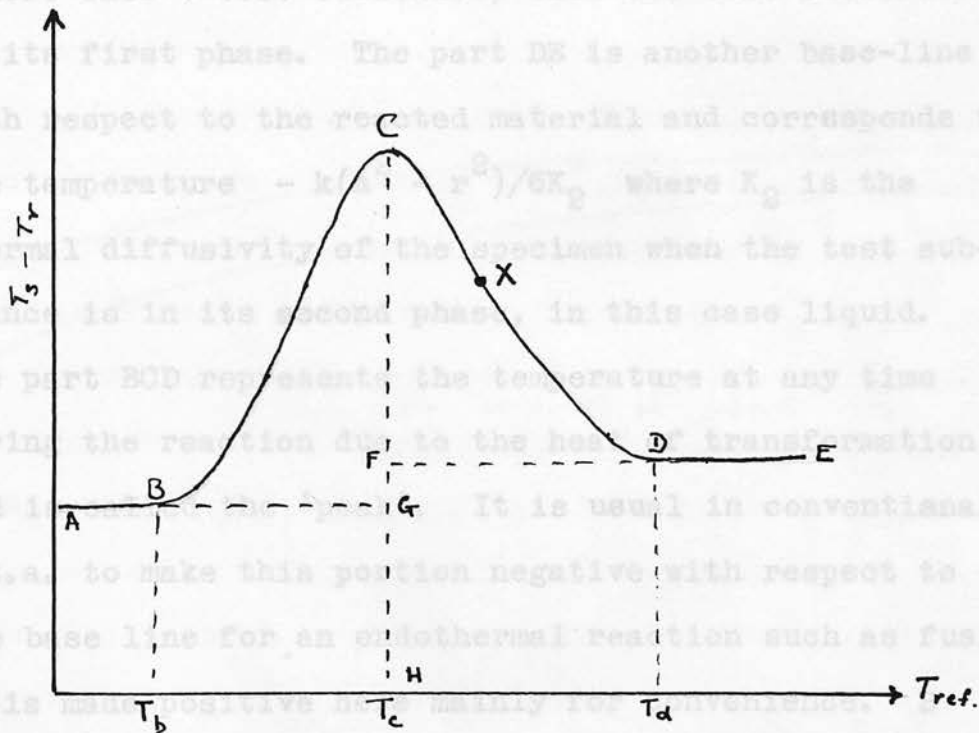


Fig. 20. Schematic representation of differential temperature curve.

The height of the peak is variously taken as  $CH$  where  $C$  is

In the rest of this thesis, the first part AB (Fig. 20) of each curve, a straight line parallel to the reference-temperature axis, is a base-line with respect to the unreacted substance and corresponds to the second term  $-k(a^2 - r^2)/6K_1$  of the equation

$$\theta = \theta_0 + kt - k(a^2 - r^2)/6K_1 \dots\dots\dots (3)$$

(see page 28) which represents the steady temperature of the steadily heated sphere at a point  $r$  from its centre and where  $K_1$  is the thermal diffusivity of the specimen (inert base + test substance) when the test substance is in its first phase. The part DE is another base-line with respect to the reacted material and corresponds to the temperature  $-k(a^2 - r^2)/6K_2$  where  $K_2$  is the thermal diffusivity of the specimen when the test substance is in its second phase, in this case liquid.

The part BCD represents the temperature at any time during the reaction due to the heat of transformation and is called the 'peak'. It is usual in conventional d.t.a. to make this portion negative with respect to the base line for an endothermal reaction such as fusion: it is made positive here mainly for convenience. B and D correspond to the points of departure from, and return to steady state respectively, and the difference in reference temperatures  $T_b$  and  $T_d$  corresponding to these points is called the width of the 'peak'. The height of the peak is variously taken as CH where C is

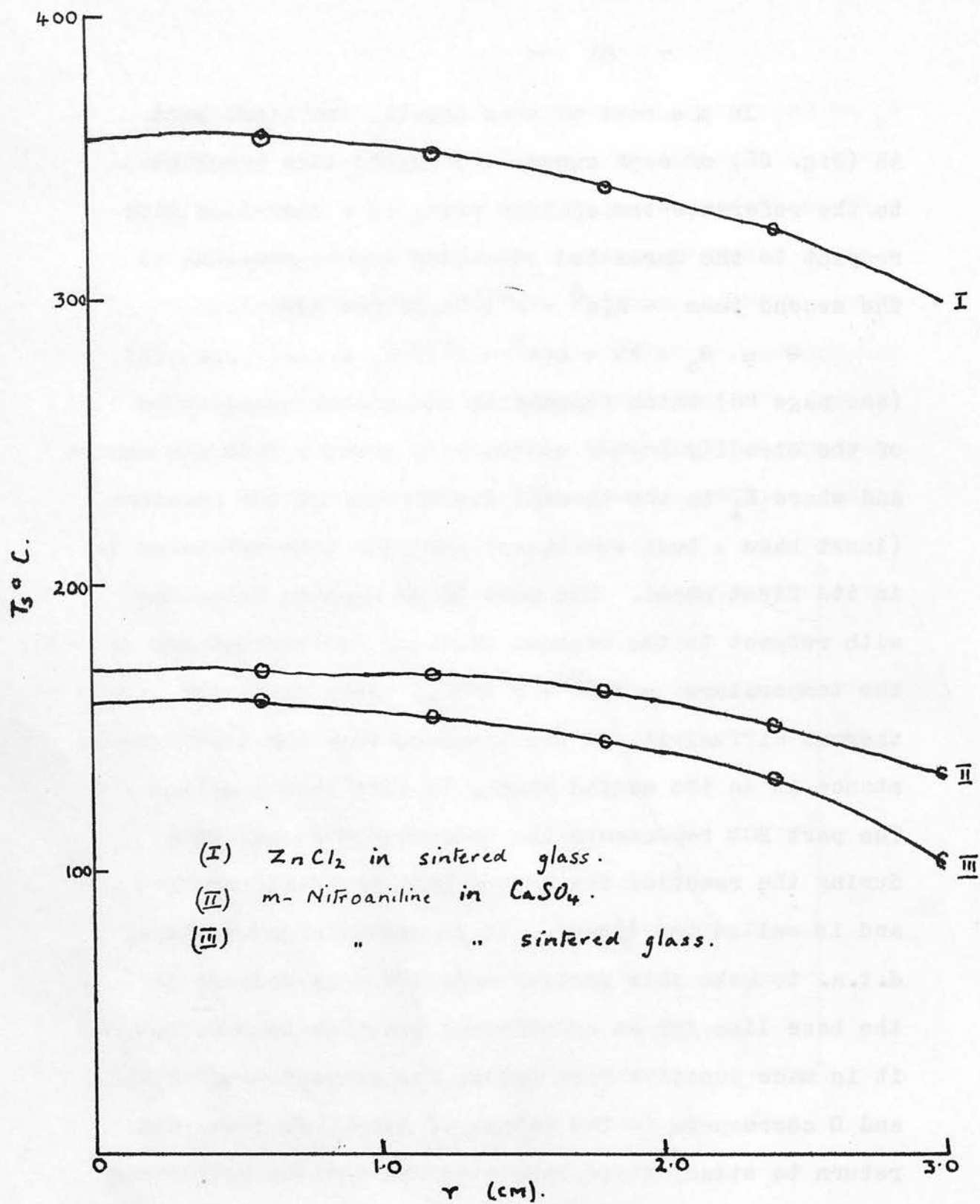


FIG. 21. SURFACE TEMPERATURES AT  $(T_s - T_R) = \text{MAX.}$   
FOR VARIOUS  $r$ .

the maximum of the 'peak' and CH is the corresponding ordinate, or CG, G being on AB produced or CF where F is on ED produced. If there was no change in thermal conductivity, density and specific heat on transformation,  $CG = CF$ . This is often (approximately) the case in crystalline inversion, but in melting and solidification, FG is normally quite large. The temperature  $T_c$  is called the temperature at the peak.

It is at once clear from a study of Figures 17 to 19 that the following features are common to all the curves:-

(a) Position of the peak. When the differential temperatures are plotted as a function of the temperatures at the surface of the specimen (curves (a)) there is a progressive shift in the temperature  $T_c$  corresponding to maximum of the peak as we move from the surface towards the centre. The extent of this shift from a fixed value, e.g. the transition temperature, varies with the rate of rise of the surface temperature. But when differential temperatures are plotted against the temperature  $T_r$  of the corresponding point inside the sphere, the maxima of the peaks for all points in the sphere tend to occur at the same value of  $T_r \approx T_i$  where  $T_i$  is the transition temperature. The factors which determine how closely  $T_r$  approaches  $T_i$  cannot be examined at this stage owing to the difficulty of

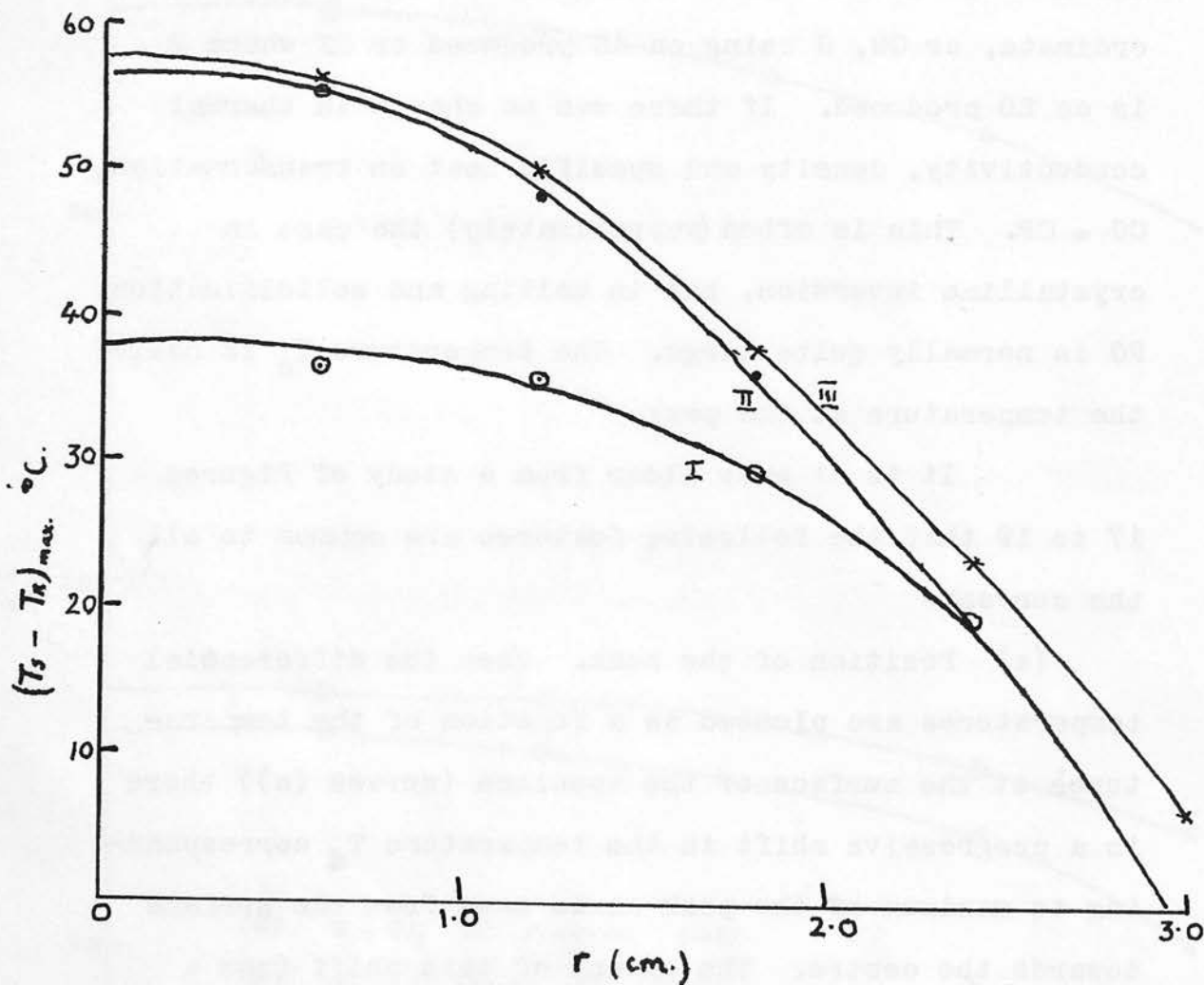


FIG. 22. MAXIMUM DIFFERENTIAL TEMPERATURE  
FOR VARIOUS r.

- (I) m-Nitroaniline in sintered glass
- (II) Zinc chloride " " "
- (III) m-Nitroaniline in calcium sulphate

carrying out more than a very few runs on the same specimen. One other factor which is essential to a full discussion of the position of the peak is the range, i.e. the quantities  $T_b$ ,  $T_d$  and  $T_d - T_b$  of figure 20. But again, this can only be fully appreciated if the experiment could be carried on to steady conditions after the completion of the reaction to realize the portion DE of figure 20. This is not possible on the scale of the experiment and using organic compounds.

(d) Height of peak. This, as is to be expected, increases with decreasing distance from the centre (Figs. 17 - 19). The variation of peak height with the other parameters of the system, especially with rate of rise of surface temperature and with the concentration of the reacting material, will be discussed more fully in the next section (IV. 2), but Fig. 22 indicates the approximate relationship between peak height and distance  $r$  from the centre for the zinc chloride and the two *m*-nitroaniline specimens whose d.t. curves are shown in Figs. 17 - 19.

#### IV. 1. 2. Propagation of reaction; Heating Curves

As has been stated before (Chapter I, p.7), in order to make a more than empirical analysis of the results of d.t. records, it is necessary to determine the history, i.e. the space-time relation, of the surface of separation between the two phases of the



reacting material. In one case, namely, that of the semi-infinite medium, it has been possible, by theoretical considerations alone, to obtain such a relationship in an exact form (41, 42). For a finite medium of a given co-ordinate system, however, the relationship is not easy to deduce mathematically, but it is very often presumed to be of the same form as that originally deduced for the semi-infinite medium, namely,

$$X = \alpha t^{\frac{1}{2}} \dots\dots\dots (4)$$

where X is the distance moved by the interface in time t.  
*the space-time relationship*

In order to determine experimentally it is necessary to know the time at which reaction may be presumed complete at a given point. According to Mackenzie (43) reaction may be presumed to be complete at any point when the differential temperature for that point is maximum, such maxima occurring at turning points or points of discontinuity in the differential temperature curve. But this is now known to be misleading, as was shown in the previous section: the temperature  $T_r = T_c$  (Fig. 20) may be greater than, equal to, or even less than  $T_i$ , (the transition temperature), and therefore it would be erroneous to attempt to follow the progress of the moving boundary by merely reading off the times at which the maxima occurs at various points in the medium. It has also been suggested (44) that the reaction is completed at a time corresponding to some

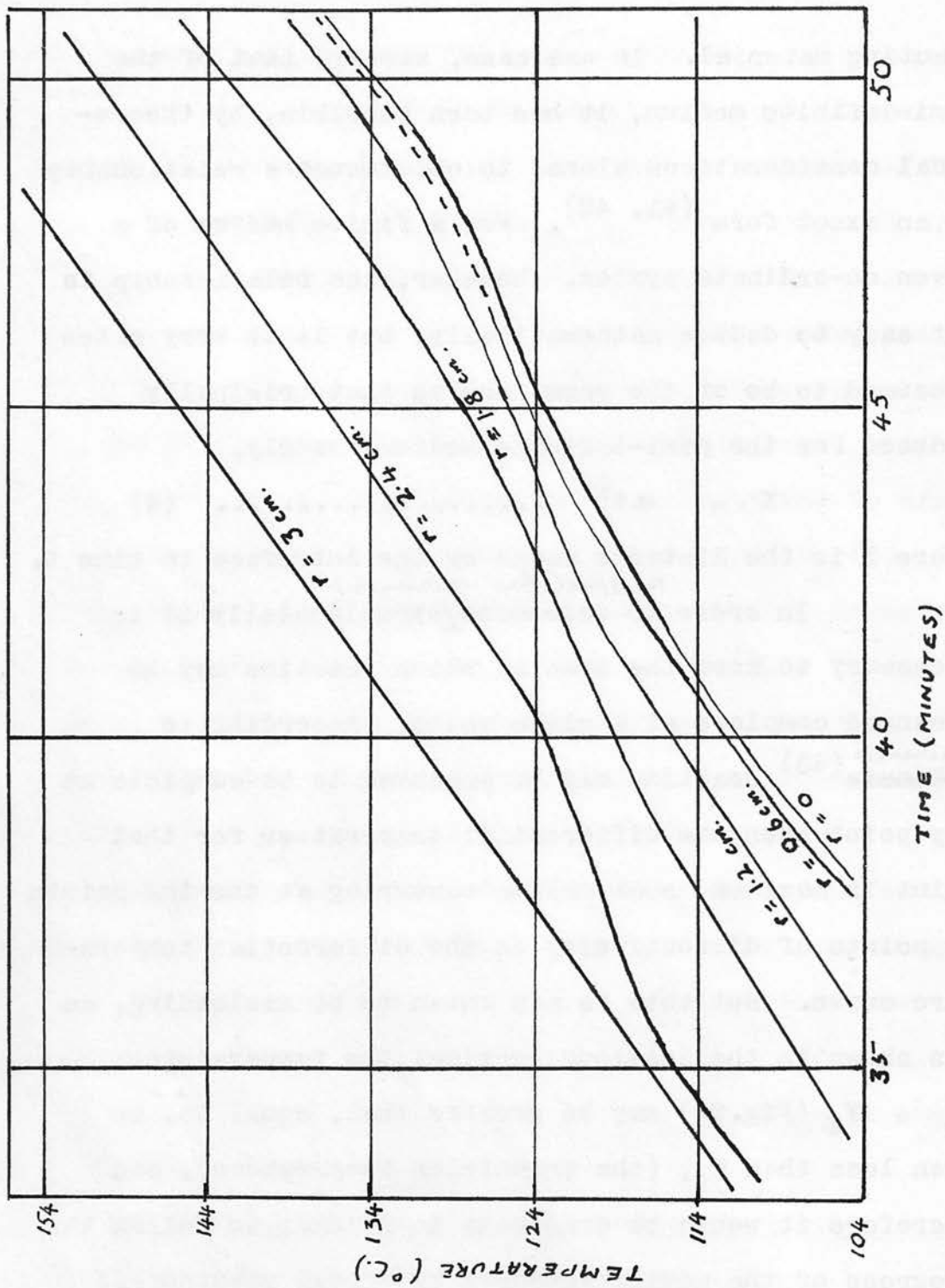


**FIG. 24.** HEATING CURVES FOR m-NITROANILINE IN SINTERED GLASS.

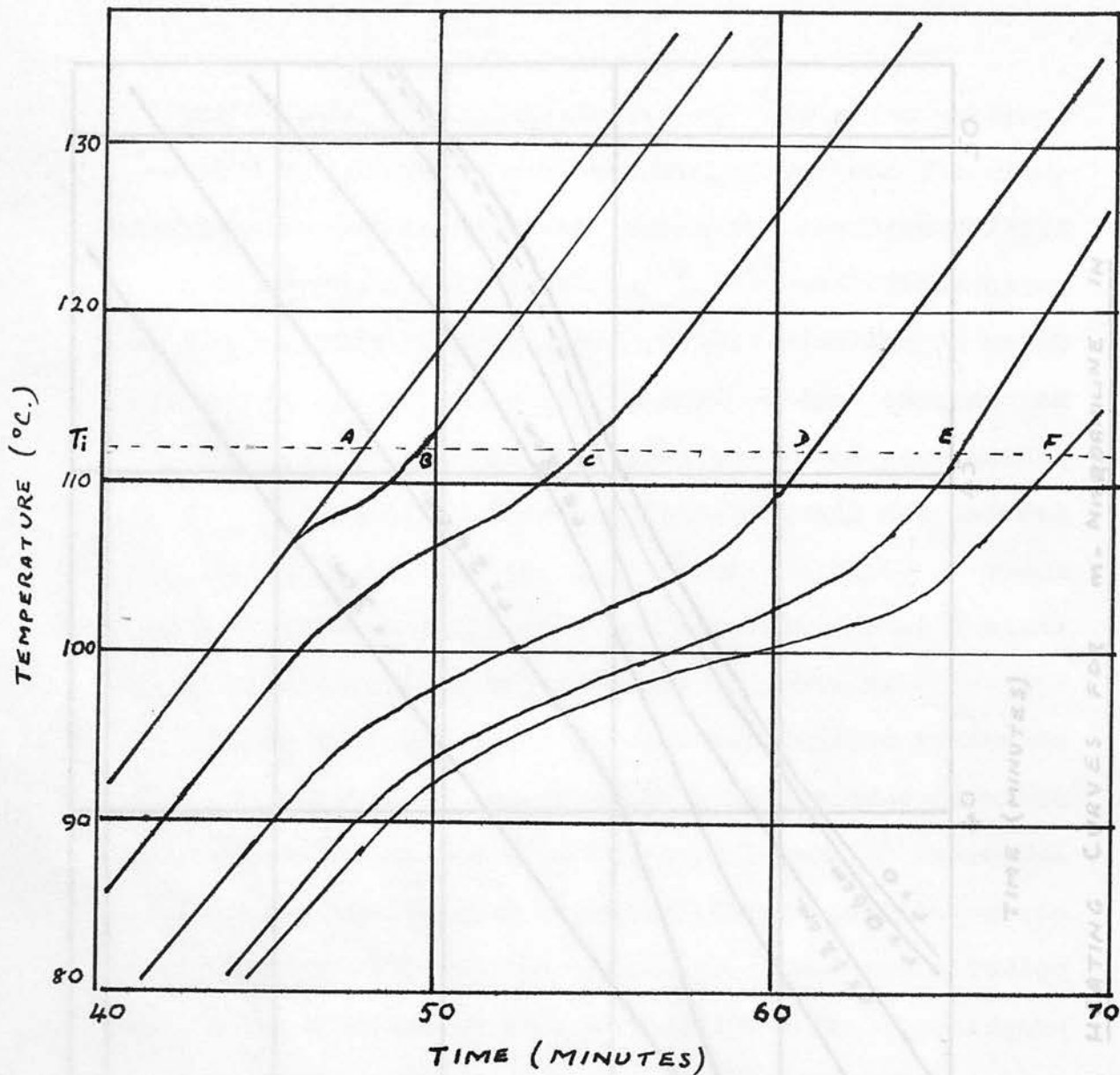


FIG. 25. HEATING CURVES FOR m-NITROANILINE  
IN CALCIUM SULPHATE

FIG. 24. HEATING CURVES FOR m-NITROANILINE IN  
SINTERED GLASS.

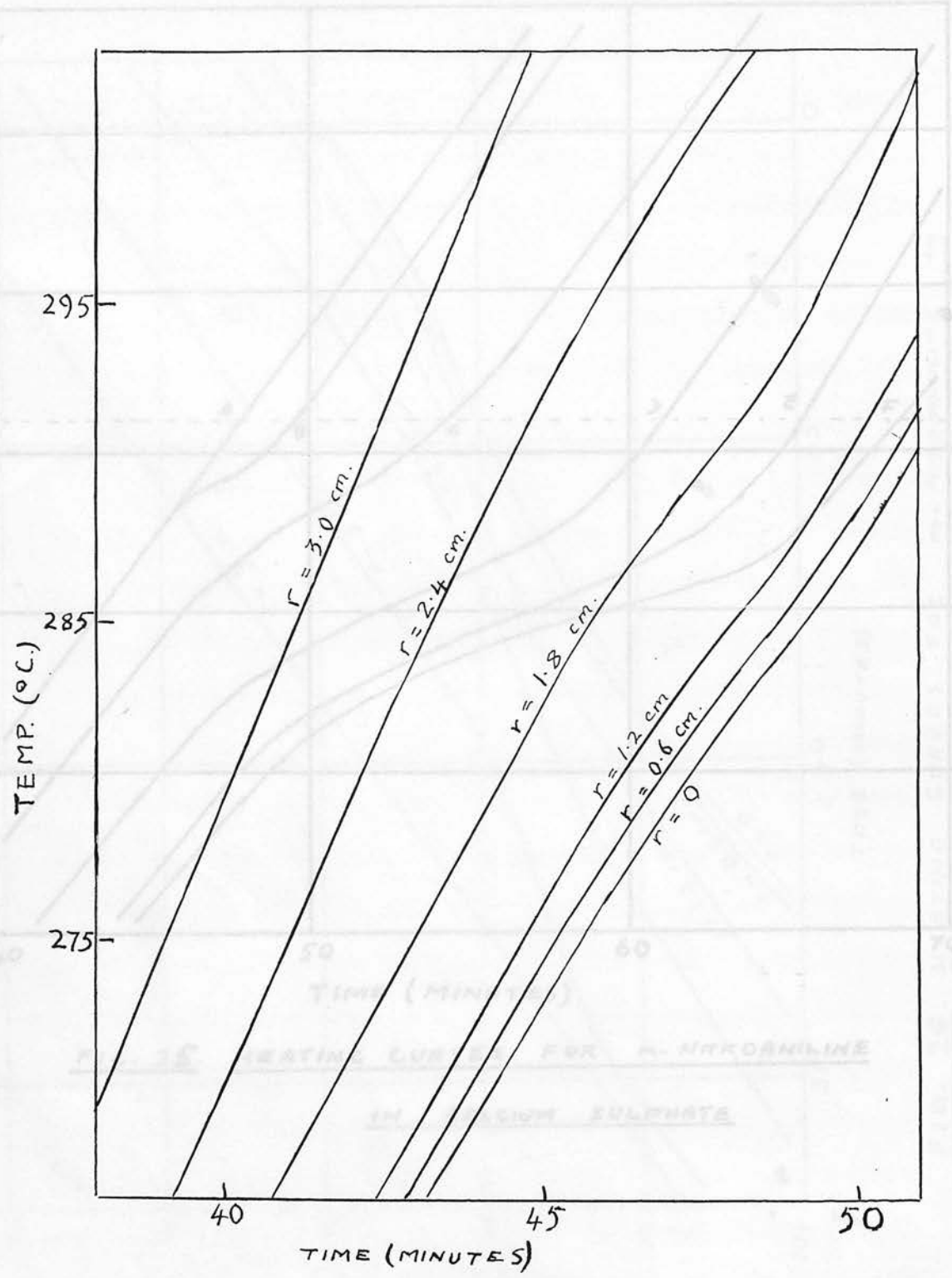


FIG. 23. HEATING CURVES FOR  $ZnCl_2$  IN SINTERED GLASS

point "X" in the portion CD of Fig.20. This will only be the case if the position of the maximum of the peak is below the transition temperature: otherwise the point in the differential thermal curve corresponding to completion of reaction may lie on the portion BC. The point on the differential thermal curve corresponding to completion of reaction is therefore indeterminate, although Vold<sup>(45)</sup> suggests that the point of completion of reaction in stearic acid on heating could be determined graphically.

In this work, however, since only substances whose transition temperatures are known or could be easily determined have been used, a more direct method has been used to trace the progress of the transition interface. This involves the drawing of conventional heating curves (temperature vs. time) for various points in the medium for temperatures in the neighbourhood of the transition point, the absolute values of temperature being deduced from the known values of differential and reference temperatures if differential thermocouples were used.

A set of heating curves are shown in Figs. 23 - 25 for the same specimens used for illustration in the previous section, viz., zinc chloride in sintered glass, m-nitroaniline in sintered glass, and m-nitroaniline in anhydrous calcium sulphate. The curves show

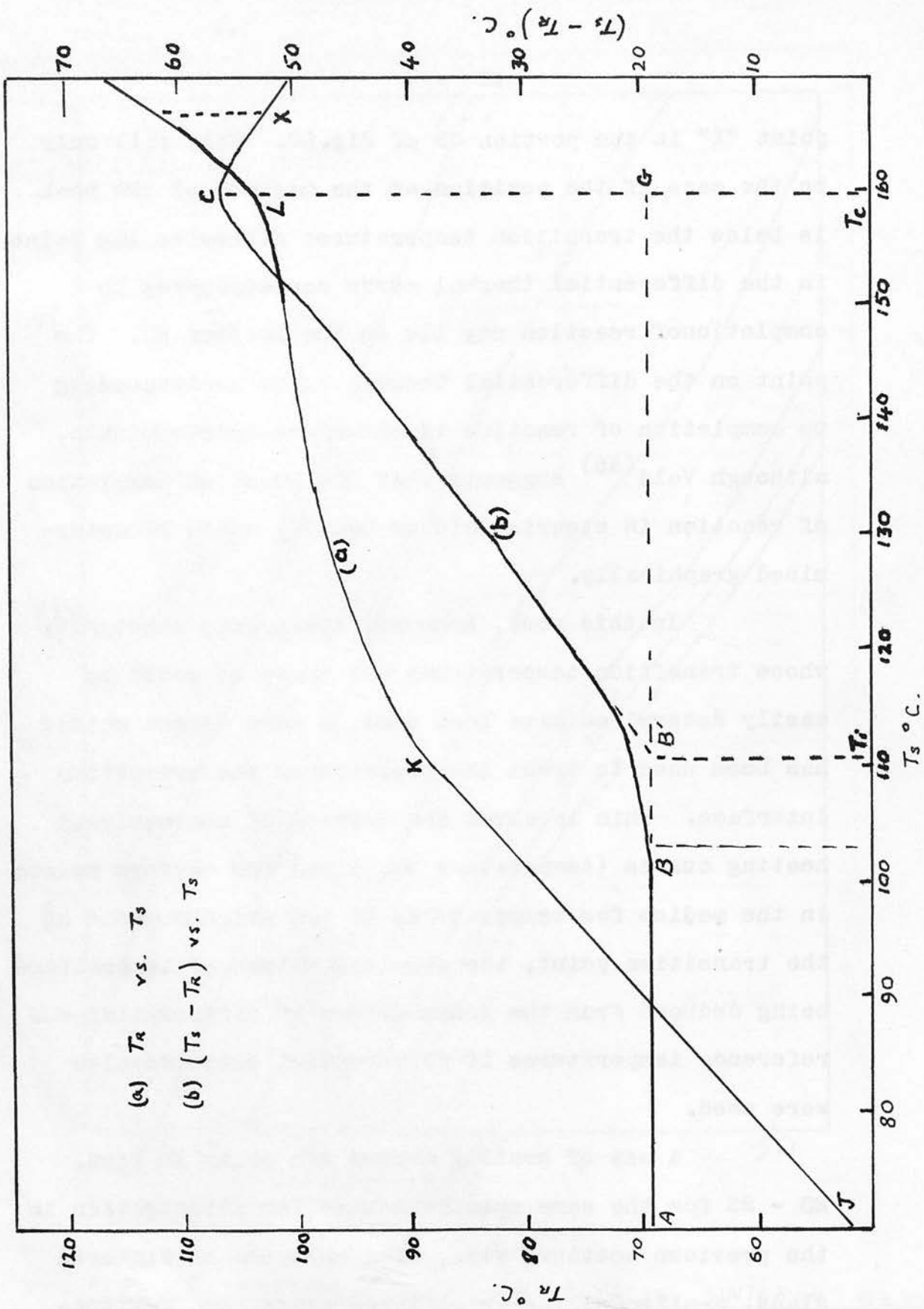


FIG. 26: HEATING AND D.T. CURVES AT  $\gamma = 0.6$  CM. IN ~~SINTERED GLASS~~ CALCIUM SULPHATE IMPREGNATED WITH m-NITROANILINE.

the usual region of diminished slope, for endothermic reactions, the flatness of the region of endothermic arrest depending partly on the heating rate and partly on the concentration of the reacting material. It will be noticed that, in general, the flat portions of the heating curves do not occur at the transition temperature except, approximately, for points near the surface of the sphere, and the divergence of the temperature of endothermic arrest from transition temperature increases with distance from the surface. Also, the endothermic arrest may occur below or above the transition temperature. This illustrates the usual difficulty of determining a transition temperature from heating curve.

It is instructive at this stage to compare the differential thermal curves (Figs. 17 - 19) with the heating curves (Figs. 23 - 26) for the same specimen. Fig 26 shows the corresponding curves for  $r = 0.6$  cm. shown in Figs. 19a and 25, the d.t. curve being lettered as in Fig. 20. As is to be expected

(i) the straight line portions AB and JK of the lead to two curves occur together, corresponding to pre-reaction steady state conditions, the

equation for JK being given by, or for very small samples

$$\theta = kt - k(a^2 - r^2)/6K$$

and that for AB by a rapid rate of a medium of low diffusivity but plotted positive for convenience; the above

(ii) the flat region, KL, of the heating curve corresponds to increasing differential, BC, the maximum of the differential temperature, C, corresponding to the point L at which recovery begins;

(iii) the transition isothermal does not pass through  $r = 0.6$  cm. until endothermic arrest has ceased: this corresponds to the case where reaction is completed at  $r = 0.6$  cm. at a time corresponding to X on the d.t. curve.

A possible explanation of the above observations is that if the heat-wave front which penetrates the sample during a transition travels fast enough, i.e., if the diffusivity  $K$  of the medium is high, thermocouples near the centre show arrest before transition temperature is reached and shortly after reaction has commenced at the surface, and recovery may in fact set in before the moving transition isothermal surface passes the thermojunction. Hence, taking the transition temperature as the point of inflexion or the mid-point of the flat region of a heating curve would lead to an underestimation of the transition temperature. A nearly correct result, however, should be obtained for points near the surface of a large sample, or for very small samples heated at a very slow rate, provided the thermojunction has a low heat capacity. On the other hand a rapid rate of heating at the surface of a medium of low diffusivity would lead to a complete reversal of the above



phenomena and an overestimation of the transition temperature.

These difficulties do not arise in the present work since only substances of known transition temperature were used. But it is interesting to note that, even if the transition points are not known, they could still be determined from the d.t. curves. It has been pointed out by Schnaid<sup>(46)</sup> that if the heating rate is sufficiently slow to produce a straight-line portion during an endothermic reaction, (e.g. the portion BC of Fig.26), an extrapolation of this line to the base line AB so as to meet the latter at B' say, will give the transition temperature, if the differential temperature is recorded against the reference temperature. Similarly, if the heating rate is adjusted to produce a vertical portion on the d.t. curve when differential temperature is plotted against actual temperature of specimen at that point, the vertical portion occurs at the transition temperature. Both of these methods have been found to yield fairly accurate values of the transition temperature: the first is illustrated in Fig.26, and the second was found applicable to the temperature of inversion of potassium nitrate described in the next section. It may be added, however, that even for a rapid rate of heating, provided the heat of reaction per unit volume of the specimen is high enough, the second method still gives a fairly accurate value of the transition temperature.

Table V: Propagation of Melting in a spherical specimen of radius 3.0 cm.

Nature of Specimen	Expt. No.	Heating Rate deg.C/sec.	Time in Seconds at r =					
			3.0	2.4	1.8	1.2	0.6	0 cm.
Zinc chloride in sintered glass	1	.090	0	102	222	324	352	357
m-Nitroaniline in sintered glass	1	.046	0	180	318	397	408	416
m-Nitroaniline in calcium sulphate (I)	1	.046	0	300	690	948	1080	1080
	2	.041	0	468	648	1008	1158	1158
	3	.042	0	204	618	984	1176	1176
m-Nitroaniline in calcium sulphate (II)	1	.028	0	624	966	1146	1230	1248
	2	.032	0	258	594	1254	1410	1410
	3	.043	0	210	666	894	966	966
	4	.043	0	156	366	606	840	840
	5	.045	0	144	297	426	546	546
m-Nitroaniline in calcium sulphate (III)	1	.036	0	168	252	324	369	381
	2	.038	0	72	150	212	249	264

Table V: Propagation of Melting in a spherical specimen of radius 3.0 cm.

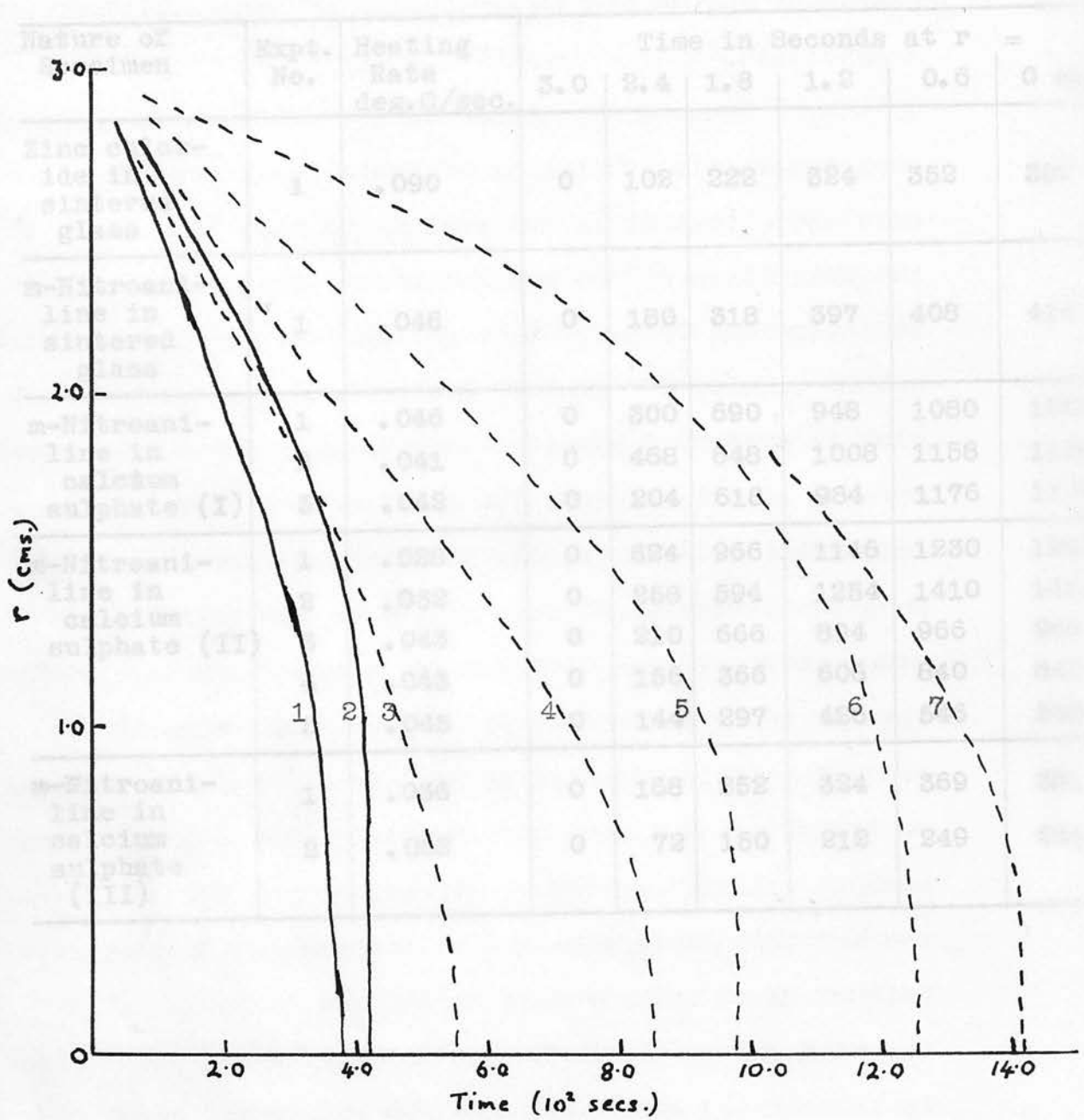


Fig. 27. Propagation Curves for fusion in Sphere of radius 3 cm.

- 1. Zinc chloride in sintered glass
- 2. m-Nitroaniline in sintered glass
- 3 - 7 " " Calcium sulphate at various heating rates.

However, in the present study, the progress of the interface was determined directly from the heating curves. A straight line, parallel to the time-axis at the known transition temperature,  $T_i$ , cuts the heating curves at points A, B, C, D, E, F (Fig. 24). The abscissae of these points give the times at which the moving boundary passes the surfaces  $r = 3.0, 2.4, 1.8, 1.2, 0.6, 0$  cm. respectively, the time for  $r = 3.0$  cm. being taken as zero. (Table V).

IV. 1. 3. Propagation of Reaction: (b) Equation of Propagation.

The first notable feature of Table V is the time required for the completion of the reaction from the surface to the centre. It will be noticed in the case of the last three specimens for which figures are shown, that the time required is an inverse function of the heating rate. Curves are shown (Fig. 27) of the distance,  $r_1$ , from the centre, of the moving boundary as a function of time. Curve (4) is that of zinc chloride and (3) to (5) are those for the second m-nitroaniline specimen in calcium sulphate and these show how strongly dependent on heating rate are the relative times required for the moving boundary to travel a given distance from the surface. One immediate consequence of the effect of the heating rate, therefore, it would seem is the

necessity of keeping this rate absolutely constant during the course of the reaction, since a change of heating rate is equivalent to the generation of an unknown heat wave-front superposed on that due to the thermal reaction in the medium, and this leads to irregularities in the propagation curve, as illustrated, for instance, by the cross-over of curves (2) and (3), and the low values of time near the surface in curve (7) of Fig.27. The effect on the d.t. curves is the existence of spurious peaks.

With the qualification in mind, the shapes of the curves, as of those of Fig.36, suggest that the rate of movement of the interface,  $-dr_1/d\lambda$ , (where  $r_1$  is the position of the moving boundary at time  $\lambda$  from the beginning of the reaction, (the negative sign indicating that the direction of increasing  $\lambda$  corresponds to decreasing  $r_1$ )<sup>+</sup>, is an inverse function of the distance

---

+ In this and subsequent discussion,  $t$  with or without subscript will be used to denote time measured from the commencement of the experiment and  $\lambda$  to denote time measured from the commencement of reaction at the surface. The necessity for the double notation will be seen more clearly in Chapter V.

in cylindrical coordinates, and of

from the centre, since the rates of movement, for different rates of heating, is small for small times, i.e. near the surface, and increases rapidly, becoming very large, as the centre of the sphere is approached.

As mentioned on page 44, a relationship of the form

$$X = k \lambda^{\frac{1}{2}} \dots\dots\dots (4)$$

(where X is the distance of the interface from the free surface at time  $\lambda$  from the beginning of the reaction), parabolic in the space variable, first deduced analytically by Lightfoot and true for the semi-infinite medium and for a medium bounded by two parallel planes with constant surface temperature<sup>(30)</sup>, has been assumed by Danckwerts<sup>(36)</sup> and others<sup>(37)</sup> to hold for media of other coordinate systems, particularly for cylindrical and spherical media, with constant surface temperature and with initial temperature  $f(X) = \text{constant}$ . This assumption is justified and the equation

$$X = k \lambda^{\frac{1}{2}}$$

will be accurately obeyed for these cases where solution of the heat equation is, or can be expressed, as, a function of  $xt^{-\frac{1}{2}}$  only. A large number of general solutions can be expressed, e.g. in terms of the function

$$-Ei(-r^2/4Kt) \dots\dots\dots (5)$$

in cylindrical coordinates, and of



Table V(a).

Propagation Rate of Melting in a spherical specimen of radius 3.0 cm.

Specimen	Expt. No.	Mean values of $\beta$ for $r_1$ (cm.) =					
		3.0-2.4	2.4-1.8	1.8-1.2	1.2-0.6	0.6-0.0	3.0-0.0
Zinc chloride in sintered glass	1	.032	.026	.023	.025	.025	.026 $\pm .002$
m-Nitroaniline in sintered glass	1	.018	.018	.019	.021	.022	.020 $\pm .001$
m-Nitroaniline in calcium sulphate I	2	.007	.009	.008	.008	.008	.008 $\pm .001$
-do- II	1	.005	.006	.007	.007	.007	.006 $\pm .001$
	3	.011	.009	.008	.009	.010	.009 $\pm .001$
	5	.023	.019	.018	.016	.017	.019 $\pm .001$
-do- III	1	.019	.023	.022	.023	.024	.022 $\pm .001$

Table V(a).

Preparation Rate of Melting in a spherical specimen of radius 3.0 cm.

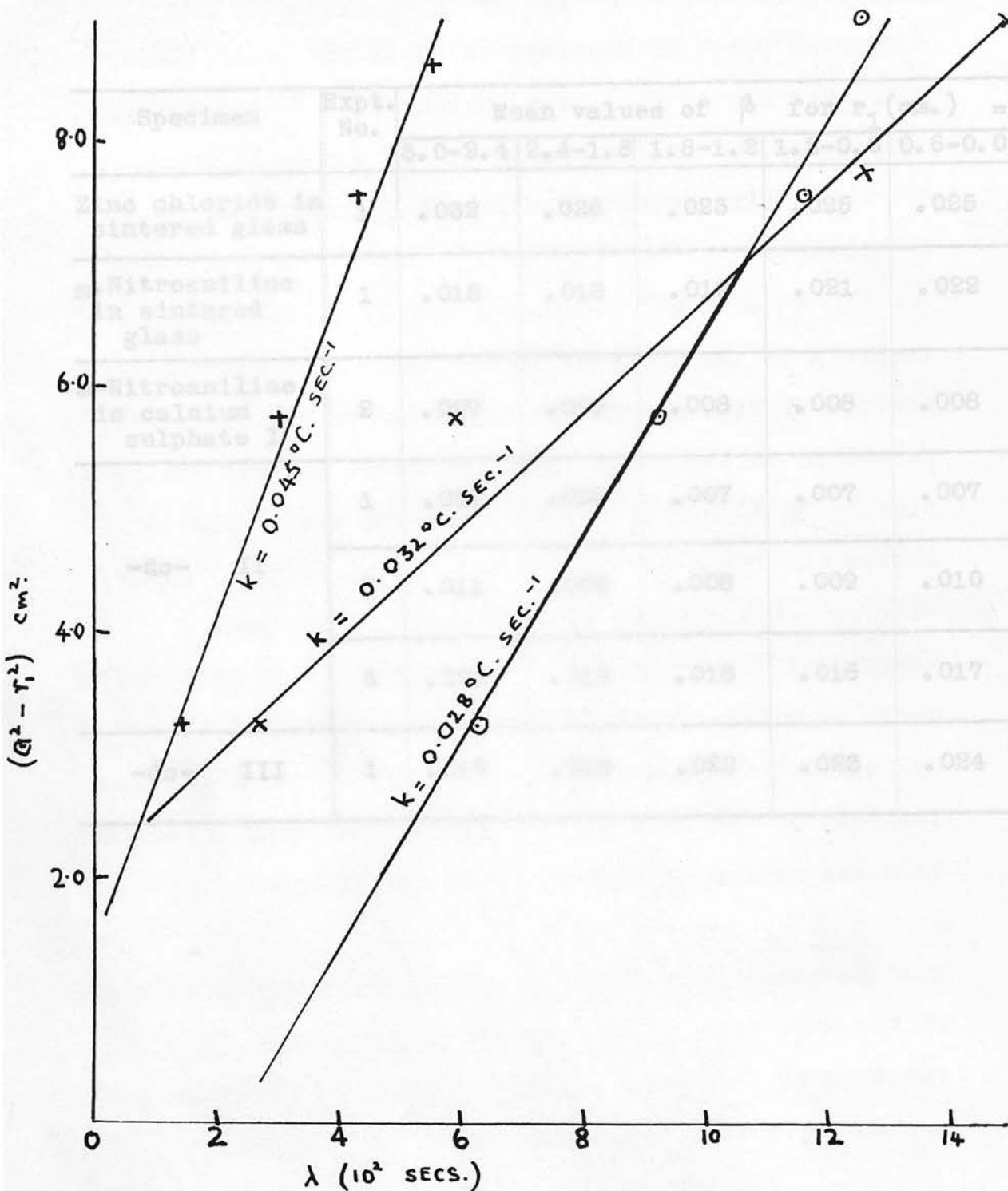


FIG. 29. FUSION OF m-NITROANILINE :  
 $a^2 - r_1^2$  vs.  $\lambda$ .



$((Kt)^{1/2}/r) \exp.(-r^2/4Kt) - \frac{1}{2} \frac{1}{2} \operatorname{erfc}(r/2(Kt)^{1/2}) \dots (6)$   
 in spherical coordinates (30).

The third term of equation (2) can be expressed as a sum of terms similarly to (6). Again, the steady state part of (2) satisfies the condition

$$-r \frac{dr}{dt} = \text{constant} \dots (7)$$

for the progress of a heat wave-front through the sphere.

Now from equation (4) we have

$$X \frac{dX}{d\lambda} = \frac{1}{2} k^2 = \text{constant} \dots (8)$$

Comparing (7) and (8), it seems therefore reasonable to suggest, for the propagation of melting through a sphere with steadily rising surface temperature, an expression similar to (7), namely,

$$-r_1 \frac{dr}{d\lambda} = \text{constant} \dots (9)$$

which, on integration, gives

$$a^2 - r_1^2 = \beta \lambda \dots (10)$$

(since  $r_1 = a$  at  $\lambda = 0$ ), where  $\beta$  is a constant which we may call, for descriptive purposes, the "propagation rate". It is the rate of change of  $(a^2 - r_1^2)$  in  $\text{cm.}^2 \text{sec.}^{-1}$ .

The mean values of  $\beta$  over various ranges in the sphere for some of the experiments of Table V are shown in Table Va, and the graphs of  $(a^2 - r_1^2)$  against

$\lambda$  for m-nitroaniline are shown in Fig.29. Having regard to the general degree of control and accuracy

attainable in these experiments and with the reservations of pages 49 - 50 and 57 - 58, the propagation equation in the present range within  $a^2 - r_1^2 = \beta\lambda$  may therefore be regarded as in fair agreement with the observation. The experiments on fusion described in preceding sections. Since the two phases are solid it is subject to no special treatment, and all parameters can be fairly rigidly controlled.

The specimen was reduced to powder of particle size below an arbitrary maximum (which was fixed for all experiments). It was hand-pressed into the specimen-holder with thermocouples in place, to an arbitrary maximum density which was then kept fixed for all further experiments by using the same mass of material every time.

#### IV. 2. Crystalline Inversion of Potassium Nitrate:

Potassium nitrate is known to exist in two crystalline forms, rhombic and trigonal columnar, the transition from one to the other taking place reversibly at the fixed temperature of 129°C. The inversion is thus not of the rate-controlled type but of the Stefan or latent-heat type (p.4). The inversion is also endothermic in the forward direction and the results therefore offer comparison with those of fusion experiments. The compound

##### IV. 2. 1. Summary of general results:

The same remarks, on the general effects of heating rate and the distance,  $r$ , from the centre on the

itself is highly stable up to its melting point ( $334^{\circ}\text{C}.$ ) The separation of the two temperatures offers a convenient range within which to carry operations to steady conditions on both sides of the transition temperature, in contrast to the experiments on fusion described in preceding sections. Since the two phases are solid it is subject to no special treatment, and all parameters can be fairly rigidly controlled.

The specimen was reduced to powder of particle size below an arbitrary maximum <sup>(0.6 mm.)</sup> which was fixed for all experiments. It was hand-pressed into the specimen-holder with thermocouples in place, to an arbitrary maximum density which was then kept fixed for all further experiments by using the same mass of material every time. Variation in concentration was easily achieved by dilution with powdered glass of roughly the same range of particle sizes, the desired concentration being obtained by removing a known amount of potassium nitrate and substituting an equivalent amount of glass, taking into account the difference in specific gravities and ease of packing. Measurements of temperature were taken for the surfaces  $r = 0.3, 0.9, 1.5, 2.1, 2.7$  cm.

#### IV. 2. 1. Summary of general results:

The same remarks, on the general effects of heating rate and the distance,  $r$ , from the centre on the

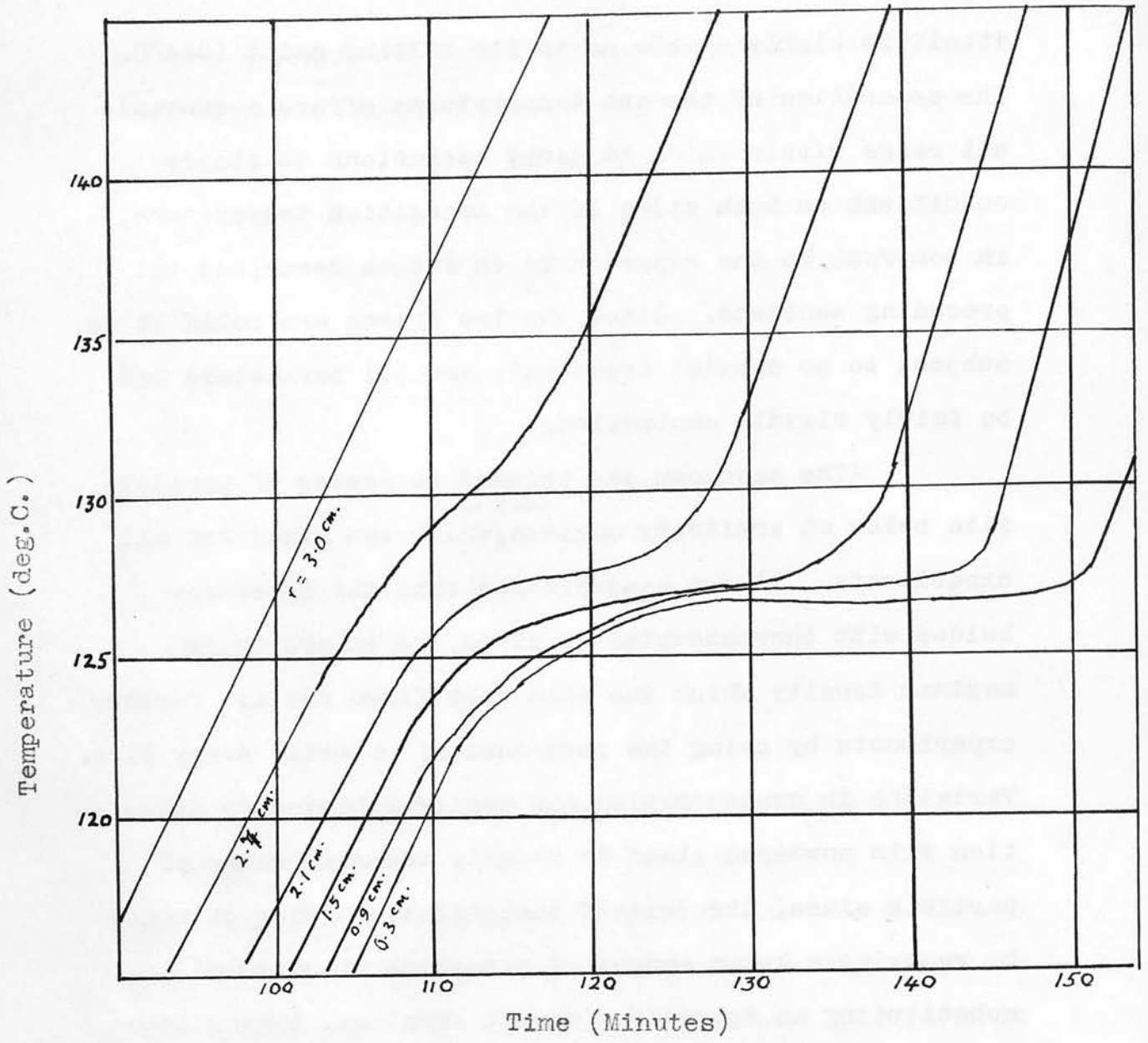


Fig. 30. Heating Curves for Potassium Nitrate, Surface Temperature =  $0.017t$  deg.C.

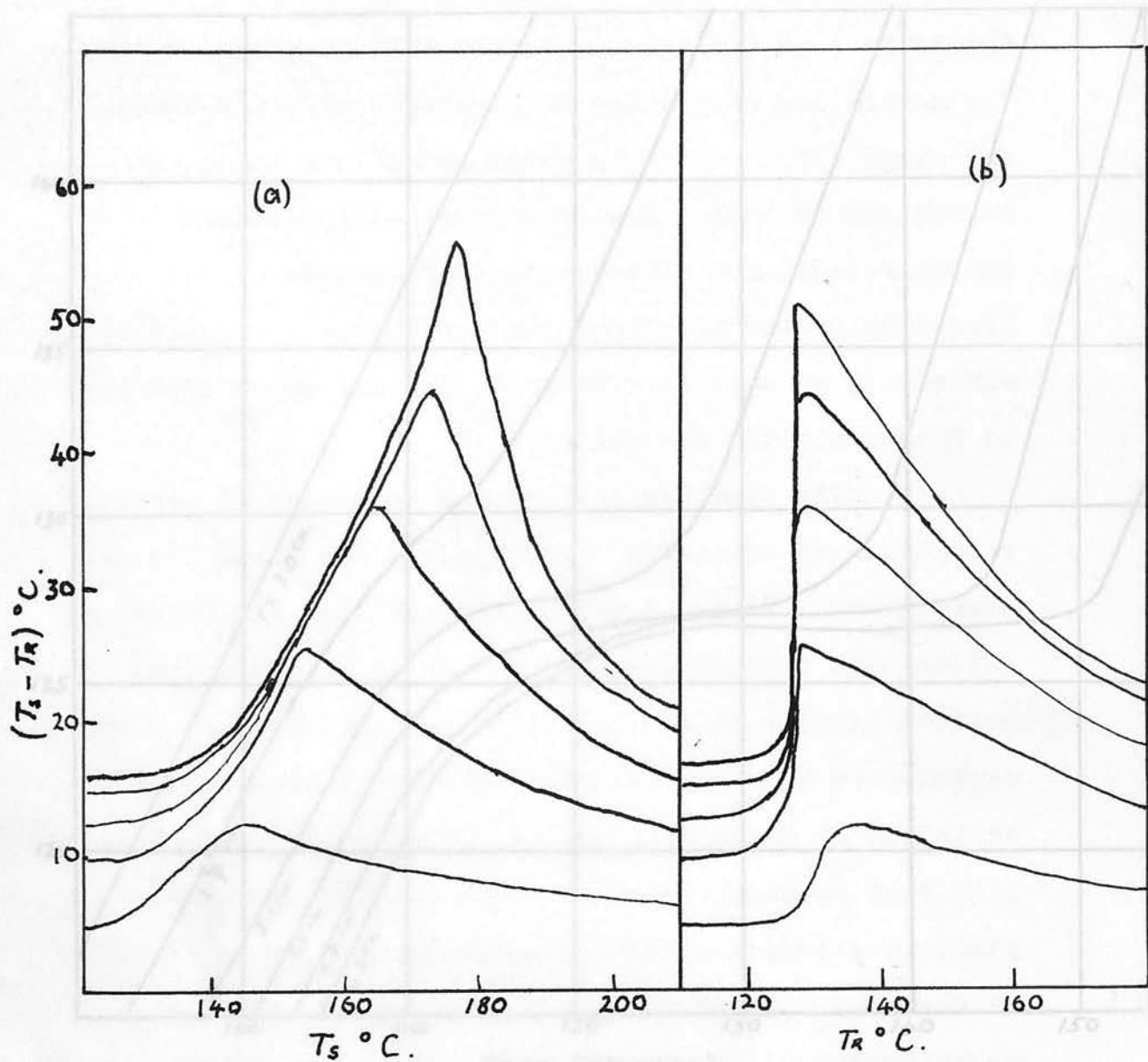


FIG. 31. DIFFERENTIAL TEMPERATURE CURVES  
FOR POTASSIUM NITRATE ( $k = 0.017^\circ\text{C./sec.}$ ).

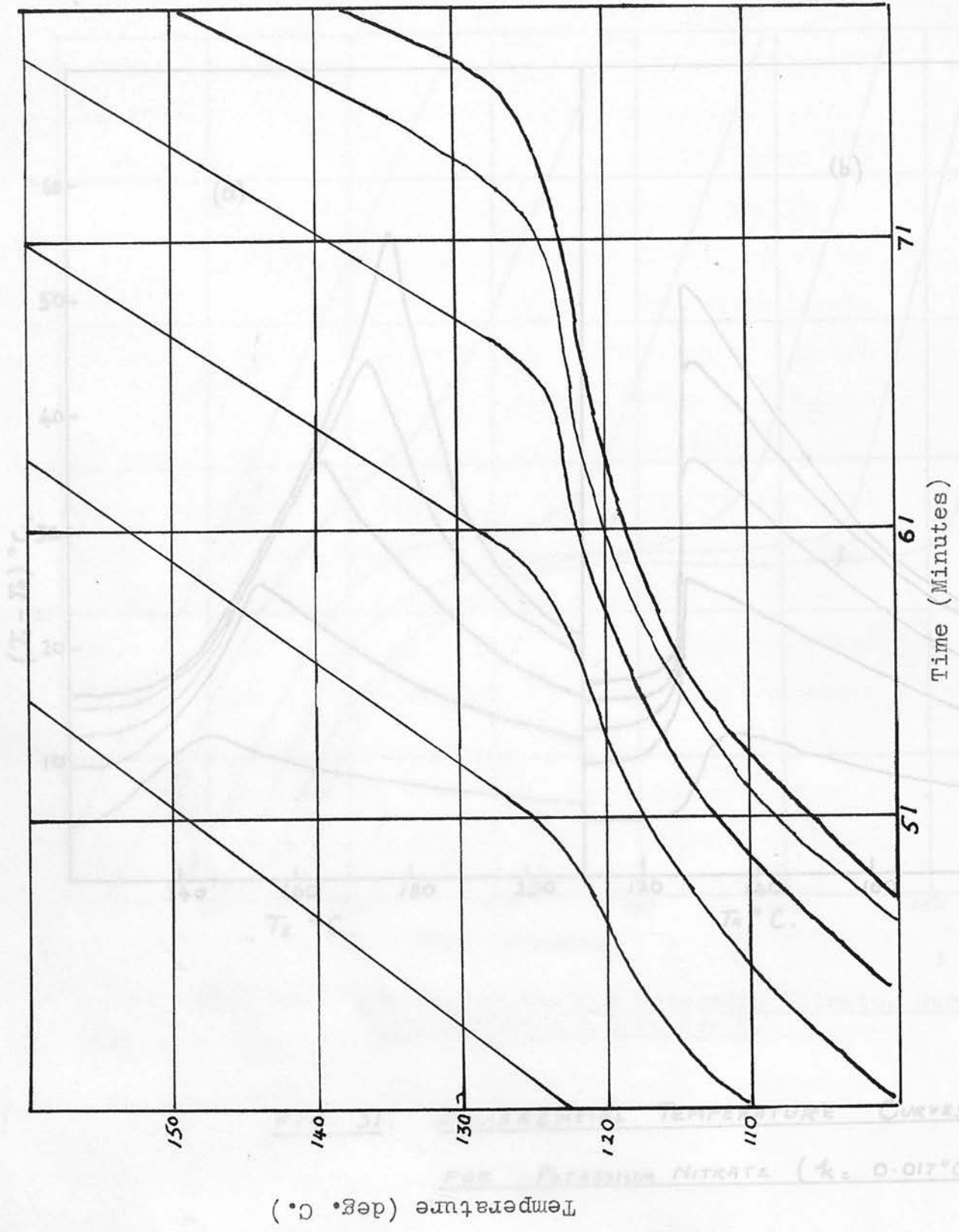


Fig. 32. Heating Curves for Potassium Nitrate, Surface Temperature = 0.041t deg.C.

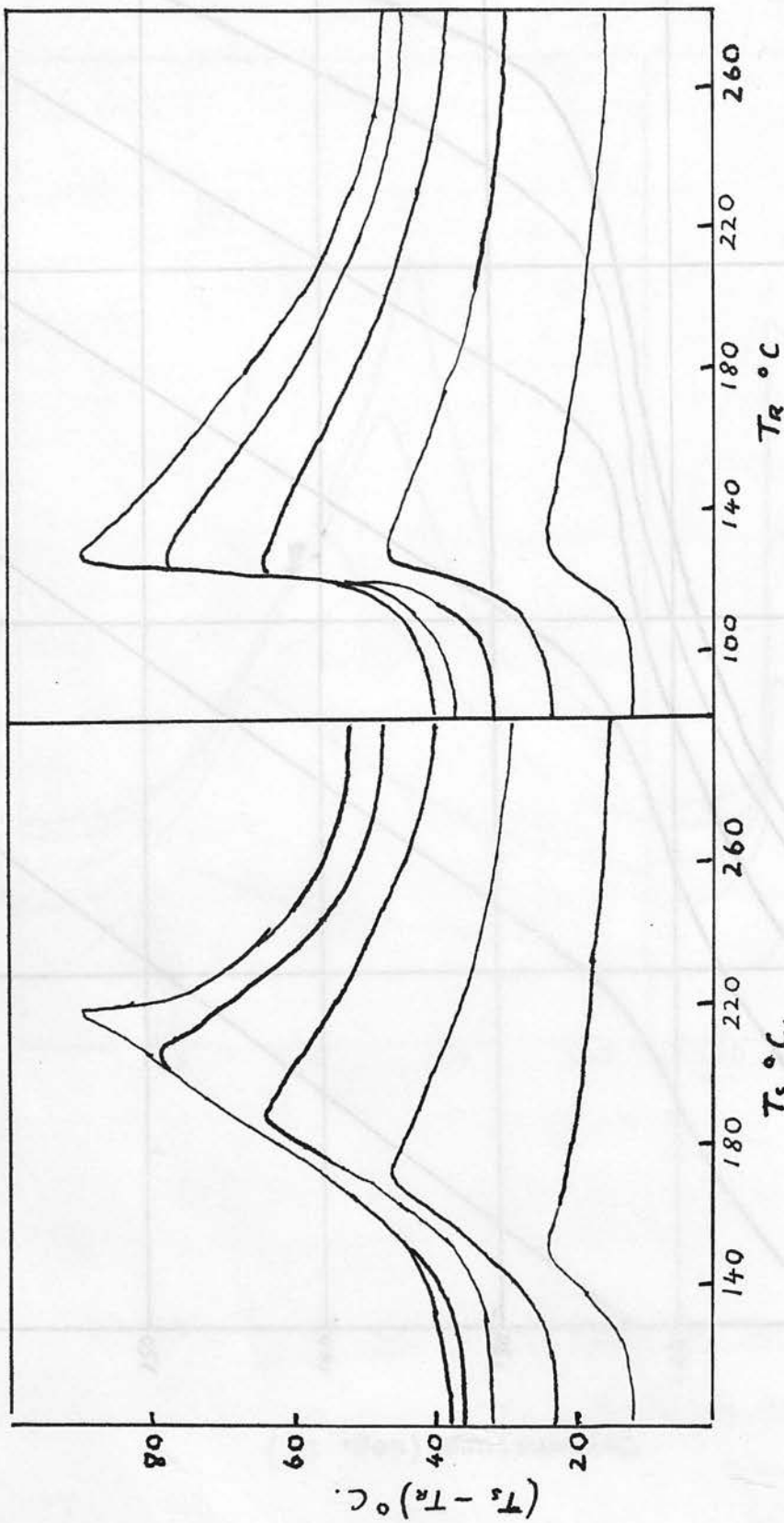


FIG. 33. DIFFERENTIAL TEMPERATURE CURVES FOR POTASSIUM NITRATE ( $k = 0.041 \text{ deg. C. sec.}^{-1}$ )

51 61 71  
Time (Minutes)

Fig. 52. Heating Curve for Potassium Nitrate. Surface  
Chemistry of the Salt.

characteristics of the heating and differential temperature curves, made in respect of the fusion experiments, apply also, without modification, to the results on crystalline inversion of potassium nitrate at  $129^{\circ}\text{C}$ .

It is also easier to study this reaction in greater detail since any concentration of the material from zero to 100 per cent. could be used.

Two pairs of heating and differential temperature curves are shown in Figs. 30 - 33 for the same specimen of undiluted potassium nitrate heated at 0.017 and 0.041 deg.C. sec.<sup>-1</sup> respectively. The main features of these curves, as of those of Figs. 17 - 19 and 23 - 25 are thus as follows:-

- (a) the endothermic arrests in general commence, for points in the interior of the sphere, at temperatures below the transition temperature, the extent of the divergence increasing with rate of heating. Recovery, in general, may also set in at a given point before that point reaches transition temperature. This means that on the corresponding d.t. curve, maximum is reached before transition temperature is attained.
- (b) the maxima on the differential temperature curve, when plotted as a function of surface temperature, show the usual progressive shift



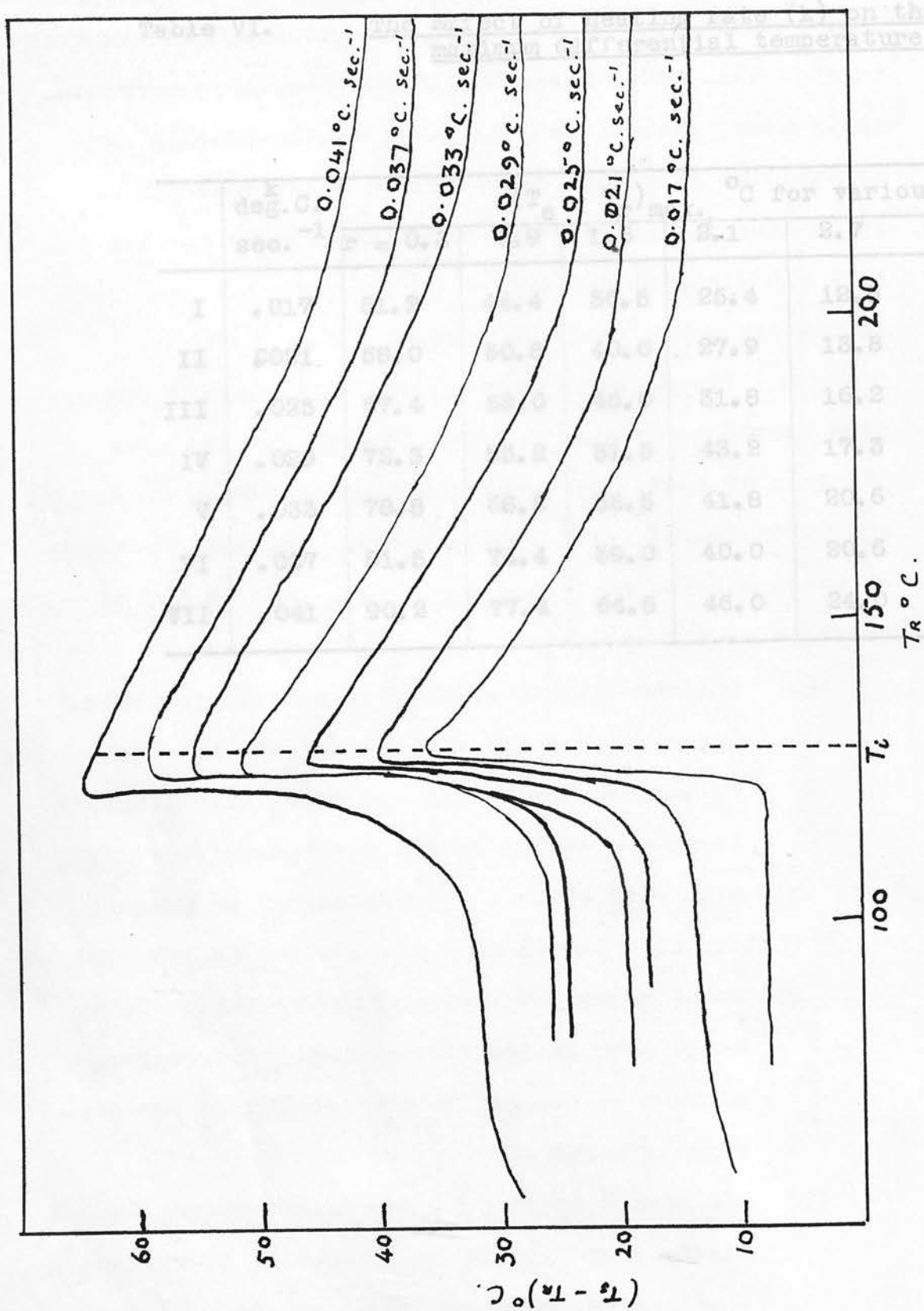


FIG. 34. D.T. CURVES FOR  $KNO_3$  AT  $\gamma = 1.5$  cm. FOR THE VALUES OF  $k$  SHOWN.

as we move from the surface towards the centre, but tend to occur at the same temperature when differential temperature is plotted as a function of temperature at that point, the actual position being usually <sup>on the low temperature side</sup> ~~to the left~~ of the transition temperature;

- (c) the propagation of crystalline inversion through the sphere obeys the same law as that for propagation of melting, namely,

$$a^2 - r_1^2 = \beta \lambda \dots\dots\dots (10)$$

For the purposes of discussion, the quantity  $\beta$  in equation (10) will be called the rate of propagation of the reaction through the sphere. As this quantity plays an important role in the mathematical theory developed in the next chapter (Chapter V), some of its properties under varying conditions of experiment will be discussed, (among other things), in fuller detail in the sections that follow.

#### IV. 2. 2. Effects of Heating Rate.

Whereas Figs. 31b and 33b illustrate the fact that the maxima on the curves of differential temperature as a function of temperature inside the sphere tend to occur, for all  $r$ , at or near the same temperature, Fig. 34 shows that this temperature lies further and further to the left of the transition temperature as heating rate is

Table VII. The effect of heating rate on the propagation of crystalline inversion through sphere of potassium nitrate.

	k deg.C. sec. <sup>-1</sup>	Time (secs.) at which 129 <sup>0</sup> C isothermal passes r(t = 0 at r = 3.0)					$\beta$ (cm. <sup>2</sup> sec. <sup>-1</sup> )
		r = 0.3	0.9	1.5	2.1	2.7	
I	.017	2904	2640	2118	1464	558	.305 x 10 <sup>-2</sup>
II	.021	2706	2394	1890	1314	684	.333 x 10 <sup>-2</sup>
III	.025	2544	2292	1812	1260	636	.350 x 10 <sup>-2</sup>
IV	.029	2436	2136	1722	1236	570	.395 x 10 <sup>-2</sup>
V	.033	2334	2034	1662	1206	564	.432 x 10 <sup>-2</sup>
VI	.037	2208	2016	1596	1056	504	.455 x 10 <sup>-2</sup>
VII	.041	2016	1800	1464	1056	540	.485 x 10 <sup>-2</sup>

Table VII. The effect of heating rate on the propagation of crystalline inversion through spheres of potassium nitrate.

Time (sec.) at which 10% isotherm passes $T(t=0) = 3.0$	Time (sec.) at which 10% isotherm passes $T(t=0) = 3.0$		Time (sec.) at which 10% isotherm passes $T(t=0) = 3.0$		Time (sec.) at which 10% isotherm passes $T(t=0) = 3.0$	
	$r = 0.3$	$r = 0.9$	$r = 1.5$	$r = 2.1$	$r = 2.7$	$r = 3.0$
I	2904	1440	2118	1464	588	$.305 \times 10^{-4}$
II	2706	1394	1690	1314	684	$.333 \times 10^{-4}$
III	2544	1298	1612	1260	536	$.350 \times 10^{-4}$
IV	2436	1212	1722	1236	770	$.395 \times 10^{-4}$
V	2394	1084	1662	1206	554	$.432 \times 10^{-4}$
VI	2194	924	1596	1056	524	$.455 \times 10^{-4}$
VII	2012	1692	1464	1086	544	$.485 \times 10^{-4}$

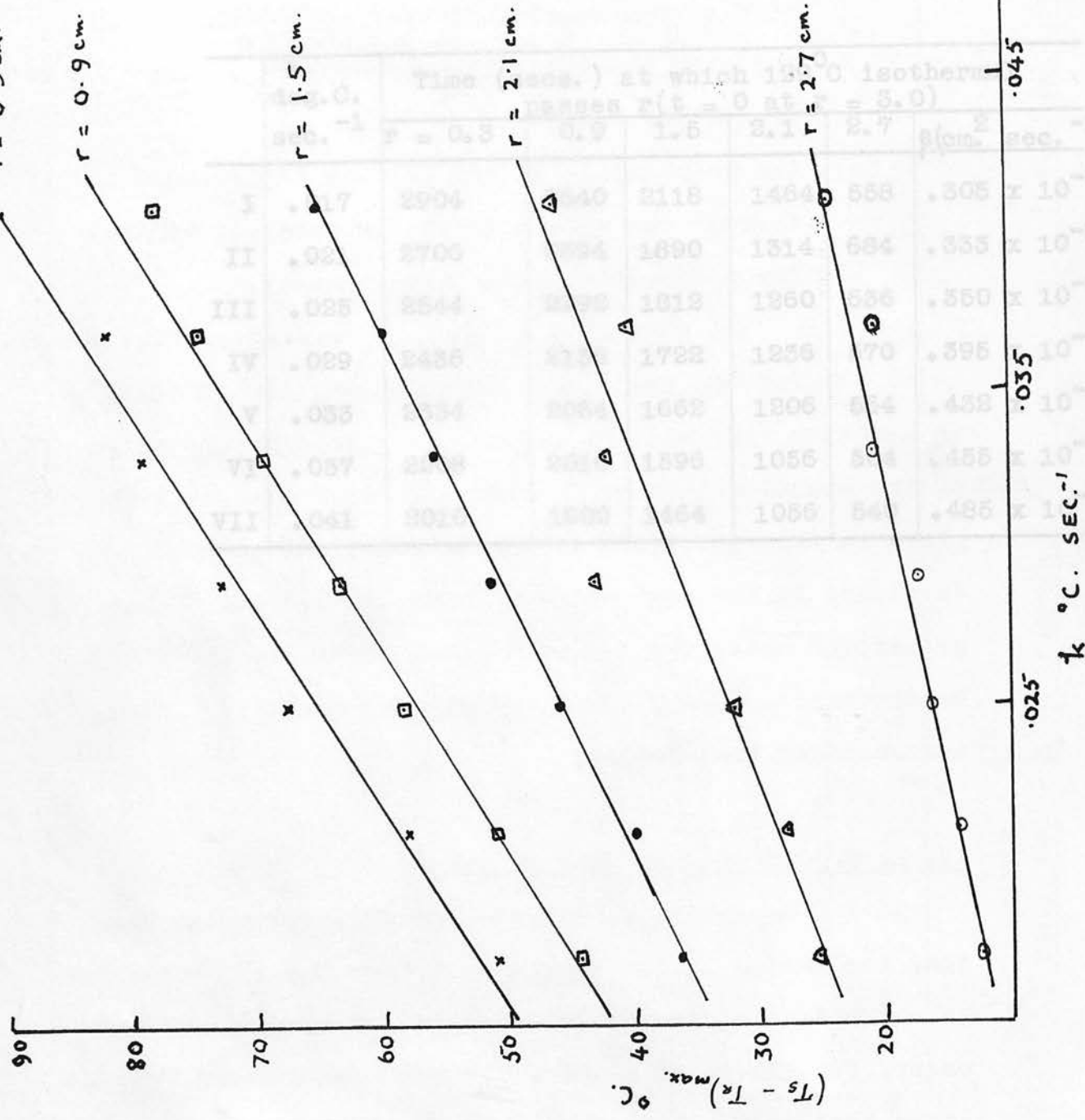


FIG. 35. VARIATION OF MAXIMUM DIFFERENTIAL TEMPERATURE WITH  $k$ .

Table VII. The effect of heating rate on the propagation of crystalline inversion through spheres of potassium nitrate.

Series	$r$ (cm.)	$T_{100}$ (°C.)	$T_{50}$ (°C.)	$T_{25}$ (°C.)	$T_{10}$ (°C.)	$\log_{10} \frac{1}{k}$	$\log_{10} \frac{1}{k}$ (sec.)
I	0.3	2904	2118	1464	868	.805	$\times 10^{-4}$
II	0.9	2766	2094	1314	684	.553	$\times 10^{-4}$
III	1.5	2544	1812	1260	536	.350	$\times 10^{-4}$
IV	2.1	2436	1722	1256	470	.395	$\times 10^{-4}$
V	2.7	2334	1662	1206	424	.432	$\times 10^{-4}$
VI	3.0	2232	1596	1056	378	.455	$\times 10^{-4}$
VII	3.0	2012	1484	1056	342	.485	$\times 10^{-4}$

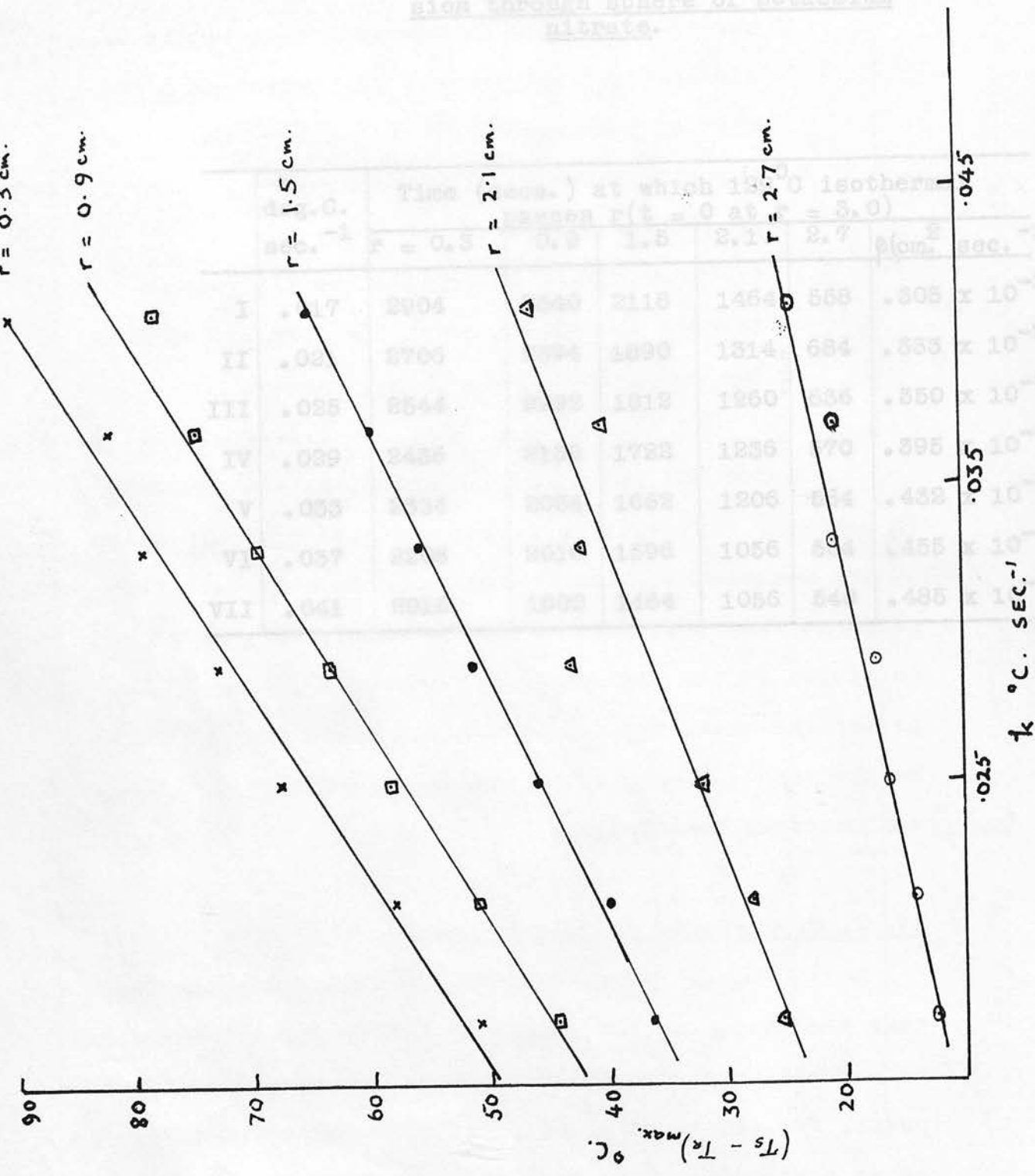


FIG. 35. VARIATION OF MAXIMUM DIFFERENTIAL TEMPERATURE WITH  $\frac{1}{k}$ .

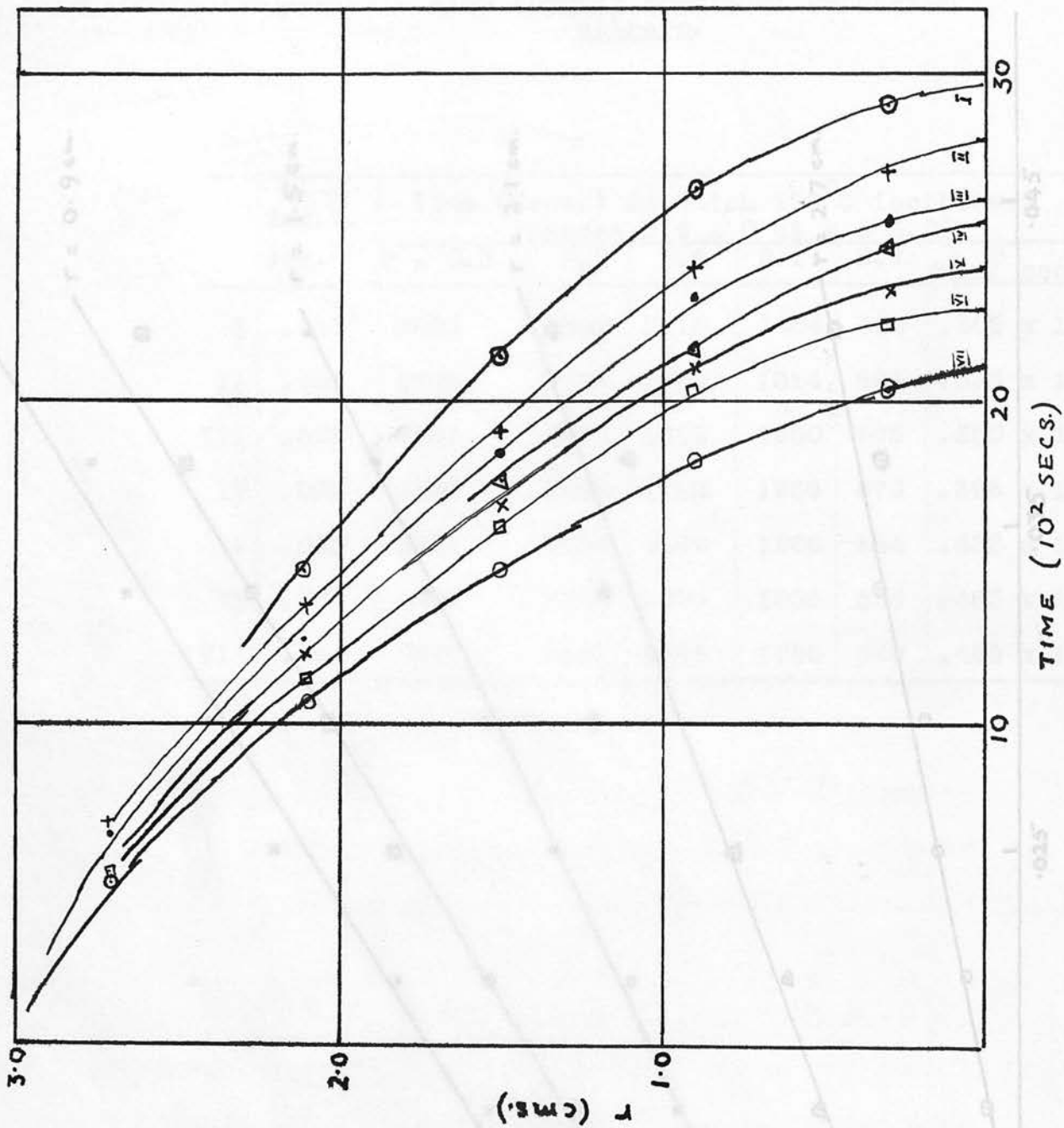


FIG. 36. CRYSTALLINE INVERSION OF  $KNO_3$ .  
PROPAGATION IN SPHERICAL MODEL.

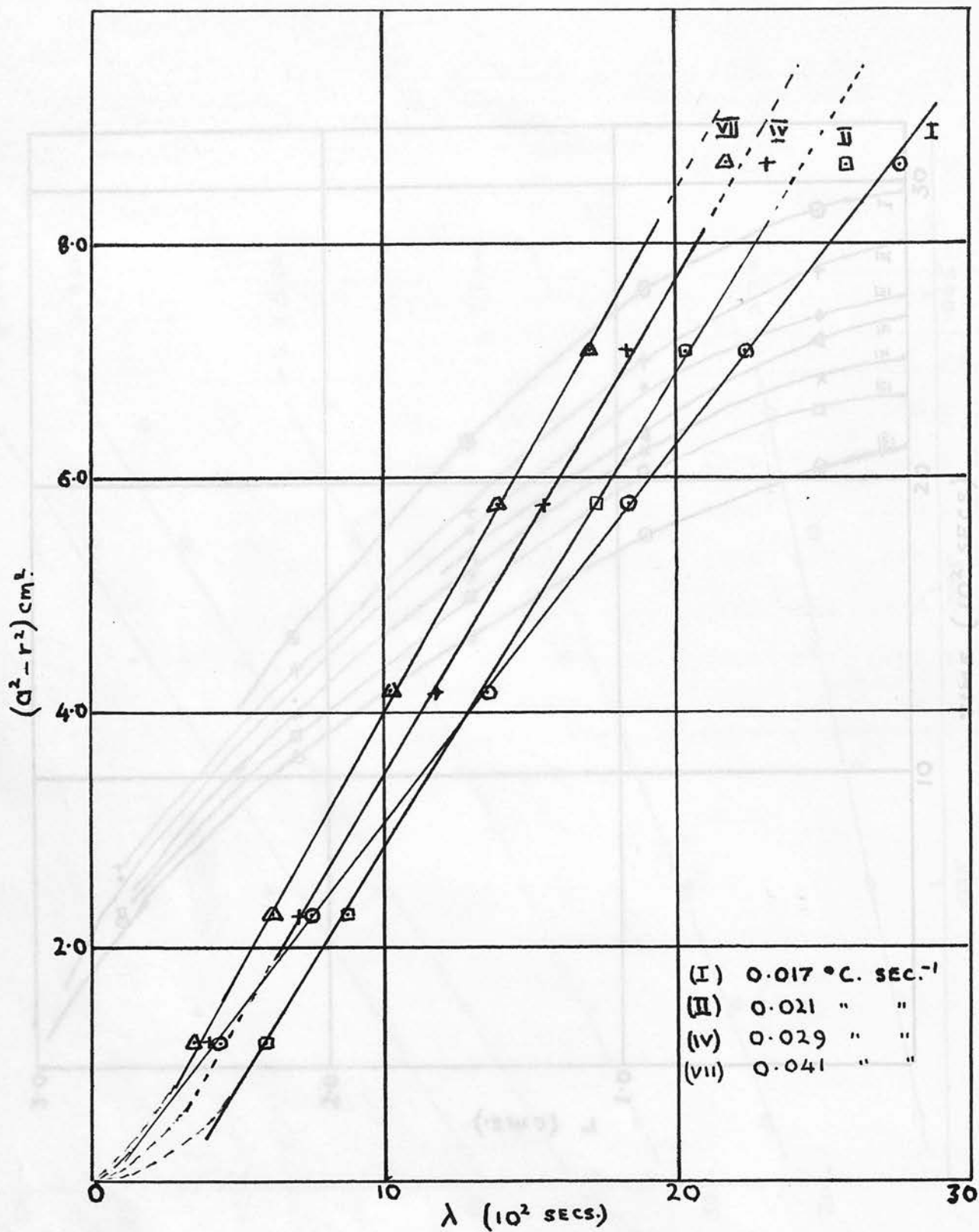


FIG. 37. INVERSION OF  $\text{KNO}_3$ :  $(a^2 - r^2)$  vs.  $\lambda$ .

increased. Table VI and Fig. 35 show the variation of peak height with rate of rise of surface temperature, the graphs indicating that, to a very close degree, the magnitude of the maximum differential temperature at all points in the sphere is proportional to the rate of heating.

The effect of the heating rate on the rate of propagation is shown in Table VII. The propagation curves are shown in Fig. 36. When the quantity  $(a^2 - r_1^2) \text{ cm.}^2$  is plotted against time (Fig. 37), the graphs are again linear, confirming the equation

$$a^2 - r_1^2 = \beta \lambda \quad \dots\dots\dots (10)$$

but the value of  $\beta$  is found to increase with increasing rates of rise of surface temperature. The <sup>agreement, as shown by</sup> ~~linearity~~ of the curves of Fig. 37, is not very good near the surface, i.e. for <sup>low</sup> ~~high~~ values of  $(a^2 - r_1^2)$ , and this is shown also when  $\beta = (a^2 - r_1^2) / \lambda$  is calculated for various values of  $r_1$  at intervals of 0.2 cm.: the values of  $\beta$  are found to be reasonably constant up to  $r_1 \doteq 2.4$  cm. when it shows a gradual drop, the relative drop increasing with heating rate. This is probably due to the fact that the reference temperature was not taken at the surface of the sphere but at a point inside the specimen holder about  $\frac{1}{8}$  inch from the surface of the specimen (see II.1), and, since the time at which this point reaches transition temperature is taken as zero, an error



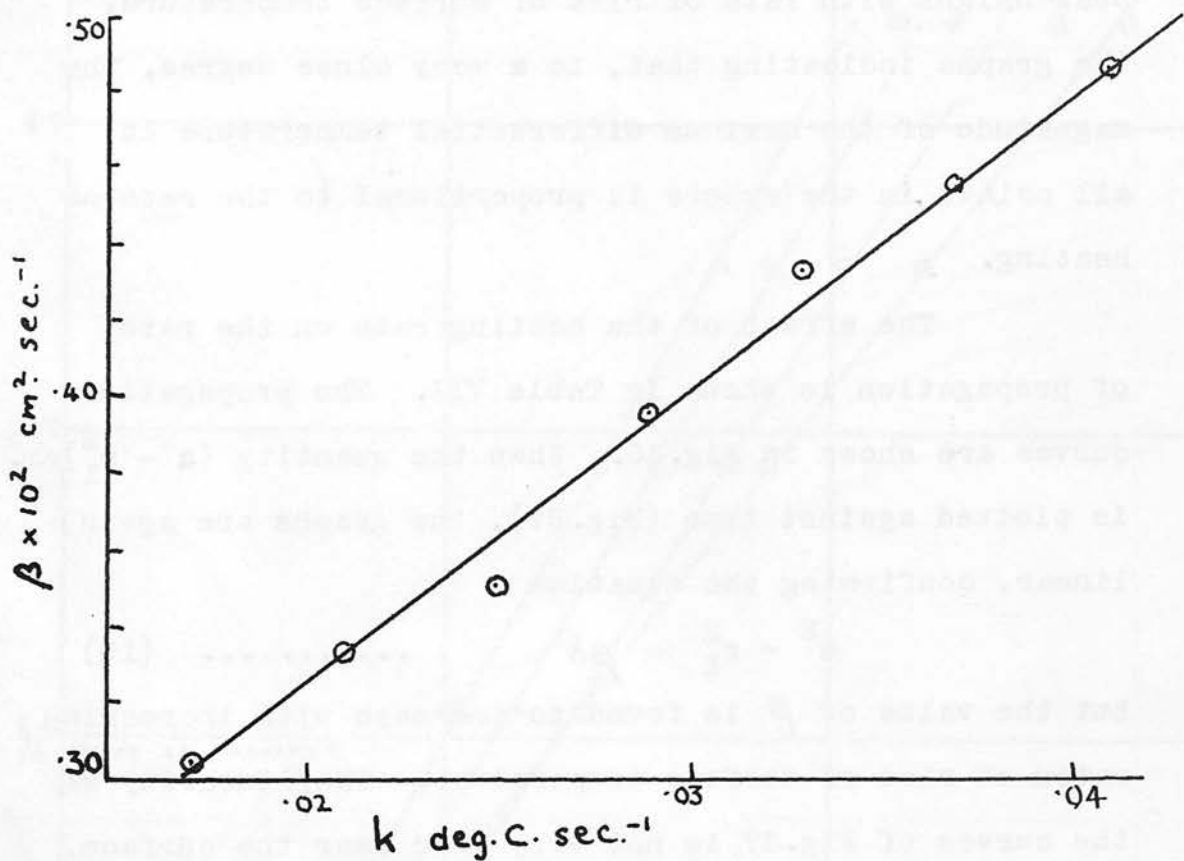


FIG. 38. INVERSION OF  $\text{KNO}_3$ : PROPAGATION RATE AS A FUNCTION OF HEATING RATE.

is introduced by the time lag between equivalent temperatures inside the specimen holder and the surface of the specimen, not so much as a result of the "relaxation time" for the specimen holder, which is only of the order of 0.5 second for  $\frac{1}{8}$  inch of mild steel, but more as a result of thermal resistance between the steel walls and the specimen, especially since it was found expedient to coat the inside walls with graphite in vaseline. The equivalent conductivity of such a skin, only 0.1 mm. thick, is about 0.04, i.e. about one-third the thermal conductivity of the specimen block. Deviation from the parabolic relation occurs also near centre when the heating rate is high as is shown increasingly by the lines II - VII in Fig. 37, where at a heating rate of  $0.017^{\circ}\text{C. sec.}^{-1}$ , there is an almost exact fit (the line I). The significance of this will be discussed in the next chapter (Chapter V).

#### IV. 2. 3. Effect of the concentration of reacting material

Experiments designed to test the effect of concentration of reacting material on the height of the maxima of differential temperatures and on the propagation rate are far less conclusive than those in which only the heating rate is altered and the same specimen used throughout, owing to the difficulty of ensuring that all experi-

Table VIII. Effect of concentration of reacting material ( $C$  grams  $\text{cm.}^{-3}$ ) on the maximum differential temperature

k deg.C. $\text{sec}^{-1}$	gm. $\text{cm.}^{-3}$	$(T_s - T_r)_{\text{max}}$ (arbitrary units) for various r				
		r = 0.3	0.9	1.5	2.1	2.7 cm.
$.033 \pm .001$	1.09	11.0	31.5	48.0	58.0	63.0
$.033 \pm .001$	0.93	8.7	25.9	40.8	53.2	60.0
$.033 \pm .002$	0.78	7.6	26.4	40.2	50.4	56.2
$.034 \pm .002$	0.62	7.8	26.2	40.8	52.3	60.4
$.033 \pm .001$	0.47	6.7	22.3	32.8	40.7	45.5

Table IX. Effect of concentration of reacting material on propagation.

C	Diffusivity $K \times 10^3$	Time (secs.) at which $129^\circ\text{C}$ isothermal passes r					
		r = 3.0	2.7	2.1	1.5	0.9	0.3 cm.
1.09	1.86	0	195	758	1050	1095	1155
0.93	1.81	0	228	600	972	1098	1152
0.78	1.80	0	98	510	723	1005	1073
0.62	1.70	0	218	758	1163	1485	1635
0.47	1.76	0	150	585	885	1050	1290

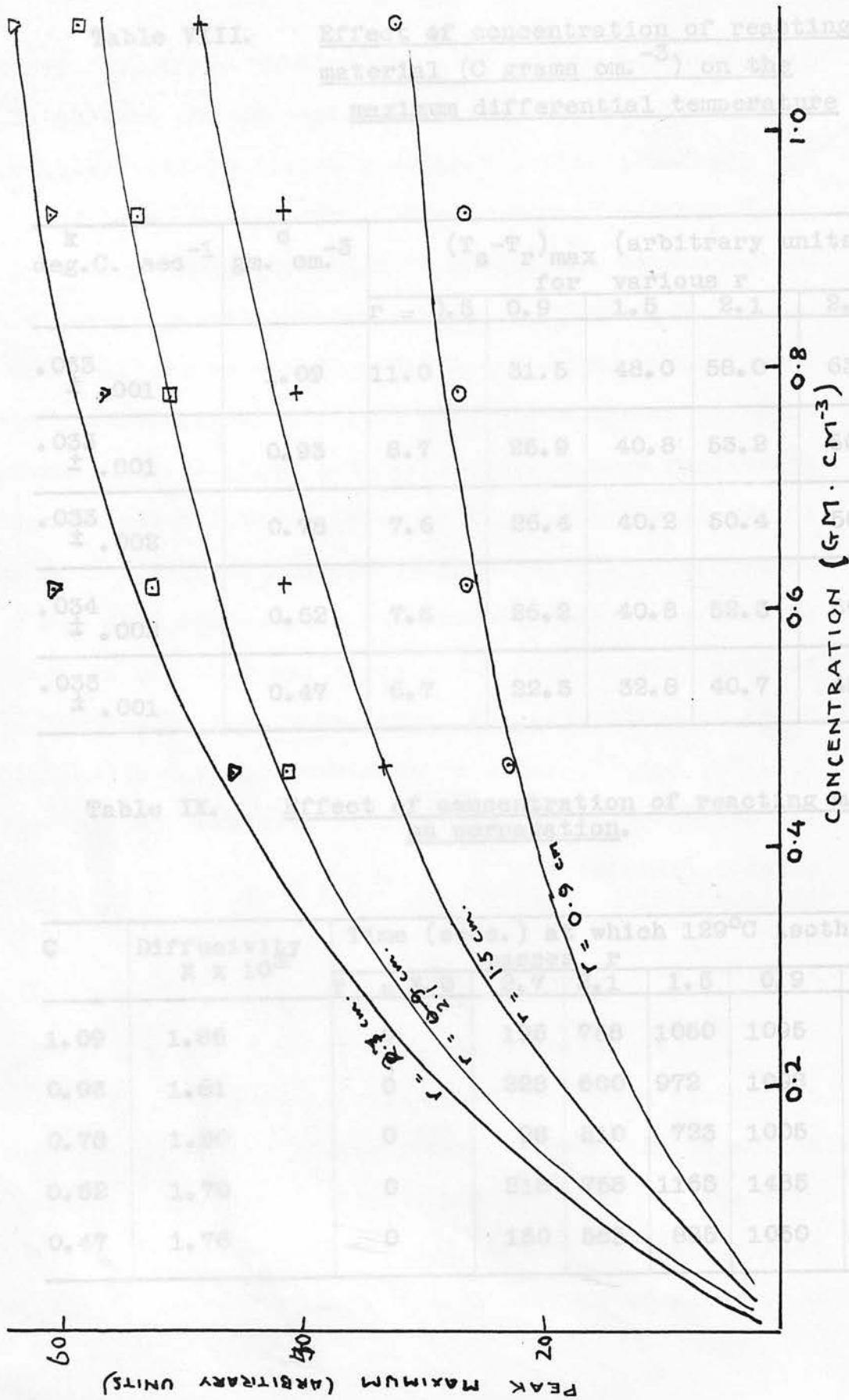


FIG. 39. EFFECT OF CONCENTRATION ON MAXIMUM OF PEAK.

mental conditions, most especially the condition of packing of the test material, are exactly reproduced as between one specimen and another.

The results for one such series of experiments, in which different samples containing varying amounts of powdered glass as diluent to obtain different distributions (grams per cm.<sup>3</sup>) of potassium nitrate, are shown in Tables VIII and IX and Figs. 39 and 40. Table VIII shows that the maximum of the differential temperature increased with concentration of reacting material for a given rate of rise of surface temperature, and, although, within the range of concentrations used, the dependence is nearly linear, it must be assumed that at zero concentration, the differential temperature, maximum or otherwise, must be zero, so that the dependence would be as shown in Fig. 39. Comparison with the results for relationship between heating rate and maximum differential temperature also shows that the increase with concentration is not so well marked as the increase with heating rate. This again underlines the importance of temperature control in differential thermal analysis, as is illustrated by the anomalous result for the concentration 0.62 gm.cm.<sup>-3</sup>, where an error of about 20% in the maximum arises from a deviation of only 3% in the heating rate. Such anomalies are more likely to occur at  $r = \frac{1}{2}a$  and least likely at  $r = 0$  because, as will be shown later, the boundary

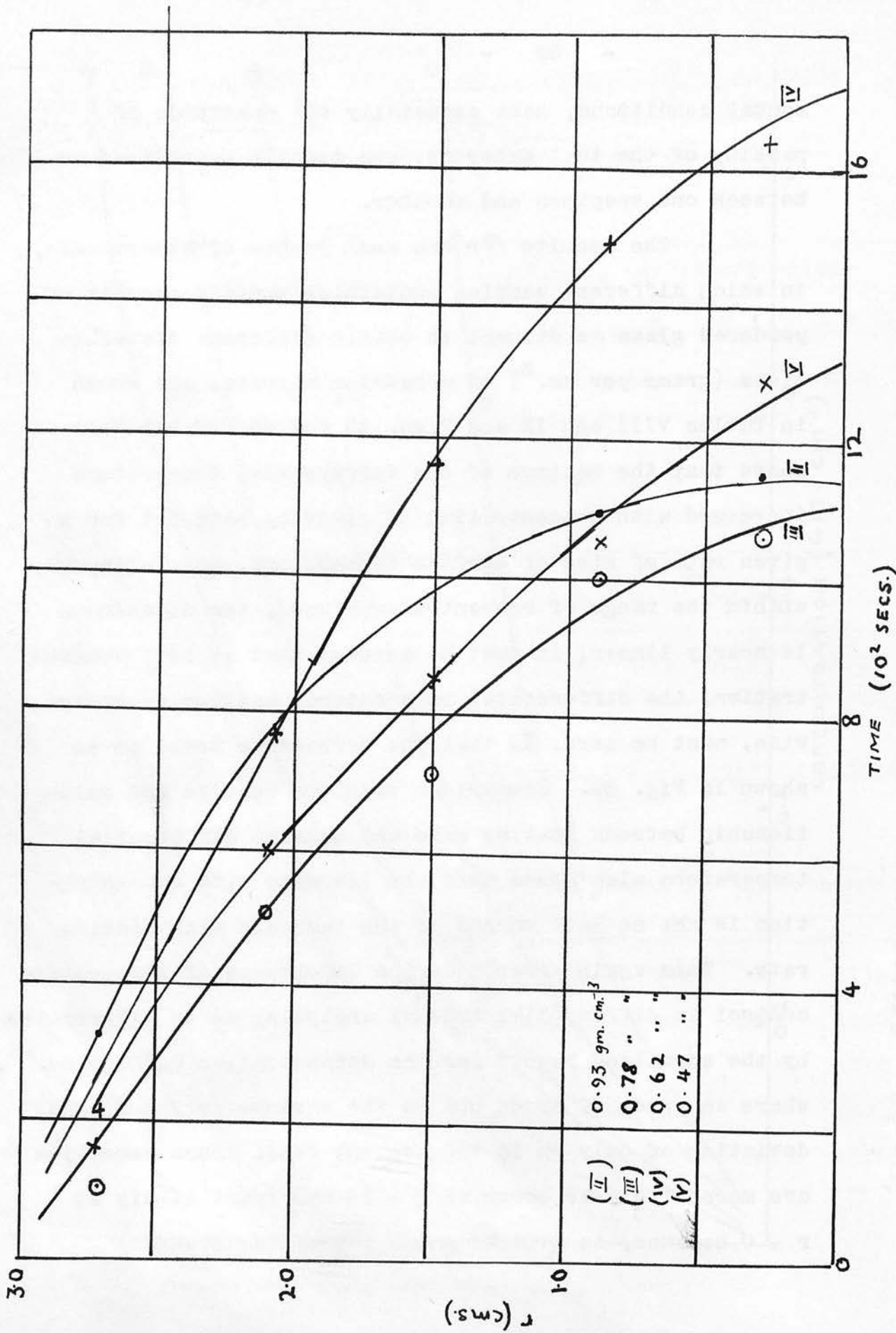


FIG. 40. INVERSION OF  $KNO_3$ . PROPAGATION FOR VARIOUS CONCENTRATIONS.

conditions demand that the contribution of the thermal effects to total temperature should be zero at  $r = a$ , and the solution of the problem is such as to make this contribution also tend to infinity (with certain limitations) at the centre, whereas at a point midway between the surface and the centre, relative errors are bound to become large.

No valid conclusions are possible on the dependence of propagation rate on concentration, as Table IX and Fig. 40 show. The times for completion of reaction throughout the sphere is of the same order of magnitude, viz., about 1200 seconds, for all concentrations used, except one, the  $0.62 \text{ gm. cm.}^{-3}$  concentration, whose results have been shown to be anomalous. A glance at the second column of that table, however, would seem to suggest that the main controlling factor on propagation rate is the thermometric conductivity of the medium, which in the case of the specimen referred to, is much lower than the average for the other specimens, which is  $1.81 \times 10^{-3} \text{ cm.}^2 \text{ sec.}^{-1}$ . This is further illustrated by the fact that two specimens of pure test material heated at equal rates of  $0.034^\circ\text{C sec.}^{-1}$  were found to require 1045 and 2410 seconds respectively for completion of reaction at  $r = 0$ , thus giving for the propagation rates

$$\beta = a^2 / \lambda_{\text{max}} \quad (\text{approximately}) \\ = .78 \times 10^{-2} \text{ and } .37 \times 10^{-2} \text{ cm.}^2 \text{ sec.}^{-1}$$

respectively. These were found to possess thermometric

conductivities. medium has reached this temperature at

$$K = 1.3 \times 10^{-3} \text{ and } 1.1 \times 10^{-3} \text{ cm.}^2 \text{ sec.}^{-1}$$

respectively. ergence between the temperature of maximum

Thus in Table IX, the effect of concentration reacting material on propagation rate seems to be negligible compared with the effect of diffusivity of the medium in the range of concentration used. It is essential, therefore, if the effect of concentration alone is to be investigated, that the specimens used and experimental conditions must be identical in all other respects and this, as we have seen, is difficult to achieve, especially when only manual handling and control is used throughout. This goes, in part, to explain some of the inconsistencies of results reported by different workers for the same or similar naturally occurring substances.

(c) the propagation of the reaction obeys the law  
IV. 2. 4. Notes on results: (10)

The similarity of the general results for the fusion of zinc chloride and m-nitroaniline on the one hand, and for the crystalline inversion of potassium nitrate on the other, tends to justify the assumption that the two types of reaction are subject to similar treatment and analysis. The main points of these results are:

- (a) endothermic arrests occur in the neighbourhood
- (d) of the transition temperature, usually before (10)



the medium has reached this temperature at the point where measurement is taken, the divergence between the temperature of maximum arrest increasing with rate of rise of temperature and with distance from the surface of the specimen; on differential temperature curves, plotted against temperature of specimen, this results in corresponds to occurrence of maximum of peaks at temperatures below transition temperature;

(b) the magnitude of the maximum differential temperature (height of peak) increased with rate of rise of surface temperature and concentration of reacting material; the relationship with concentration is nearly linear over limited ranges of concentration;

(c) the propagation of the reaction obeys the law

$$a^2 - r_1^2 = \beta \lambda \dots\dots\dots (10)$$

a relation which is analogous to that for a semi-infinite reacting medium, with constant surface temperature, viz.,

$$x^2 = \beta \lambda$$

and also to that for the progress of an isothermal through a sphere heated at the rate  $k$  and in which no reaction is taking place, i.e.

$$a^2 - r^2 = 6Kt$$

(d) the magnitude of the constant  $\beta$  in equation (10)

increases linearly with rate of rise of surface temperature, and there are indications that its value increases with the thermometric conductivity of the medium, but no general conclusions on the effect of concentration or reacting material. The theory given here also provides an attempt will be made to explain some of these results in the next chapter.

Methods of calculation based on an empirical relationship between the concentration of reacting material, on the one hand, and the area bounded by the differential temperature curve and the axes of coordinates on the other, have been studied in detail by various workers, notably Spell<sup>(48)</sup>, Vold<sup>(49)</sup>, Kerr, Kulp and Hamilton<sup>(50)</sup>. Discrepancies have been found in the calculated results owing partly to poor reproducibility of experimental technique and apparatus, and partly to the error of taking the whole of the area under the peak as proportional to the total heat liberated, instead of that portion of the area bounded by the ordinate corresponding to completion of reaction at the centre (See Fig. 20). This error has been indicated by Tsang<sup>(51)</sup> and is discussed further in this chapter.

#### V. 1. Symmetrical radial flow with temperature

$$P = \frac{4\pi k l}{r} \text{ at } P = \frac{4\pi k l}{r}$$

In the absence of heat generation or absorption

Chapter V.

THEORETICAL ANALYSIS OF THE STEFAN PROBLEM.

In this chapter an attempt is made to explain some of the properties of the differential temperature in terms of heat flow within the sphere, using known solutions of the heat equation. The theory given here also provides an easy but quite effective method for the calculation of the heat of reaction from the differential temperature curve. Methods of calculation based on an empirical relationship between the concentration of reacting material, on the one hand, and the area bounded by the differential temperature curve and the axes of coordinates on the other, have been studied in detail by various workers, notably Speil<sup>(48)</sup>, Vold<sup>(49)</sup>, Kerr, Kulp and Hamilton<sup>(50)</sup>. Discrepancies have been found in the calculated results owing partly to poor reproducibility of experimental technique and apparatus and partly to the error of taking the whole of the area under the peak as proportional to the total heat liberated, instead of that portion of the area bounded by the ordinate corresponding to completion of reaction at the centre (See Fig.20). This error has been indicated by Tsang<sup>(51)</sup> and is discussed further in this chapter.

V. 1. Symmetrical radial flow with temperature

$$\theta = kt \text{ at } r = a.$$

In the absence of heat generation or absorption

within the medium, the temperature,  $\theta(r,t)$ , in the sphere  $0 < r \leq a$  with initial uniform temperature  $\theta_0$  and surface temperature  $kt$  at  $t \geq 0$  is given by

$$\theta(r,t) = \theta_0 + kt - k(a^2 - r^2)/6K - (2ka^3/K\pi^3r) \sum_{n=1}^{\infty} (-1)^n n^{-3} \sin(n\pi r/a) \times \exp. (Kn^2\pi^2t/a^2) \dots \dots \dots (2)$$

which after a sufficient time  $t$  depending on  $K$ , the thermometric conductivity of the medium, and  $a$ , the radius of the sphere, becomes, for all practical purposes,

$$\theta(r,t) = \theta_0 + kt - k(a^2 - r^2)/6K \dots \dots \dots (3)$$

In differential thermal analysis, the temperature recorded is

$$\theta(a,t) - \theta(r,t),$$

so that, we can write

$$\theta_{diff.} = k(a^2 - r^2)/6K \dots \dots \dots (12)$$

for the case where the only thermal effect is a rise in temperature. For this to be true, it must be assumed that the thermal conductivity, density and specific heat of the medium remain constant throughout the range of temperatures of the experiment. Thus, after a sufficient time  $t$ , the differential temperature curve as a function of time becomes sensibly constant, the steady state plot of differential temperature against time (or surface temperature, since this is proportional to time) becomes a straight line parallel to the  $t$ -axis. In practice, this is generally the case, i.e. the instruments of d.t.a.

are not usually sensitive enough to show changes in K, so that the assumption of the constancy of physical constants mentioned earlier on are justifiable.

V. 2. Inclusion of the source.

The solution of the heat equation for problems with radial symmetry and for sources within the medium must, to satisfy the experimental conditions, vanish at r = a. Such a solution can be expressed in the form

theta\_inst = (Q / (2 \* pi \* a \* r \* r\_1)) \* sum\_{n=1 to infinity} exp(-Kn^2 \* pi^2 \* t / a^2) \* sin(n \* pi \* r / a) \* sin(n \* pi \* r\_1 / a) ... (13)

which is the temperature at any time t at r due to an instantaneous spherical source of strength Q at t = 0 and situated at r\_1, the strength of a spherical source being defined as Q when a quantity of heat Q \* rho \* c is liberated at the surface of the sphere.

The problem of the moving source may be solved by taking the sum-over-all effect of a series of such sources integrated between the appropriate limits of time lambda, the position r\_1 of the source at any time lambda being a function of lambda. This procedure is due to Lightfoot.

Thus, if the source moves a distance -dr\_1 in time d lambda, the heat liberated is

H\_tr = -(4 \* pi \* r\_1^2) \* (dr\_1 / d lambda) \* d lambda \* rho \* L ... (14)

where rho = concentration of reacting material in gms.cm^-3, c = specific heat of medium

$t_1$   $L_{inst} =$  "latent heat" of transformation of reacting material, cal. gm.  $^{-1}$

This constitutes an instantaneous spherical source of strength  $Q$  given by

$$Q = -(4 \pi r_1^2 L/c) (dr_1/d\lambda) d\lambda \dots\dots\dots (15)$$

Hence the instantaneous temperature at  $r$  at time  $t > \lambda$  due to this source is given by

$$\theta_{inst.} = -(2Lr_1/acr) (dr_1/d\lambda) d\lambda \sum_{n=1}^{\infty} \exp. (-Kn^2 \pi^2 (t-\lambda)/a^2) \times \sin(n \pi r/a) \sin(n \pi r_1/a) \dots\dots\dots (16)$$

Hence the temperature at  $r$  at time  $t_2$  due to all the heat liberated from the commencement of reaction at the surface at time  $t_1$  is

$$\theta = -(2L/acr) \sum_{n=1}^{\infty} \sin(n \pi r/a) \int_{t_1}^{t_2} r_1 (dr_1/d\lambda) \exp. (-Kn^2 \pi^2 (t-\lambda)/a^2) \times \sin(n \pi r_1/a) d\lambda \dots\dots\dots (17)$$

V.3. Properties of the differential temperature.

Now it has been shown (IV. 1.3 and IV. 2. 1)

that, for the moving source,  $r_1$  is given, to a good degree of approximation, by

$$r_1^2 = a^2 - \beta \lambda \dots\dots\dots (10)$$

Substituting in (17) we have

$$\theta_q = (L \beta /acr) \sum_{n=1}^{\infty} \sin(n \pi r/a) \int_{t_1}^{t_2} \exp. (-Kn^2 \pi^2 (t_2 - \lambda)/a^2) \times \sin n \pi (1 - \beta \lambda/a^2)^{1/2} d\lambda \dots\dots\dots (18)$$

The contribution to the temperature at  $r$  by the moving boundary between the two phases of the reacting substance is thus given by equation (18), in which times  $t_1$  and  $t_2$  are measured from the commencement of the experiment,

$t_1$  being the time at which reaction starts at the surface and  $t_2$  the time at which measurement is taken,  $t_2 > t_1$ . This contribution is superimposed on the differential temperature

$$k(a^2 - r^2)/6K - \theta_0 \dots \dots \dots (12)$$

due to supply of heat from outside. Since this is independent of time, no confusion arises by making  $t_1 = 0$  and  $t_2 = t$  in equation (18), where  $t$  is now time measured from commencement of reaction at the surface. This convention will be adhered to in all that follows, as no further interest attaches to the surface temperature  $kt$ . The total differential temperature is thus the sum of (12) and (18).

V.3. Properties of the differential temperature.

These depend entirely on the expression in equation (18) since the term due to outside source remains constant and may therefore be ignored. In d.t.a. it serves as the base-line. Examination of equation (18) suggests at once that the contribution of the moving source to the differential temperature depends on

- (a) the "latent heat" of transformation,  $L$  cal.s.gm.<sup>-1</sup>, of the reacting substance, but since the quantity  $\beta$  which appears under the sign of integration as well as a factor is also known to depend on  $L$ , although this has not been conclusively shown by these experiments, the relation between  $L$  and

at a value  $\theta$  cannot be exactly linear: (see Fig.39);

(b) the quantity,  $\beta$ , which has been called the "propagation rate" for the reaction, and since this has been shown to vary linearly with heating rate (Fig.38), the dependence of the differential temperature on heating rate thus becomes obvious, although, again, the relationship depends on the magnitude of the integral in equation (18) for various values of  $\beta$ ;

(c) the distance,  $r$  from the centre, at which measurement is taken: the relationship with  $1/r$  is also in this case not exactly linear owing to the presence of the term  $\sin(n \pi r/a)$  under the summation sign.

Equation (18) shows that if  $\lambda$  is limited, the differential temperature is purely transient. The equation may be written in the form

$$\theta = \sum_{n=1}^{\infty} \left\{ \exp.(-Kn^2 \pi^2 t/a^2) \sin(n \pi r/a) \frac{L\beta}{acr} \int_0^t \exp. (Kn^2 \pi^2 \lambda /a^2) \sin n \pi (1-\beta \lambda/a^2)^{\frac{1}{2}} d\lambda \right\} \dots (18a)$$

The second factor represents a growth factor and remains predominant as long as reaction is taking place, although the rate of growth diminishes exponentially, being controlled by the first term whose effect depends on the magnitude of  $K$  and  $a$ . But after a time  $t = a^2/\beta$ , reaction ceases and the growth factor remains constant



at a value

$$\sum_{n=1}^{\infty} \int_0^{a^2/\beta} \exp. (Kn^2 \pi^2 \lambda / a^2) \sin n \pi (1 - \beta \lambda / a^2)^{1/2} d\lambda \dots \dots \dots (19)$$

and the decay factor becomes predominant, so that the contribution of the reaction to the differential temperature becomes, for all practical purposes, zero after a time  $t$  depending on the thermometric conductivity  $K$  of the reaction product and the size of the specimen

The time of return to base-line as well as the shift in the base-line away from the  $t$ -axis thus depends largely on  $K$  and  $a$ , but since, in general, the value of  $K$  for the reaction products may differ very much from that for the reactants, the shift in base-line may be quite appreciable. This is generally the case where one of the phases is solid and the other liquid, and this has caused a certain amount of difficulty in evaluation of peak area.

But since it is now clear that only a portion of the area should be taken into account, the second base-line should not enter into consideration.

Thus, for  $t < a^2/\beta$ , we have

$$\theta_1 = (L \beta / a c r) \sum_{n=1}^{\infty} \left\{ \sin(n \pi r / a) \exp. (-Kn^2 \pi^2 t / a^2) \int_0^t \exp. (Kn^2 \pi^2 \lambda / a^2) \sin n \pi (1 - \beta \lambda / a^2)^{1/2} d\lambda \right\} \dots \dots \dots (20)$$

and for  $t > a^2/\beta$ , if  $t_1 = \lambda_{\max} = a^2/\beta$ ,

methods. But care is required in this respect since

$$\theta_2 = (L \beta / a c r) \sum_{n=1}^{\infty} \exp. (-K n^2 \pi^2 (t - t_1) / a^2) \sin(n \pi r / a) \\ \times \int_0^{t_1} \exp. (K n^2 \pi^2 (t_1 - \lambda) / a^2) \sin n \pi (1 - \beta \lambda / a^2)^{1/2} d \lambda \\ \dots \dots \dots (21)$$

since all the heat generated up to  $t > a^2 / \beta$  is the heat generated up to  $t_1 = a^2 / \beta$ . It may be noted from equation (21) that the time  $(t - t_1)$  of return to base-line depends entirely on the term

$$\exp. (-K n^2 \pi^2 (t - t_1) / a^2)$$

and hence is an invariant for any given system, i.e. for any given value of K and a, irrespective of the maximum differential temperature reached. This is why the area represented by equation (21) should not be taken into account in evaluation of heat of reaction.

V. 4. Evaluation of the differential temperature.

If the relationship between  $r_1$  and  $\lambda$  obeys a fractional power of the type of equation (10), the evaluation of the integral

$$\int_0^t \exp. (-K n^2 \pi^2 (t - \lambda) / a^2) \sin n \pi (1 - \beta \lambda / a^2)^{1/2} d \lambda$$

becomes one of great difficulty. This militates to some extent against a more general discussion of the behaviour of the differential temperature. But an approximate value for particular values of  $\beta$  and K for a given size of specimen is easily and quickly obtained by numerical methods. But care is required in this respect since

TABLE X.

$$f(\lambda) = \int_0^t \sum_{n=1}^{\infty} \exp.(-Kn^2 \pi^2 (t-\lambda)/a^2) \sin(n\pi x/a) \sin n\pi(1-\beta\lambda/a^2)^{1/2} d\lambda,$$

for  $r/a = 0.5$  and  $t \leq a^2/\beta$

$\beta/a^2 =$	$0.04 \times 10^{-2}$		$0.08 \times 10^{-2}$		$0.20 \times 10^{-2}$	
$\beta t/a^2 \backslash K =$	$.18 \times 10^{-2}$	$.16 \times 10^{-2}$	$.18 \times 10^{-2}$	$.16 \times 10^{-2}$	$.18 \times 10^{-2}$	$.16 \times 10^{-2}$
0.2	24.7	25.3	9.4	8.2	-4.2	-3.4
0.4	146.0	144.0	62.5	64.5	16.0	12.8
0.6	323.0	342.0	217.0	222.0	81.2	75.3
0.8	374.5	452.5	378.0	405.0	243.4	254.0
1.0	460.0	515.0	415.0	450.0	282.0	344.0

TABLE Xa.

$$\theta = (L\beta/acr)f(\lambda)$$

with  $L = 10.5 \text{ cal. gm.}^{-1}$   
 $c = 0.214 \text{ cal. deg. C}^{-1}$  } for potassium nitrate

$\beta/a^2 =$	$0.04 \times 10^{-2}$		$0.08 \times 10^{-2}$		$0.20 \times 10^{-2}$	
$\beta t/a^2 \backslash K =$	$.18 \times 10^{-2}$	$.16 \times 10^{-2}$	$.18 \times 10^{-2}$	$.16 \times 10^{-2}$	$.18 \times 10^{-2}$	$.16 \times 10^{-2}$
0.2	1.1	1.1	0.8	0.7	-0.9	-0.7
0.4	6.4	6.3	5.5	5.6	3.5	2.8
0.6	14.1	14.9	19.0	19.4	17.6	16.6
0.8	16.3	19.7	33.9	35.3	53.0	55.4
1.0	17.9	22.5	36.1	39.4	61.5	75.0

TABLE XI.

$$f(\lambda) = \sum_{n=1}^{\infty} \frac{M_n}{a} \exp.(-Kn^2 \pi^2 (t - t_1)/a^2) \sin(n\pi r/a) \times \int_0^{t_1} \exp.(Kn^2 \pi^2 (t_1 - \lambda)/a^2) \sin n\pi (1 - \beta\lambda/a^2)^{1/2} d\lambda$$

for  $r/a = 0.5$ ,  $t \geq t_1 = a^2/\beta$ .

K =	$1.8 \times 10^{-3}$			$1.6 \times 10^{-3}$		
	$\beta/a^2 = .04 \times 10^{-2}$	$.08 \times 10^{-2}$	$0.2 \times 10^{-2}$	$.04 \times 10^{-2}$	$.08 \times 10^{-2}$	$0.2 \times 10^{-2}$
500	174.0	148.0	90.0	210.0	174.0	102.0
1000	65.0	55.0	33.5	89.0	73.0	43.0
1500	24.2	20.5	12.5	36.6	30.0	17.8
2000	8.8	7.5	4.6	15.2	12.6	7.4
2500	3.3	2.8	1.7	6.6	5.4	3.2
3000	1.5	1.2	0.7	2.5	2.1	1.2
3500	0.5	0.4	0.2	1.2	0.8	0.5
4000	-	-	-	0.5	0.4	0.2

TABLE XIa.

$$\theta = (L\beta/acr)f(\lambda)$$

K =	$1.8 \times 10^{-3}$			$1.6 \times 10^{-3}$		
	$\beta/a^2 = .04 \times 10^{-2}$	$.08 \times 10^{-2}$	$0.2 \times 10^{-2}$	$.04 \times 10^{-2}$	$.08 \times 10^{-2}$	$0.2 \times 10^{-2}$
500	7.6	12.9	19.6	9.2	15.1	22.1
1000	2.8	4.8	7.3	3.9	6.4	9.3
1500	1.1	1.8	2.7	1.6	2.6	3.9
2000	0.4	0.7	1.0	0.7	1.5	1.6
2500	0.1	0.2	0.4	0.3	0.5	0.7
3000	-	0.1	0.2	0.1	0.2	0.3
3500	-	-	-	-	0.1	0.1
4000	-	-	-	-	-	-

I - III. THEORETICAL D.T. CURVES FOR  
 $\beta = 0.20 \times 10^{-2}$ ,  $0.08 \times 10^{-2}$ ,  
 $\& 0.04 \times 10^{-2}$   $\text{cm}^2 \cdot \text{sec}^{-1}$   
 $K = 1.6 \times 10^{-3}$   $\text{cm}^2 \cdot \text{sec}^{-1}$

IV & V. EXPERIMENTAL CURVES FOR  
 $k = 0.041$  &  $0.021$   $^{\circ}\text{C} \cdot \text{sec}^{-1}$   
 $K = 1.54 \times 10^{-3}$   $\text{cm}^2 \cdot \text{sec}^{-1}$

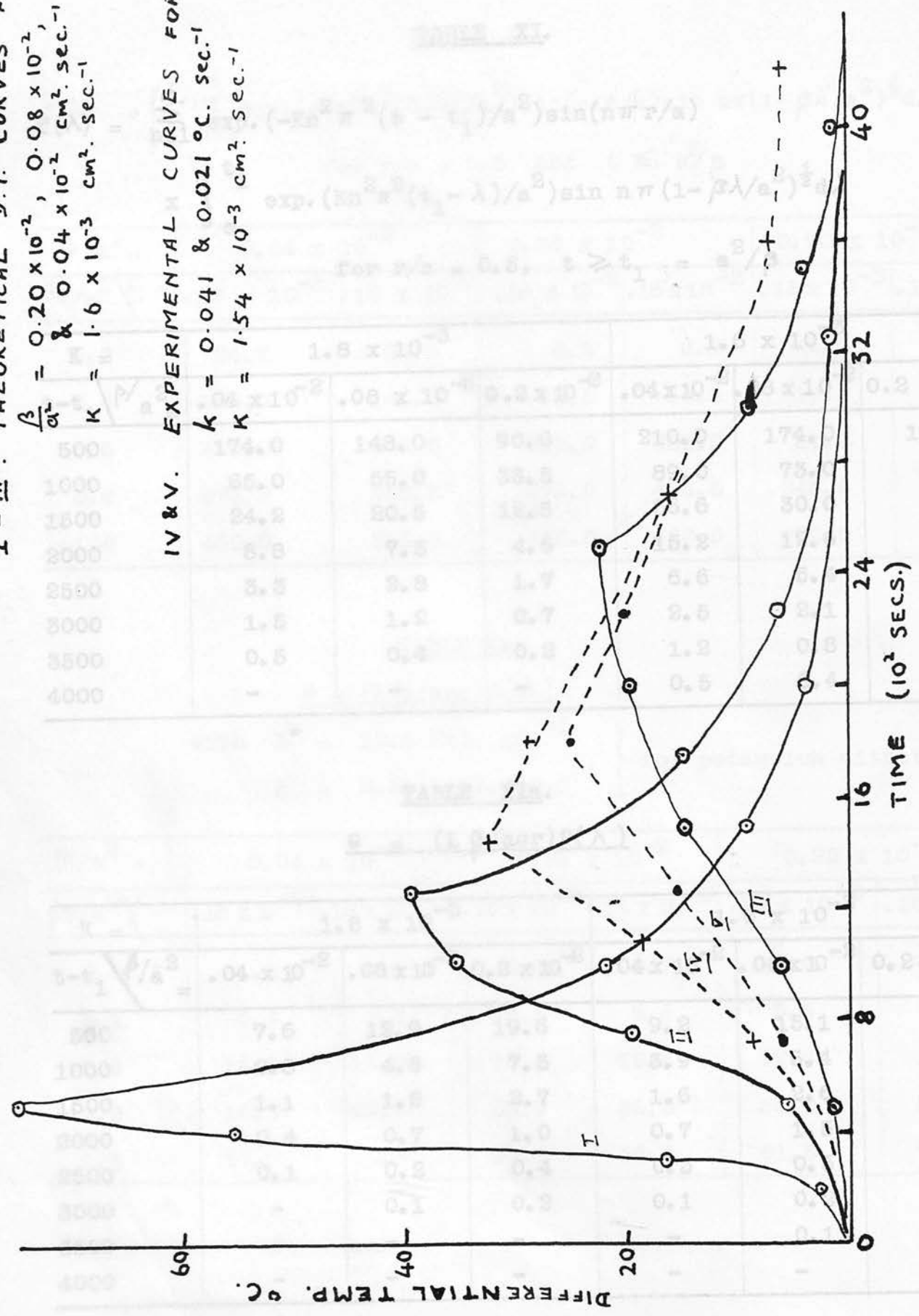


FIG. 41. D. T. CURVES, THEORETICAL & EXPERIMENTAL.

I-III. THEORETICAL D.T. CURVES FOR  
 $\frac{\beta}{a^2} = 0.20 \times 10^{-2}, 0.08 \times 10^{-2},$   
 $\& 0.04 \times 10^{-2} \text{ cm}^2 \text{ sec}^{-1}$   
 $K = 1.6 \times 10^{-3} \text{ cm}^2 \text{ sec}^{-1}$

IV-V. EXPERIMENTAL CURVES FOR  
 $k = 0.041 \& 0.021 \text{ } ^\circ\text{C. sec}^{-1}$   
 $K = 1.54 \times 10^{-3} \text{ cm}^2 \text{ sec}^{-1}$

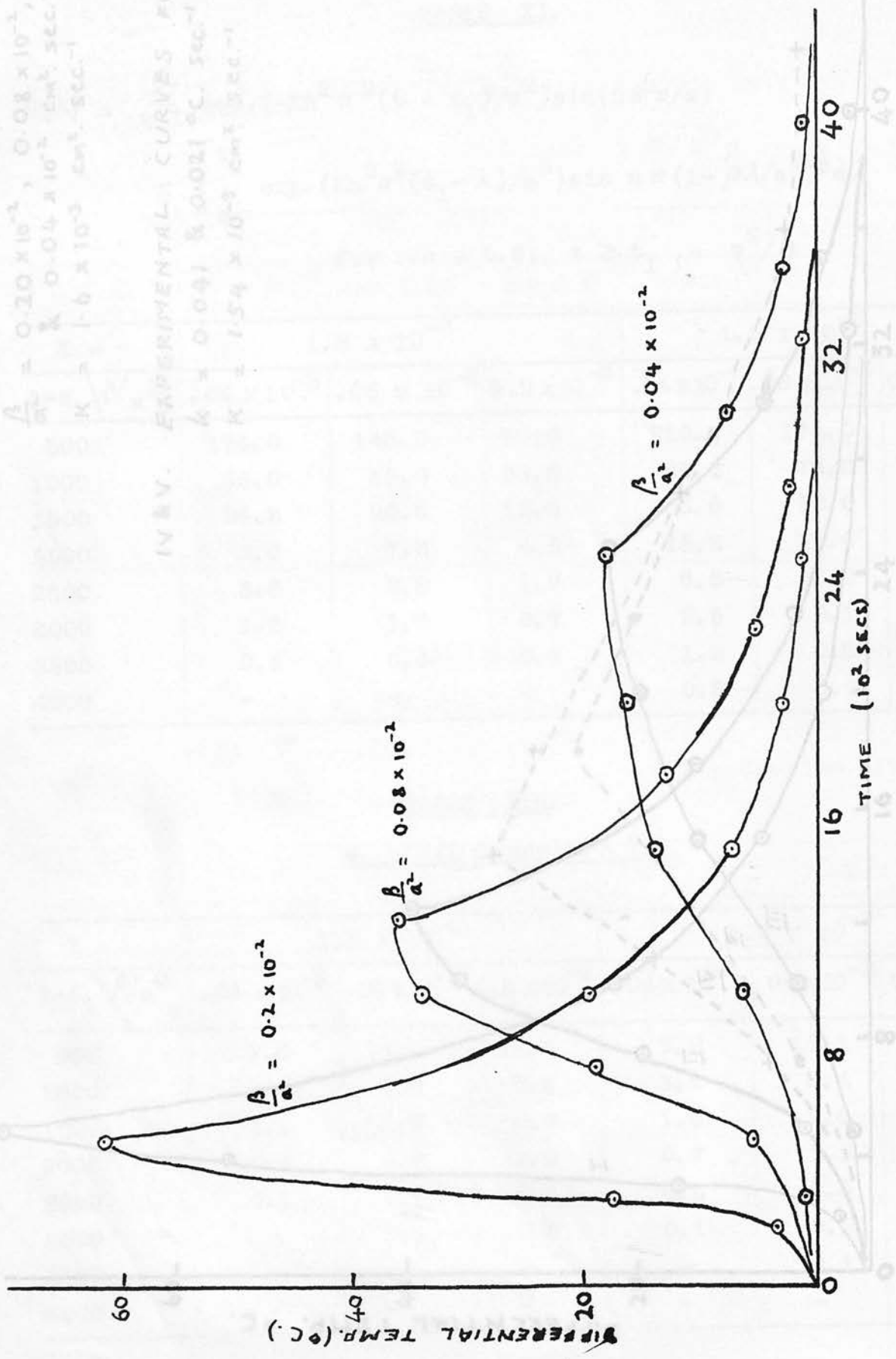


FIG. 42. THEORETICAL D.T. CURVES:  $K = 1.8 \times 10^{-3} \text{ cm}^2 \text{ sec}^{-1}$

FIG. 41. D.T. CURVES, THEORETICAL & EXPERIMENTAL

the numerical value of the function becomes anomalous at  $\lambda = t$ ,  $\lambda = 0$

and at  $\lambda = a^2/\beta$  corresponding to  $r_1 = 0$ .

This limits rather severely the choice of particular methods since most methods of numerical integration require the values of  $f(\lambda)$  at these points. (See Appendix).

The values of  $\lambda$  for the two values  $0.04 \times 10^{-3}$

$$\sum_{n=1}^{\infty} \int_0^t \exp.(-Kn^2 \pi^2 (t-\lambda)/a^2) \sin(n\pi r/a) \sin n\pi(1-\beta\lambda/a^2)^{1/2} d\lambda$$

have been evaluated for  $r/a = 0.5$  and for two values of  $K$  and three values of  $\beta$ , the values of  $K$  and  $\beta$  being those within the range of the experiments in the preceding

pages. Table X shows the values of the integral and the

corresponding temperatures for  $t \leq a^2/\beta$ , i.e. during the course of the reaction, and Table XI the values for  $t > a^2/\beta$ , i.e. during recovery. The values of differential temperature from

Tables Xa and XIa are plotted together in Figs.41 and 42

for the two values of thermometric conductivity respectively. The values of differential temperature were obtained by making

$$L = 10.5 \text{ cal. gm.}^{-1}$$

$$c = 0.215 \text{ cal. gm.}^{-1} \text{ deg.C.}^{-1}$$

There is some doubt as to the value of  $L$  for potassium nitrate transformation at  $129^\circ\text{C.}$ : the value  $12.8 \text{ cal. gm.}^{-1}$  is sometimes used, and this would raise the temperatures by about 22 per cent. Also the value of  $c$  used is the known value at  $0^\circ\text{C.}$  The graphs therefore are only

approximate representation of ideal differential thermal curves.

maximum, time from maximum to complete recovery, and general shapes of curves are concerned. The curve I

#### IV. 5. Discussion

employed For purposes of comparison, two experimental

curves are plotted on Fig. 41. The basis for this is

taken from Fig. 38 in which the two values  $0.04 \times 10^{-2}$

and  $0.08 \times 10^{-2}$  for  $\beta/a^2$  would correspond to heating

rates of 0.218 and 0.436 deg.C. per second respectively.

The curves IV and V shown are those for a sample of pure

potassium nitrate heated at 0.21 and 0.41 deg.C. per

second respectively, the mean value of the thermometric

conductivity of the specimen being found to be  $0.154 \times 10^{-2}$ ,

so that the parameters of the experiment are comparable

to the hypothetical values used to obtain curves II and

III respectively. The base-line for the experimental

curves are taken as that value of the differential tempera-

ture for  $r/a = 0.5$  at the commencement of reaction at

the surface. The density of packing of the material was

$1.24 \text{ gm. cm.}^{-3}$  as against the mean density of potassium

nitrate itself of  $1.42 \text{ gm. cm.}^{-3}$ .

In view, therefore, of previous remarks on the

reproducibility of experimental conditions and the diffi-

culty of realizing the ideal in practice, the results may

be regarded as in fairly good agreement with the theory

outlined in the previous two sections, in so far as the



relative magnitudes of maximum differential temperature, time to maximum, time from maximum to complete recovery, and general shapes of curves are concerned. The curve I represents an extreme of very high heating rate not employed in the experiments here described. But in other respects the agreement is not so good, and the following qualifications must be made:

(a) Although the theoretical and experimental curves represent experimental conditions which are only approximately similar the discrepancy in times to reach maximum differential temperature are serious ones. But, as mentioned before, the theoretical curves represent only the ideal conditions in which reaction is assumed to be completed in the centre when  $t = a^2/\beta$ . We have seen, however, that this is usually only the case when limiting conditions of very low heating rates are employed, otherwise completion of reaction usually corresponds to a point on the recovery side of the d.t. curve, and not to the maximum of the peak. In order to account for this, consideration must be given to the fact that the ideal propagation law applies accurately only at low heating rates, and, as we have seen (IV.2.2), deviation occurs at  $r \rightarrow 0$  to an increasing extent as the heating rate is increased. The departure of the temperature or time at which maximum is reached on the experimental curve from that on the experimental curve may be taken, therefore,

as a measure of the <sup>deviation of the</sup> <sup>law</sup> propagation of the reaction from equation (10), as illustrated by Fig. 43.

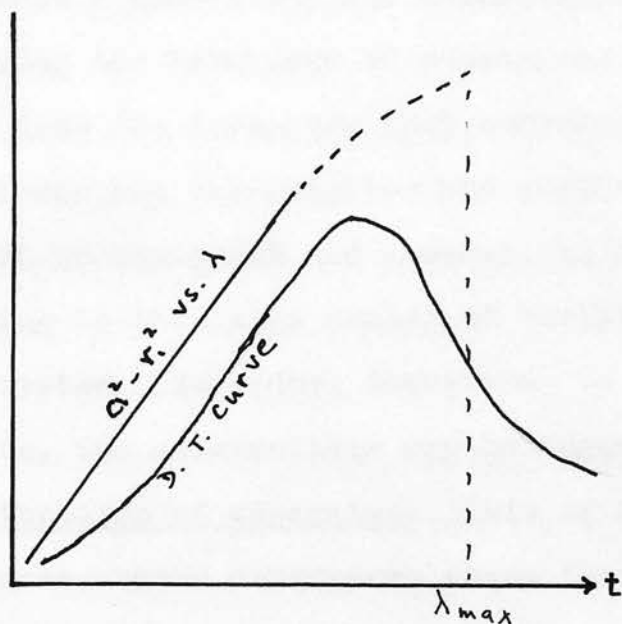


Fig. 43.

We should therefore expect increasing deviation, for a given heating rate, for media of increasing thermometric conductivities  $K$ , since the rate of decay of the differential temperature depends on the quantity  $\exp(-Kn^2\pi^2t/a^2)$ .

(b) The theory does not take into account the changes in  $K$  during the course of heating. This change is primarily due to expansion and hence, change in density, so that  $K$  increases. In the case of solid-liquid transitions there is also, apart from change in density, a change in thermal conductivity. This shows up in experimental

d.t. curves as a shift in base-line away from the t-axis.

Although the method of differential thermal analysis provides a convenient and systematic means of studying the kinetics of reactions as well as it is evident from the foregoing that correlation of results as between one investigator and another and as between one set of equipment and another, is extremely difficult, owing to the wide number of variable parameters of any given system. In order, therefore, to make the method absolute, the following are suggested:

1. Calibration of standards. This is being increasingly done, since substances whose thermal constants are accurately known, especially the temperature and heat of transition. The only standard available is quartz with a transition temperature of 573°C. There are two objections to this: (1) the use of a substance which undergoes a first or "latent heat" type of reaction to standardize equipment for other reactions is bound to lead to error unless a unified theory can be developed for both types; (2) as has been shown in Chapter IV, serious error results in correlation unless the important parameter  $K$ , the thermoelectric sensitivity, is made the same for the standard substance, the reference material, and the test substance.

2. Internal Correlation. The approximate theory

Chapter VI. CONCLUSION.

Although the method of differential thermal analysis presents a convenient and relatively simple means of studying the behaviour of substances on heating it is evident from the foregoing that correlation of results as between one investigator and another and as between one set of equipment and another, is extremely difficult, owing to the large number of variable parameters of any given system. In order, therefore, to make the method absolute, two alternatives may be suggested:

1. Calibration of apparatus: This is being increasingly done, using substances whose thermal constants are accurately known, especially the temperature and heat of transition. The usual standard substance is quartz with a transition temperature at  $575^{\circ}\text{C}$ . There are two objections to this: (a) the use of a substance which undergoes a Stefan or "latent heat" type of reaction to standardize equipment for other reactions is bound to lead to error unless a unified theory can be developed for both types; (b) as has been shown in Chapter IV, serious error results in correlation unless the important parameter K, the thermometric conductivity, is made the same for the standard substance, the reference material, and the test substance.

2. Internal Correlation: The approximate theory

outlined in Chapter V makes it possible to determine the required thermal constants from a single experiment. It has been shown that the differential temperature is related to the function  $f(\lambda)$  of tables X and XI by

expression for 
$$\theta = \frac{L\beta}{acr} f(\lambda).$$

All the constants of this equation can be determined from a single experiment as follows:

this (a) the quantity  $\beta$  may be determined by assuming the approximate relationship

$$a^2 - r_1^2 = \beta\lambda \quad \dots\dots\dots (10)$$

in the case of a spherical model;

(b) the parameter K which occurs in the expression for  $f(\lambda)$  can be determined from the final steady differential temperature from the relation

$$\theta = \frac{k(a^2 - r^2)}{6K}$$

for a spherical model;

(c) the point X in Fig. 20 corresponding to completion of reaction can be determined also from equation (10), and from this that portion of the area required to estimate the total heat liberated may be found.

From the total heat liberated,  $H_{tr}$ , and the heat of transition per gram, L, the amount of reacting material present may be evaluated.

Limitations: Apart from experimental conditions

imposed by the inaccuracy of equation (10) at high heating rates, the expression for differential temperature given in Chapter V creates serious difficulties at  $r = 0$  if numerical methods are used. In the absence of a closed expression for the integral

$$\int_0^t \exp.(-Kn^2 \pi^2 (t - \lambda)/a^2) \sin n\pi(1 - \beta\lambda/a^2)^{1/2} d\lambda$$

where  $\lambda_1 = 0.1 t$   
 $\lambda_2 = 0.4 t$   
 $\lambda_3 = 0.5 t$   
 $\lambda_4 = 0.9 t$   
this must remain a serious limitation.

This formula has been found to be the most suitable since it does not involve the difficulties associated with the anomalies of  $f(0)$  and  $f(t)$ . The errors are negligible for low values of  $\beta$  in equation (13a), only five terms of the series being found sufficient to make errors less than 0.001 in the value of the integral

$$\int_0^t \exp.(-Kn^2 \pi^2 (t - \lambda)/a^2) \sin n\pi(1 - \beta\lambda/a^2)^{1/2} d\lambda .$$

But, for high values of  $\beta$ , the formula is less accurate unless up to seven or even nine terms of the series are taken.

APPENDIX

FORMULA FOR INTEGRATION

The formula used to compute the values in

Tables X and XI was

$$\int_0^t f(\lambda) d\lambda = \frac{t}{4} (f(\lambda_1) + f(\lambda_2) + f(\lambda_3) + f(\lambda_4))$$

where  $\lambda_1 = 0.1 t$

$\lambda_2 = 0.4 t$

$\lambda_3 = 0.6 t$

$\lambda_4 = 0.9 t$

This formula has been found to be the most suitable since it does not involve the difficulties associated with the anomalies of  $f(0)$  and  $f(t)$ . The errors are negligible for low values of  $\beta$  in equation 18a, only five terms of the series being found sufficient to make errors less than 0.001 in the value of the integral

$$\int_0^t \exp.(-Kn^2 \pi^2 (t-\lambda)^2 / a^2) \sin n\pi (1 - \beta\lambda/a^2)^{1/2} d\lambda .$$

But, for high values of  $\beta$ , the formula is less accurate unless up to seven or even nine terms of the series are taken.

17. Vold, M.J. Anal. Chem., 21, 583-8 (1949)  
 18. Hattingsdi, Vold, & Vold. Ind. Eng. Chem., 41, 2320-2324, 2311-2320 (1949).  
 19. Ullman, D. Thesis, Göttingen (1932).  
 20. Kofler, L. Chem. Ztg., 68, 43-45 (1944).  
 21. Orsel, J. Bull. soc. franc. d. Min., 59, 273-322 (1927).

REFERENCES

1. Le Chatelier. Bull. soc. franc. mineral., 10, 204 - 211 (1887).
2. Roberts-Austen, W.C. Proc. Mech. Engrs., 543-604 (1891); 102-138 (1893); 145-198 (1893); 238-297 (1895); 31-100 (1897); 35-102 (1899).
3. Fenner, C.N. Am. J. Sci., ser. 4, 38, 331-384 (1913).
4. Sandonini. Atti. acad. Lincei, 21, II, 634-640 (1913).
5. Pascal. Compt. rend., 154, 883-6 (1913)
6. Germs, H.C. Acad. proefschrift Gronigen, 1917; Chem. Weekblad, 14, 1156.
7. Kracek, F.C. J. Phys. Chem., 33, 1857 - 1879 (1929)
8. Perrier & Wolfers. Arch. Sci. phys. nat., 2, 372-8 (1920)
9. Gosman, 1927. The Properties of Silica
10. Andre-Boulle. Compt. rend. 200, 832-4 (1935)
11. Kracek, F.C. J. Phys. Chem. 33, 1281-1303
12. Segawa, Kiyoshi. J. Japan Ceram. Assoc., 56, 7-10, 59-62, 99-101; 57, 1-3, 97-99.
13. Guillisan, J. Bull. sci. acad. roy. Belg., 13, 233-8 238-40, (1927).
14. Chatelet, R. Bull. soc. Chim. (5), 4, 1996-2016, (1937)
15. Shinkichi-Horiba. Sci. Repts., Tohoku Imp. Univ. First Series, 430-43 (1936).
16. Juffray, J., & Viloteau, J. Compt. rend., 226, 1701-2 (1948).
17. Vold, M.J. Anal. Chem., 21, 683-8 (1949)
18. Hattingdi, Vold, & Vold. Ind. Eng. Chem., 41, 2320-2324, 2311-2320 (1949).
19. Ullman, D. Thesis, Gottingen (1932).
20. Kofler, L. Chem. Ztg., 68, 43-45 (1944).
21. Orsel, J. Bull. soc. franc. d. Min., 50, 278-322 (1927).



22. Orcel, J. VII. Cong. Int. d. Min. Geol. appl., 1, 357 (1935)
23. Caillere, Henin & Turc. Compt. rend., 223, 383-4 (1946)
24. Grim, R.E., 1953. "Clay Mineralogy" (McGraw-Hill).
25. Stefan, J. Wied. Ann., 42, 269 (1891)
26. Mackenzie, R.C. (ed.), 1957. "The Differential Thermal Investigation of Clays". (Mineralogical Society, London.)
27. Stefan, J. *Op. cit.*
28. Weber, "Differential Gleichungen" (Riemann), II, p.117
29. Tamara, Monthly Weather Review, 33, 55 (1905)
30. Lightfoot. Proc. Lond. Math. Soc. (2), 31, 97 (1929)
31. Lachmann. Zeits. fur angew. Math. Mech., 15, 345 (1935)  
17, 379 (1937).
32. Huber, Zeits. fur angew. Math. Mech., 19, 1 (1939).
33. Perkeris & Slichter, J. Appl. Phys. 10, 135 (1939)
34. Miles, J.W. Quarterly of Appl. Maths. 8, 81 (1950)
35. Landau, Quarterly of App. Maths. 8, 85 (1950)
36. Danckwerts, P.V. Trans. Farad. Soc. 46, 701-712 (1950)
37. Carslaw & Jaeger, "Heat Conduction in Solids"
38. *Ibid.*
39. Berg & Sveschnikova. Izvest. Akad. Nauk, SSSR., Otdel. Khim. Nauk, 19-24 (1946)
40. British Standards Institution. B.S. 1827: 1952.
41. Carslaw & Jaeger *Op. cit.*
42. Danckwerts, P.V. *Op. Cit.*
43. Mackenzie *Op. Cit.*
44. Smothers, W.J. & Chiang, Yao. " Differential Thermal Analysis" (1958).
45. Vold, M.J. *Op. Cit.*

46. Smothers & Chiang. Op. Cit.
47. Wagner, C. Trans. A.I.M.E. (1954), Journal of Metals (Feb. 1954)
48. Spiel, S., et al. U.S. Bur. Mines Tech. Paper 664 (1945)
49. Hattingdi, Vold & Vold. Op. cit.
50. Kerr, P.F., Kulp, J.L. and Hamilton P.K. A.P.I. Project 49, Prel. Rpt. No.3, Colum. Univ., 1-48 (1949)
51. Tsang, N.F. Article in Smothers & Chiang, "Differential Thermal Analysis".
52. Carslaw & Jaeger. Op. cit.

P L A T E

Photograph of Apparatus Assembly

